POLITECNICO DI TORINO

III Faculty of Engineering

Degree in Mechatronics Engineering

Master Thesis

DESIGN AND CONSTRUCTION OF AN EMG MULTICHANNEL ACQUISITION SYSTEM PROTOTYPE

Relator:
Prof. Marcello Chiaberge

Sebastián Aced López

DLR
German Aerospace Center
Dipl. Inf. Holger Urbanek

September 2012

Summary

This thesis presents the design and construction of an Electromyography (EMG) high−density acquisition system prototype at the Deutschen Zentrums für Luft und Raumfahrt (DLR) Bionics group in Munich− Germany. It does not intend to come up with new principles of EMG recording, but its scope is to search, compare, simulate, construct and validate nowadays available solutions that fulfill the imposed requirements.

The design consists in ten functional blocks that cover all the system aspects from the power supply to the measuring electrodes. In order to construct the circuit prototype, some classical solutions were implemented and some novelty configurations were explored, for instance: a novelty DC rejection filter without grounded resistors, to prevent degradation of the front−end amplifier Common Mode rejection (CMR) and the driven shields that solved the problem of amplifying the EMG signal at a considerable distance from the source.

This document covers all the way in between the muscles and the computer, that EMG signals go through: electrodes, esd protection, shield cables, DC rejection, amplification, Driven Right Leg feedback, filtering, isolation and digitization.

Acknowledgements

I would like to thank all the people at the DLR in Germany that helped me and thought me so many things during this six intense months. Specially I want to thank to Patrick van der Smagt, for the great opportunity of working in his lab, to Holger my supervisor and Robert my other supervisor. Thanks also to Nikolaus Seitz and his help during the circuit manufacturing, to Markus and his soldering tips, Robin and the equipment he lent me and to Franz Hacker for his help in the debugging process.

Ringrazio anche a tutti i miei amici a Torino, per l'incontro che mi hanno fatto fare, la compagnia e i buoni momenti che mi hanno regalato. A Agni per il supporto durante i lunghi mesi a Monaco, per il bene che mi vuole, davvero grazie.

A Roa, Male, Willi, Jorge e Ivancho por su valiosa amistad durante estos años lejos de casa.

Por último agradezco a las tres personas al otro lado del mundo, sin las cuales nada de ésto habría sido posible: Mariela, Santiago e Isabel.

Contents

Summary III

Acknowledgements IV

1 Introduction 1
- 1.1 Ambition . . . 1
- 1.2 Overview . . . 1
- 1.3 Electromyography . . . 3
  - 1.3.1 Basic physiology of EMG signals generation . . . 3
  - 1.3.2 Historical notes . . . 8
- 1.4 Electronics review . . . 11
  - 1.4.1 Noise . . . 11
  - 1.4.2 Operational Amplifiers . . . 16
  - 1.4.3 Filters . . . 22
  - 1.4.4 Analog to digital conversion . . . 25
  - 1.4.5 PCB Design . . . 29

2 EMG system: design specifications and functional blocks division 31
- 2.1 System design implications . . . 32
  - 2.1.1 Signal model . . . 32
  - 2.1.2 Blocks Diagram . . . 38

3 Functional blocks 41
- 3.1 Electrodes . . . 41
- 3.2 ESD protection . . . 45
- 3.3 DC Rejection . . . 49
- 3.4 Amplification . . . 51
  - 3.4.1 Amplifier . . . 52
  - 3.4.2 Integrator . . . 57
- 3.5 Shield Driver . . . 58
- 3.6 Driven Right Leg . . . 60

3.7 Filtering 63
3.8 Isolation 65
3.9 Power Supply 67
3.9.1 The DC−DC converter 69
3.9.2 Power supply filtering 71
3.10 ADC 72

4 Circuit construction 75
4.1 PCB design considerations 76
4.2 Prototype structure 80

5 Validation 87

6 Conclusion 99

Bibliography 101

Chapter 1

Introduction

1.1 Ambition

The human body is an outstanding system, complex and fascinating at the same time. Muscles are part of this masterpiece of "natural engineering" and in order to understand them, the study of EMG is mandatory. Although many signal software processing techniques and high level applications of EMG signals are available and being developed nowadays, the first step in between the live muscle and the computer display is the acquisition system. This thesis does not pretend to come up with new topologies or methods to measure *surface EMG*, but to review the available ones, the theory behind them and combine them into a multichannel acquisition system design. The construction of a prototype based on such design is also intended to set the basis for the first fully functional EMG high−density acquisition system prototype, customized for the needs of the Deutschen Zentrums für Luft und Raumfahrt (DLR) Bionics group.

1.2 Overview

This thesis will take the reader along the design process, construction and prototype validation of a EMG acquisition system developed in the DLR bionics group in Munich, Germany. At the beginning, the document presents a review of the physiology behind the EMG signal production and some historical notes that summarize the long way between the first observations of electrical phenomena, to the actual EMG signal detection techniques. Then some basic electronics concepts used during the design and construction stages will be presented.

After the introductory sections, the design process itself will be discussed: from the initial blocks diagram derived from the user specifications, to the prototype PCB construction. Each of the blocks will be explained in detail, with a theoretical

background, alternative choices and final practical considerations. Simulations will be annexed when necessary.

Finally the testing plan will be presented alongside the encountered problems during the realization, concluding with tips for future prototypes development.

The thesis is divided in the following parts:

- **Chapter 1** Introduction

In this chapter the physiology behind the EMG signals is explained. Short historical notes of EMG systems will be provided with some basic electronics review.

- **Chapter 2** EMG system: design specifications and functional blocks division

In this chapter the characteristics required by the user are presented, and the translation of them into project specifications is done. The proposed division in functional blocks will be discussed too.

- **Chapter 3** Functional blocks

In this chapter each block will be explained in detail. Design and practical considerations are discussed.

- **Chapter 4** Prototype PCB construction

In this chapter the practical aspects concerning the PCB construction will be discussed.

- **Chapter 5** Validation: Tests and further improvements

In this chapter the tests and validation setups will be shown with their corresponding results. Further improvements and tips for future prototypes are presented.

- **Chapter 6** Conclusion

In this chapter the conclusions of the overall process, from the theoretical background, passing through the design process until the construction of the prototype, are presented.

1.3 Electromyography

1.3.1 Basic physiology of EMG signals generation

Electromyography (EMG) signals are subject of study because there is a direct relationship between them and the muscles exerted force.[17] So it is possible to understand the muscle activity by understanding the EMG signals they produce. The first step in order to comprehend this biopotential (EMG) is to measure it through a sensor, and in order to construct a good sensor is necessary to know *what* has to be sensed.

Muscles

Before starting the study of muscles electrical activity and their force producing processes, a definition of muscle should be given first: a muscle is a body tissue consisting of long cells that contract when stimulated and produce motion[1]. There are three type of tissue that fit this definition:

- *Smooth muscle* Is an involuntary muscle controlled by the enteric and autonomous nervous system, meaning that it cannot be consciously controlled. Is called "smooth" because it does not present striations unlike the other two muscle types. It can be found in the walls of many organs like the stomach, bladder etc. Its contraction is much slower and longer lasting than the one produced by the skeletal muscle, in part because it does not consume as much energy as the voluntary muscles.
- *Cardiac muscle* Is only present in the heart, and although is very similar in structure to the skeletal muscle, it is also an involuntary muscle. The bioelectrical signals it produces, called Electrocardiography (ECG), are studied apart and are not treated in this document.
- *Skeletal muscle* Is the one in charge of the body movement and the posture maintenance, whence is controlled voluntarily. It is also the one from which EMG signals are taken. The skeletal muscle cells attach to the tendons, and through them, they fasten to the bones. Each muscle is constituted by a set of fibers surrounded by conjunctive and adipose tissue, these fibers are approximately 6 width, and can be as long as $4cm$ in adults.[2]. The Figure 1.1 shows how the skeletal muscles are seen as dark and light fibers repeated along the fiber, approaching and moving away during muscle contraction and relaxation.

[1] http://www.merriam-webster.com/medlineplus/muscle

[2] Projeto Ciência e Arte, Instituto de bioquímica médica UFRJ. http://www.bioqmed.ufrj.br

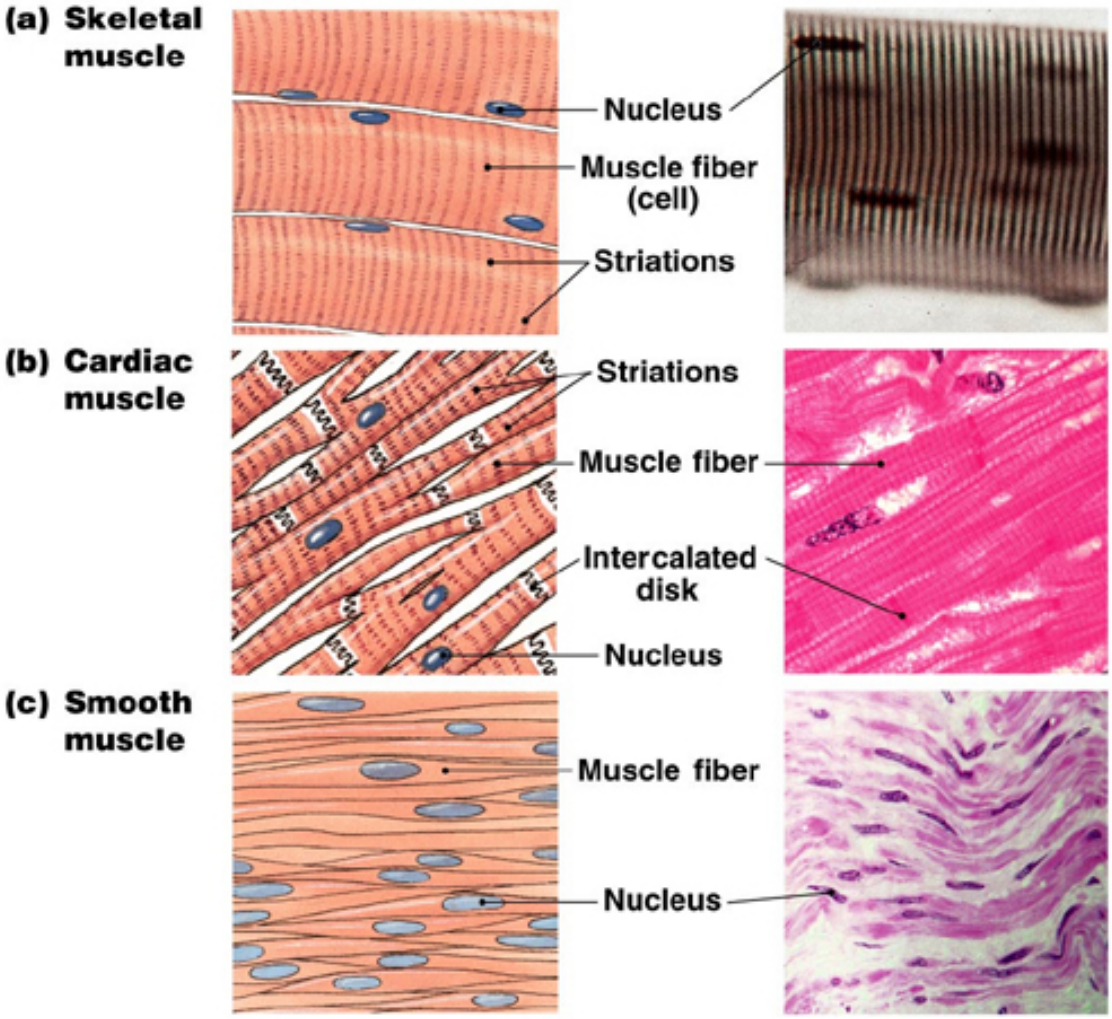

Figure 1.1. Detail of different types of muscle. Copyright ©Pearson Education Inc.

Motor Unit

The muscular system is intimately linked to the nervous system because is across the latest that the control commands arrive to the muscles. The central nervous system is organized in a hierarchical fashion [17], and the conscious movement of a muscle starts at the top of the hierarchy, in the *premotor cortex*, where the motion programming takes place. Then the stimulus travels to the spinal cord across the pyramidal tract, passing by the basal ganglia which modifies, improves, and increases the precision and finesse of the movement command, and by the cerebellum which regulates the movement.

Then, in the spinal stage, the impulse travels across the spinal cord until the

corresponding segment of the muscle to stimulate and continues its propagation to the muscle fibers through the *motoneurons*. Once in the muscle, the electrical signal is transformed into a chemical signal which causes the muscle contraction wanted by the cortex.

The motoneuron ($\alpha - motoneuron$) and the muscle fibers it innervates constitute the *motor unit*[3]. These motor units vary in size (from $5 - 7mm$ to $7 - 10mm$) and in number of innervated fibers. When fine movements are required, for example in the fingers or the eyes, less fibers are innervated by the same motoneuron, on the other hand, in clumsy movements each motoneuron covers hundreds of fibers at the same time.

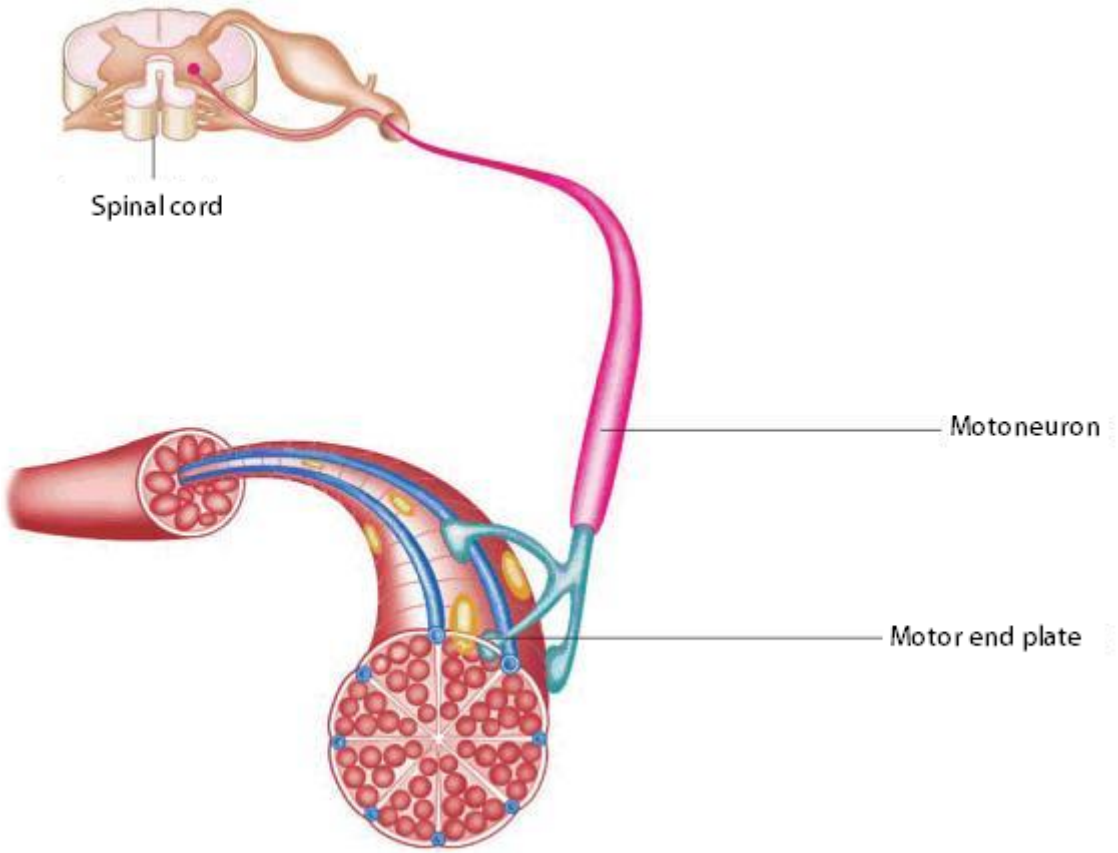

Figure 1.2. The Motor Unit (MU) consists of an $\alpha - motoneuron$ and the muscle fibers it innervates. Adapted from [19]

In Figure 1.3 the contractile elements of a muscular fibre known as *myofibrils* are shown. Each myofibril exhibits alternate dark and light bands called *myofilaments*.

[3]The concept of Motor Unit was originally described by Sherrington in 1906.

The light bands are the isotropic bands (I) formed by the protein *actin.* The dark ones are the anisotropics bands (A) and are composed of thicker filaments formed by the protein *myosin* which have paddle−shaped structures to attach to the actin filaments creating "crossbridges" between the two filaments. These crossbridges use ATP energy to pull the actin filaments closer. In this way the two types of filaments get closer, resulting in the muscle contraction. A series of actin−myosin filaments is called *sarcomere.*

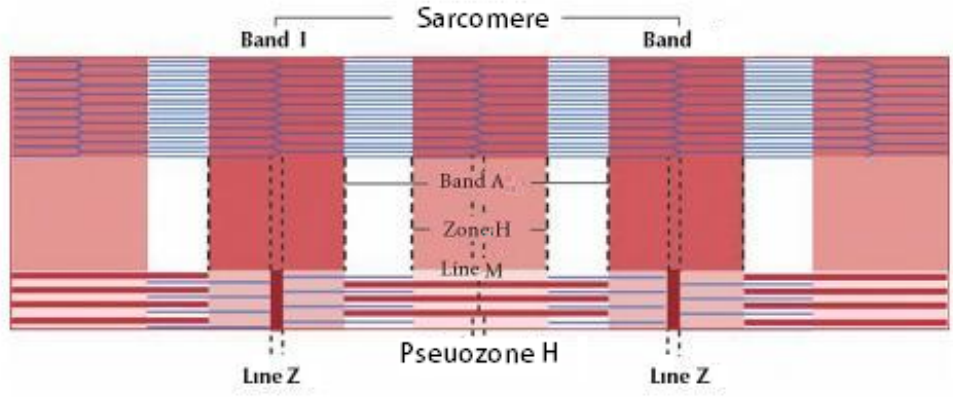

Figure 1.3. The myofilaments in a sarcomere. A sarcomere is defined as the section between two consecutive Z lines.

Action Potential

Muscle cells are surrounded by a semipermeable lipid membrane called *sarcolemma.* Under resting conditions there is a voltage across the membrane such that the inside of the fiber membrane lies around −90mV with respect to the outside. This potential gradient is produced by the difference in ionic concentrations between the inside and outside of the cell. In normal resting conditions, the concentration of Na^+ is higher at the outside of the membrane than it is at the inside; the opposite occurs with K^+ ions (relatively low at outside and high at the inside). Those conditions create the *resting potential.*

When the muscular tissue is excited , the muscle fiber depolarizes. First, the sodium (Na^+) permeability of the membrane changes, allowing the Na^+ ions to enter the tissue. If the depolarization is enough and the threshold of −65mV is reached, the sodium channels (controlled by voltage) open and the Na^+ rushes into the cell reversing the polarity of the cell momentarily to about +10mV.[11] A refractory period follows, and for a short time, the membrane do not respond with any action potential at all to additional stimuli. The voltage controlled sodium channels are closed and the potassium channels open, allowing the K^+ ions to cross the membrane

to the outside. At this point, the situation is the opposite than at the beginning: the high concentration of K^+ is in the outside, and a high Na^+ concentration in the interior of the tissue. Finally, the sodium−potassium pump resets the Na^+ and K^+ concentrations with an energy expenditure (active transport of three molecules of sodium and two molecules of potassium). Since multiple muscle fibers are innervated

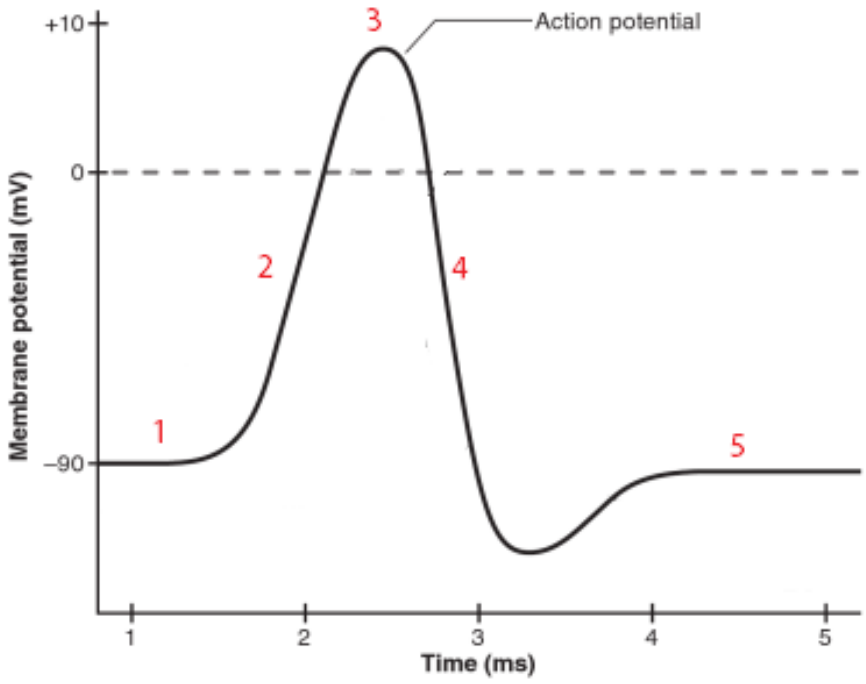

Figure 1.4. Muscle fiber action potential (MFAP). In the first stage (1) the membrane is resting at −90mV. At (2) the depolarization takes place and if the threshold is reached, the potential rises up until +10mV. During (3) the sodium channels close and the fiber cannot produce any new action potential at all. (4) is the repolarization that ends with the same initial conditions in (5). Adapted from [11]

by the same motoneuron, the firing of such neuron results in the activation of many muscle fibers. The summed activity of all the muscle fibers generates the *MUAP (motor unit action potential)*. See Figure 1.5.

Recruitment and firing rate

At this point, how the muscle activity relates to the EMG signals is quite clear, but there are factors that modulate the force exerted by the muscles that still need to be discussed. These "strategies" change *the number* and *the frequency* of the motor unit activations and thereby affect the algebraic sum of the motor unit action

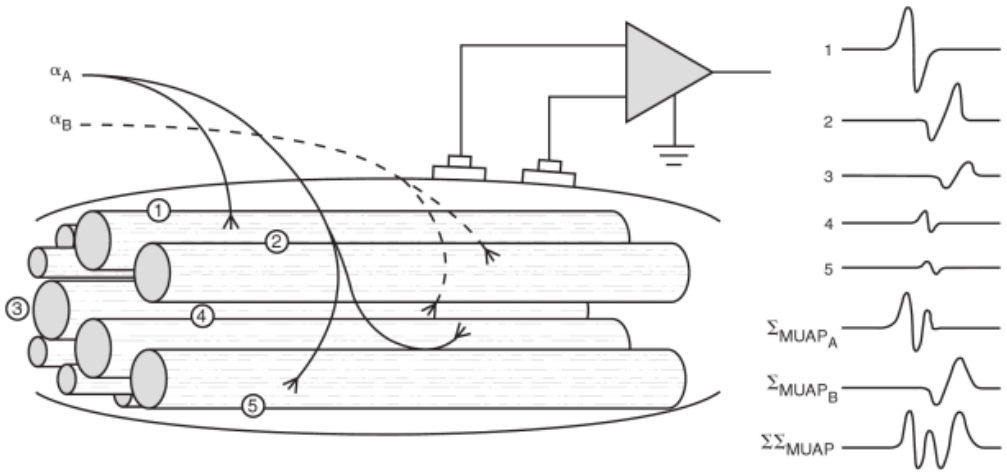

Figure 1.5. The surface electromyogram is composed by the algebraic sum of all motor unit action potentials. Adapted from [11]

potentials that compose the EMG signals.

The first strategy to increase the force is known as *motor unit (MU) recruitment* and consists in the activation of more motor neurons. Almost invariably, motor units are recruited by increasing size. In other words, the smallest motor units (the motoneurons that innervate less muscle fibers) are recruited first, and larger MUs are recruited with the force demand increasing. More motor units means increased EMG amplitude [11]. The second strategy to augment muscular force is to increase the frequency with which motor units are activated, known as *firing rate*. As in the previous case, the greater the frequency of MUs activation, the greater the EMG amplitude. However, there are other mechanisms (besides the firing rate increasing and the MUs recruitment) affecting the EMG amplitude such as: fatigue, MU firing synchronization, doublet firing etc. [17] Anyway is reasonable to assume a direct relationship between EMG and exerted muscle force, with correlation ranges from 0.97 to 0.99 [17].

To conclude, a *raw EMG signal* (unfiltered and unprocessed) recorded for three static contractions of the biceps brachii muscle is presented in Figure 1.6 to show the observable characteristics from the surface of the skin of the internal phenomena that transform the "intention of movement" into a measurable muscle force.

1.3.2 Historical notes

The first record of electrical phenomena is from the year $600BC$ when Thales of Miletus observed that the amber could be rubbed with fur to attract a small feather. The word electricity was used for the first time in the XVI century, when the english

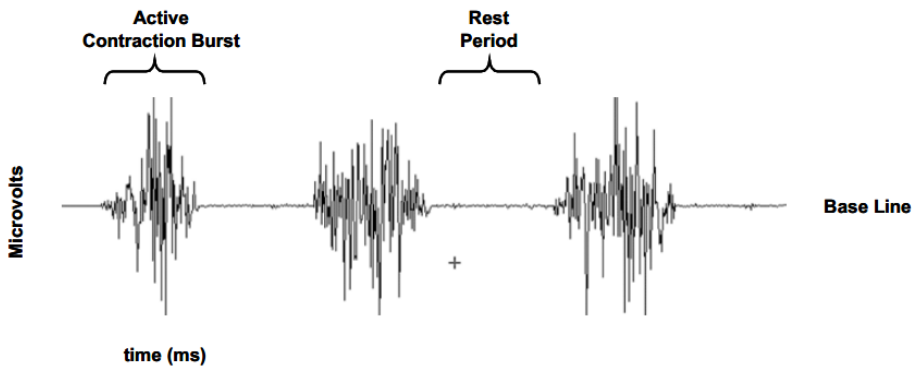

Figure 1.6. EMG recording of 3 contractions bursts of the biceps brachii muscle. Adapted from [13]

doctor William Gilbert in "De magnete" proposed the first hypothesis about the mysterious phenomenon. He referred to it with the adjective *electricus* from the old greek word for amber $\eta\lambda\epsilon\kappa\tau\rho o\upsilon$ (elektron).

Historical evidence suggests that in ancient Egypt ($2750BC$) the electrical discharges of the electrogenic fish (*Malopterurus electricus*) were used with therapeutic purposes. After thirty centuries, Scribonius Largus, medical officer of the Emperor Claudio, compiled a form of prescriptions, in which recommended, for treat the gout, to put an alive black torpedo (*Torpedo torpedo*) under the feet of the patient in a wet beach washed by the sea and remain so until the whole foot and leg to the knee were numb.

Many years later and in another location on the planet, early explorers and settlers in South America reported that the native indians treated various types of disease with the powerful electric shocks of the electric eel *(Electrophous electricus)*. Similarly, in China, electric catfish *(Parasilurus asota)* was recommended for treatment of ptosis (drooping eyelid) and facial paralysis.

In the XVII century, Otto von Guericke invention of the electrostatic generator would change everything because it provided scientists with a tool for conducting electrical experiments including Galvanis accidental discovery of animal electricity over a century later. Then, in 1750 Benjamin Franklin proposed his famous kite experiment, he discovered the principle of charge conservation and classified it in positive and negative.

Although in the fifteenth century, Francesco Redi $(1626-1697)$, an italian physician and naturalist physiologist, and later his disciple Stefano Lorenzini, described in detail a very specialized muscle of the electric ray, it was not until the pioneering work of Luigi Galvani $(1737-1798)$ when it was began to sense that electricity was a phenomenon that occurred in living tissues.

In 1783, Luigi Galvani dissected a frog on a tabletop where he had previously

been performing experiments involving static electricity. When his assistant touched an exposed sciatic nerve on the frog leg with a metal scalpel, the dead frog leg moved. Allesandro Volta then demonstrated that muscle twitching was also possible through his *Voltaic cell* and argued that the basis for the observed "animation" was not bioelectricity, but metallic electricity.

Many bioelectrical phenomena were being observed by an always increasing number of scientists (Mateuci, Emil du Bois-Reymond etc) but the first investigator to study EMG signals would not appear until 1912 in Germany, when H. Piper made the first measurements with a string galvanometer [17]. In 1924 Gasser and Erlanger did similar investigations with an oscilloscope. In 1928 Proebster observed signals generated by denervated muscles and opened the field of clinical EMG. With the passing of the years and thank to the Vacuum tube amplifiers and, later, solid state circuits, quantitative analysis of the Motor unit action potential (see Subsection 1.3.1) were introduced. Big contributions were made with publications such as Muscles Alive **??** and by important researches like De Luca. In 1964, Willson [17] introduces the amplitude analysis of EMG signals.

With the founding of the International Society of Electromyography and Kinesiology in 1966, the electromyography field was strongly promoted. Between the 70s and 90s there was a multitude of contradictory EMG publications creating confusion among the researchers. And because of that, the Surface EMG for Noninvasive Assessment of Muscles was founded in 1996: to seek consensus and collaboration between different European laboratories active in this area.

But the history of the actual interpretation techniques and applications of surface EMG would have been very different without the technical support that developed in parallel. Many prototypes and devices enabled the evolving from the DISA A/S (Denmark) 13A67 model, a 1950 cutting-edge three channel EMG system, to the newest wireless active sensors commercially available: in the early 1960s, Medelec Ltd. (UK) and DISA introduced transistorized EMG systems that were developed on printed circuit boards. Then, digital models began to appear (DISA 1500, MS6from Medelec) and with the microprocessor and PCs new complex EMG systems arrived, wireless, handheld etc. An example of a typical handheld EMG system is the MYOTRAC INFINITI introduced in 2003 (Thought Technology Ltd). This unit is a dual channel, handheld portable EMG device with three distinct operating modalities: Surface Electromyography (SEMG), Neuromuscular Electro-stimulation (NMES) and SEMG-triggered Stimulation (ETS).

Nevertheless, one common thing to all EMG systems, wired or wireless, multichannel or not, PC based is that they need an analog input stage: a front end amplifier, some filtering and conditioning before digitalization; and the main characteristics of these configurations will be discussed in the next chapters through the design of an EMG system prototype.

1.4 Electronics review

After the theoretical background about EMG signals, EMG measurements, and its importance, is convenient to do an electronics review. Key concepts relative to the design and construction of the EMG acquisition system prototype are going to be explained in order to give the reader the necessary tools for a full understanding of this document. Theoretical aspects involved in the design process, as noise and interference picking up, differential measuring etc will be covered; and practical considerations in the construction stage will be clarified (OPAM important parameters, AC and DC coupling, impedance restrictions etc).

1.4.1 Noise

Noise can be basically defined as "any unwanted disturbance that obscures or interferes with a desired signal" [18], in other words, everything that is not part of the signal wanted to be measured is considered *noise*. However, a differentiation can be made between *disturbances or interferences* and the word *noise*. Disturbances often come from sources external to the circuit under study, and result from electromagnetic or electrostatic coupling with the power lines, fluorescent lights, cellphones, cross talk between adjacent circuits, even mechanical vibration could also cause disturbances. Most of these types of disturbances and possible sources of interference are "man made" and can be minimized or eliminated.

On the other hand, the *noise* is a random signal, with random amplitude and phase components, and although a long term RMS value can be measured, is impossible to predict its instant values. Noise is the result of spontaneous fluctuations [4] in the materials from which the electrical systems are made [18] , and it is impossible to be completely eliminated, it just can be manipulated.

In 1928 Johnson [9] showed that electrical noise [5] was a significant problem when designing sensitive circuits, as sensitive amplifiers or sensors, because of the *noise floor*, which is the noise level when all input sources are turned off and the output properly terminated, [14] often determines the limit resolution of a sensor. In fact, the dynamic range of the EMG acquisition system, as for any other system, is determined by noise, because the smallest detectable level is set by it.

[4] "The term spontaneous fluctuations, although, perhaps, theoretically the most appropriate, is not commonly used in practice; usually it is simply called noise". Aldert van der Ziel

[5] "Statistical fluctuation of electric charge exists in all conductors, producing random variation of potential between the ends of the conductor. The electric charges in a conductor are found to be in a state of thermal agitation, in thermodynamic equilibrium with the heat motion of the atoms of the conductor. The manifestation of the phenomenon is a fluctuation of potential difference between the terminals of the conductor. J.B. Johnson"

Types of Noise

There are three main types of noise mechanisms which are *Thermal Noise*, *low-frequency or flicker noise* and *shot noise*, being the first of them the most often encountered. Though burst noise and avalanche noise are normally not problems are mentioned as well to give the reader a more complete view of the noise nature.

- **Shot Noise**

  This type of noise is common in diodes, transistors and other electronic devices with "potential barriers", as PN junctions. Shot noise is the result of the random potential barrier crossing by the charge carriers in these types of devices, which do not flow in a smooth or continuous way, but as the effect of the sum of a large number of randomly independent current pulses (off course, with an average value equal to the I instantaneous current flowing through the device).

  Shot noise has a uniform power density and is independent of the temperature. The equation 3.1 shows the RMS value of the shot noise current.

$$I_{sh} = \sqrt{2qI_{DC}\Delta f} \tag{1.1}$$

Where $q = 1.59 \times 10^{-}19C$ is the charge of a single electron, I_DC is the direct current in Amperes and Δf is the bandwidth in Hz.

- **Thermal Noise** Thermal noise is caused by a random vibration resulting of thermal excitation of the charge carriers in a conductor (holes or electrons). This type of carrier motion is similar to the Brownian motion of particles, and in fact, was predicted from studies in this field. It was first observed by J.B. Johnson of Bell Telephone Laboratories in 1927, and a theoretical analysis was provided by H. Nyquist in 1928 [18]. In every conductor above the absolute zero, the electrons are in constant random motion, vibrating according to the temperature; each electron has a charge of $1.59 \times 10^{-}19$ C, so there are many little currents along the conductive material, and although the average current is zero, instantaneously this current fluctuations produce a voltage across the conductor. This noise is present in all passive components, and is independent of the current flow, and it is important to observe that pure reactive components do not generate thermal noise (also known as white noise because it has a uniform power density, which means that there is equal noise power in each hertz of bandwidth).

  This type of noise is modeled by a voltage generator in series or a current generator in parallel to the noisy element. The average mean square value of

the model voltage source, for example, is calculated as in the equation 1.2. $k = 1.38 \times 10^{-}23$ J/K is the Boltzmann's constant, T is the temperature of the conductor in degrees Kelvin, R is the resistance of the conductor in ohms, and df is differential frequency.

$$e^2 = \int 4kTRdf \tag{1.2}$$

Although equation 1.2 will be very useful when deriving the noise voltage and current model for noise analysis, is easier to remember that $1K\Omega$ resistor will produce $4nv$ of noise per each Hz of bandwidth and take advantage of the proportionality of thermal noise to the bandwidth, when doing noise calculations.

- **Low-frequency Noise** This type of noise was first observed in vacuum tubes and was called *flicker effect* because of the flickering observed in the plate current. Is also called "pink noise", but no matter how it is called, the characteristic is always the same: its spectral density increases without limit as frequency decreases. Flicker noise is present in all active devices, from transistors, diodes and resistors, to even membrane potential in biological systems [18]. In the equation 1.3 are presented the expressions for average mean-square voltage and current values. K_e and K_i are constants relative to each device, f is frequency, and df is differential frequency.

$$e^2 = \int \frac{K_e^2}{f} df \quad i^2 = \int \frac{K_i^2}{f} df \tag{1.3}$$

- **Burst Noise** Also known as "popcorn" because the sound it produces when played through a speaker at frequencies lower than $100Hz$. This noise seems to be related to imperfections in semiconductors but it can be minimized with optimal components choosing.

- **Avalanche Noise** Avalanche noise is a typically associated to Zener diodes and is created when a pn junction is operated in the reverse breakdown mode. When the junctions depletion region is reverse biased with a strong electric field, electrons acquire enough kinetic energy that, when they collide with the atoms of the crystal lattice, create additional electron-hole. These collisions are seen as a series of large spikes. [14]

Noise Units and Noise Voltage Addition

- In components datasheets or in literature, noise is often specified as a RMS volts or RMS amps per root Hertz. This means that for actual noise calculations, a bandwidth is *always* needed. From the five types of noise seen in

1.4.1, the first three are the most important (because are unavoidable); and from those three, two are bandwidth proportional and the other one (the flicker noise) is proportional to $1/f$. This frequency dependence is the reason why is not the same to calculate the noise in a system of $2MHz$ bandwidth than to calculate it in a $1KHz$ bandwidth system. Systems with larger bandwidths tend to be noisier than narrow bandwidth ones, and that is something to have in mind when selecting a suitable frequency response.

With a defined frequency band and a noise specification, in $nV/\sqrt{Hz}$, for example, other interesting indicators as equivalent input noise (E_{in}) and signal-to-noise ratio (SNR) can be calculated.

- Adding noise voltages is equivalent to summing up a very large number of component frequencies with a totally random distribution of phases and amplitudes, and therefore a RMS summation is used to found a resulting RMS voltage amplitude. When separate independent noise generators are series connected, *the output power is the sum of the separate output powers, and consequently it is valid to combine such sources so that the resultant mean square voltage is the sum of the mean square voltages of the individual generators.* A problem arises when the voltage noise sources are not fully independent. In this case a correlation factor must be included. Equations 1.4 and 1.5 illustrate how to sum the voltage noise sources (see Figure 1.7) in the special case that they are independent from each other, and in the general case when they are correlated by means of the correlation coefficient C. Assuming $-1 \leq C \leq 1$.

$$V = \sqrt{E_1^2 + E_2^2} \tag{1.4}$$

$$V = \sqrt{E_1^2 + E_2^2 + 2CE_1E_2} \tag{1.5}$$

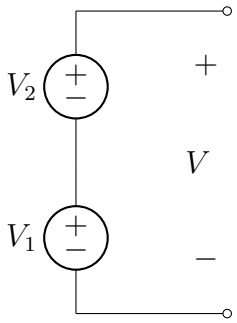

Figure 1.7. Addition of two voltage sources.

The Corner Frequency

In order to determine the noise in an Operational Amplifier is mandatory to know how to read the equivalent input noise vs frequency graphs that come in the datasheets. This graphs are divided into regions: the pink noise in the lower frequencies region, and the white noise which affects the higher frequency regions. The Figure 1.8 shows the Input referred noise vs frequency graph of the INA114 of Texas Instruments. It can be seen that the curves are not only frequency dependant, but *gain* dependant. The red circle spots the *Corner frequency*, which refers to the point in the frequency spectrum where $1/f$ noise and white noise are equal [14]. If that occurs at f_c frequency, then f_c is the corner frequency of the amplifier at the specified gain.

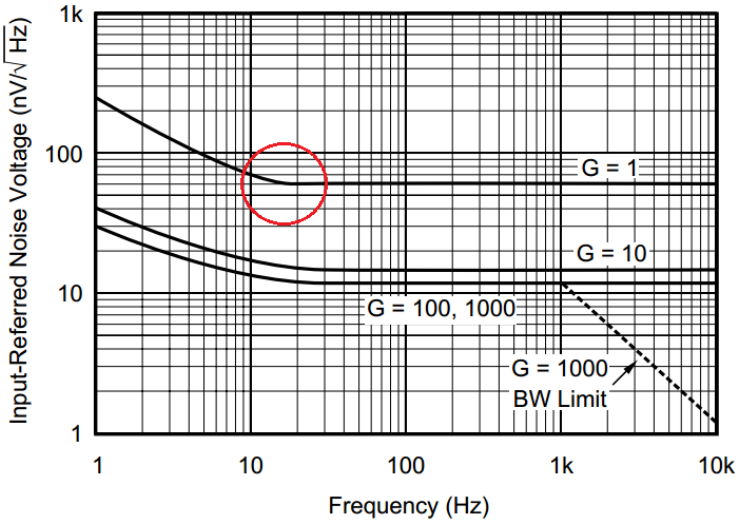

Figure 1.8. Input referred noise voltage vs Frequency graph. Adapted from Texas Instruments INA 114 datasheet.

The corner frequency is an important parameter because if it is present in the system bandwidth of operation, the two noises (white and pink) must be combined to obtain a complete noise equivalent. On the other hand, if the frequency band of operation of the circuit is below f_c, just pink noise is considered in the calculations as a contribution to the equivalent noise. Similarly, if the bandwidth is very large and extends to three decades or so above f_c [14], the $1/f$ noise contribution can be ignored.

Putting all together, when doing noise analysis in an Operational Amplifier there are three things to be calculated: the resistor noise, the voltage noise and the current noise (representing the most important types of noise presented above. See Subsection 1.4.1). The first one can be calculated with the $1K\Omega \rightarrow 4nV$ rule. The current noise must be written as a voltage noise in order to combine it with the other noises. The last noise (voltage noise) can be read directly from the datasheet,

(usually when dealing with *instrumentation* amplifiers two voltage noises are given: one referred to the output, which is gain dependant, and one referred to the input. Both have to be considered). Finally everything is combined following the equation 1.4, if fully noise sources independence is assumed.

1.4.2 Operational Amplifiers

Operational Amplifiers are among the most widely used electronic devices today, they are the core unit of many analog applications and the prototype discussed in this thesis is not the exception. The ideal Op-amp model is very diffuse and allows quick startup in the early stages of a circuit design process. The main properties of the mentioned model are listed below:

- Infinite bandwidth
- Infinite input impedance
- Zero input offset voltage
- Zero input current
- Zero output impedance
- Zero noise
- Infinite Common mode rejection ratio
- Infinite Power supply rejection ratio

And although is very useful as a first step to get into the design process, the real characteristics have to be clear in order to get a functional prototype "out of the paper". That is why in this section, a quick review of some Operational Amplifier concepts will be presented. In addition, the most relevant datasheet parameters for the design and construction of the EMG system are going to be further explained, because *to successfully apply any electronic component, a good understanding of its specifications is required. That is to say, the numbers contained in a data sheet are of little value if the user does not have a clear picture of what each specification means* [12].

Differential and Common mode signals

A differential signal is simply the difference between two signals, they are the best option to transmit information to one point to another because of their high immunity to external interference and noise. On the other hand, when single ended signal transmission takes place, both sender and receiver shares a common ground potential which with the signal is compared; making the interferences with the common ground obscure the signal of interest.

In other words, in a differential transmission or measurement the useful information *is* the difference between the signals and not between one signal's end and the common ground of the sense or receiving circuit. Usually, where there is a differential signal, there is also a common mode overlapped to it, produced for example by, parasitic coupling between the differential signal and a common ground point. This overlapped signal is called the *common mode*, and is undesirable in measurements because it does not contain any information of interest. What is more, it worsens the sensing process.

A differential signal has the form of the Equation 1.6, meanwhile Equation 1.7 shows the common mode one.

$$V_{diff} = V_p - V_n \tag{1.6}$$

$$V_{common} = \frac{V_p + V_n}{2} \tag{1.7}$$

When measuring biopotentials, an amplification stage is mandatory to get the low level signals into a suitable voltage level (see Chapter 2). The Figure 1.9 shows both differential and common mode voltages applied to an Op-amp input.

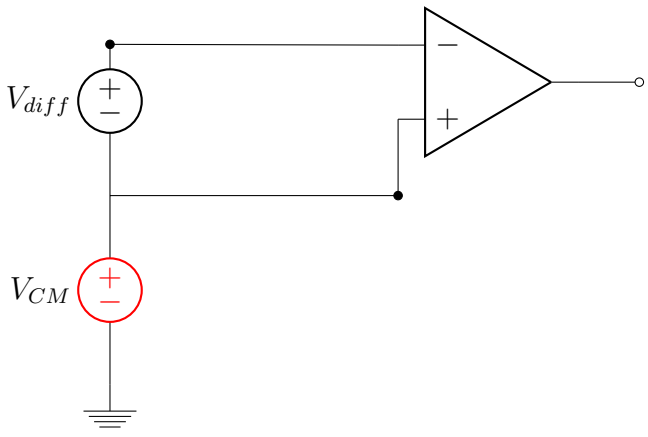

Figure 1.9. Op-amp amplifying differential and common mode

In the ideal model of the Op-Amp, the amplifier should provide infinite rejection against the V_{CM} voltage; in reality the CMRR is not infinite but is very large ($> 100db$, usually). However this value could be meaningless if the designer does not take into account phenomena like the Common to differential mode conversion. (See Subsection 2.1.1). So in order to do good differential measurements, the balance of the differential amplifier inputs paths must be as accurate as possible.

The instrumentation amplifier

In-amps (instrumentation amplifiers) are used in many applications, from motor control to data acquisition to automotive. An instrumentation amplifier is a closed-loop gain block that has a differential input and a single ended output (with respect to a reference terminal). Usually, the impedances of the two input terminals are balanced and have high values. The input bias currents (see Subsection 1.4.2) use to be low, typically 1nA to 50nA, or exceptionally low as 3fA like the LMP7721 of Texas Instruments[6]. As with op amps, output impedance is very low, especially at low frequencies.[12] The gain of these devices is set by only one resistor, if it is not preset internally, which is isolated from the terminal inputs.

Although Op-amps, differential amplifiers, and In-amps provide common mode rejection, Op-amps are not designed to prevent the common mode signal from appearing in the output. In typical configurations, like the one shown in the Figure 1.10, op-amps process common mode signals, passing them to the output, but do not reject them.

For example, if the only input connected to an operational amplifier is a common mode voltage signal (as in Figure 1.10), the voltage output will reflect this common mode. The explanation is simple: the common voltage in the non inverting input, forces the inverting input terminal to be at its same potential (in this case, the common mode potential of the voltage source). This forced potential will be amplified by the resistors net to finally appear at the output terminal.

From Op-amp model:

$$\mathrm{V}_{-} = V_{+}$$

then

$$\begin{aligned} \mathrm{V}_{out} - V_{-} &= I_x R_2 \\ \mathrm{V}_{-} - V_{CM} &= I_x R_1 \end{aligned}$$

but

[6] From LMP7721 datasheet, available in Texas Instruments site with the literature number SNOSAW6B

$$V_{-} = V_{CM}$$

which means that

$$\mathrm{I}_x = 0$$

and finally,

$$\mathrm{V}_{out} = V_{CM}$$

Even Though the common mode voltage does not get amplified, is not totally rejected, and in presence of large common mode voltages, the system could be easily saturated.

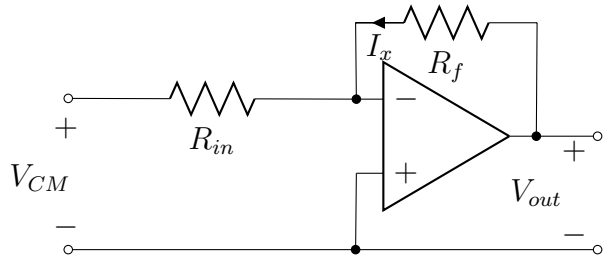

Figure 1.10. Typical Op-Amp configuration with Common mode input

The In-Amps are the best choice when extracting weak signals because, as it has been said before, they only amplify the difference between the two input terminals while reject any common signals to both. The Figure 1.11 shows a classical instrumentation amplifier with a $10mV$ peak to peak differential signal and a common mode signal CMV. The configuration and values of the resistors make the output of the *buffering* amplifiers be equal to one-half the peak to peak input voltage $\times 1000$, plus any common mode voltage that is present on the inputs (the common-mode voltage will pass through at unity gain regardless of the differential gain).[12]. Splitting the *gain resistor* R_G (see Figure 1.11) into two equal resistors of value $\frac{R_G}{2}$ creates a node in between, which allows the designer to pick up the common mode signal CMV and use it, for example, in feedback loops to achieve additional common mode rejection like in the *body driven potentials*. This is what actually will be used in the *DRL* block to get larger common mode interference reduction in the measurement. See 3

The equations for an instrumentation amplifier can be easily derived splitting the device in two parts: the input buffering stage, and the differential amplifier stage. In the first part, the difference between the signals present in the inverting and

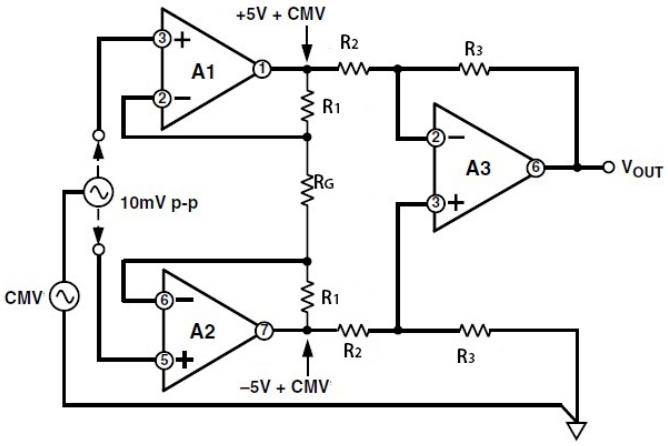

Figure 1.11. Classical Instrumentation amplifier. Adapted from [12]

noninverting inputs, is amplified by a gain factor G, while the common mode appears *without* amplification in the output. The second stage is a differential amplifier which only amplifies the difference (in practice the common mode is amplified by really small the common mode gain A_cm) between the outputs of both previous buffering stages. Equation 1.8 express the instrumentation amplifier gain in function of the network resistors.

First

$$\mathrm{V}_{in} = 10mVV_{pp} + CMV$$

Applying the ideal model of Op Amps, the final result is

$$\frac{V_{out}}{V_{in}} = (1 + 2\frac{R_1}{R_{gain}})\frac{R_3}{R_2} (1.8)$$

Concepts applicable to operational amplifiers like gain bandwidth product, input bias current, voltage offset etc. are also valid when talking about instrumentation amplifiers, and a quick review of them is presented in the following paragraphs.

Gain Bandwidth product

Is one of the typical five parameters relating to frequency characteristics of an operational amplifier, being the others the *unity gain bandwidth*, the *gain bandwidth product*, *phase margin at unity gain*, the *gain margin* and *maximum output-swing bandwidth*. This parameter express that the gain of the amplifier is not independent of its operation frequency; the higher the gain, the lower the bandwidth at which

it operates (See Figure[7] 1.12). For voltage feedback amplifiers the *Gain Bandwidth product* (GBW) is constant: $GBW = G \times f$.

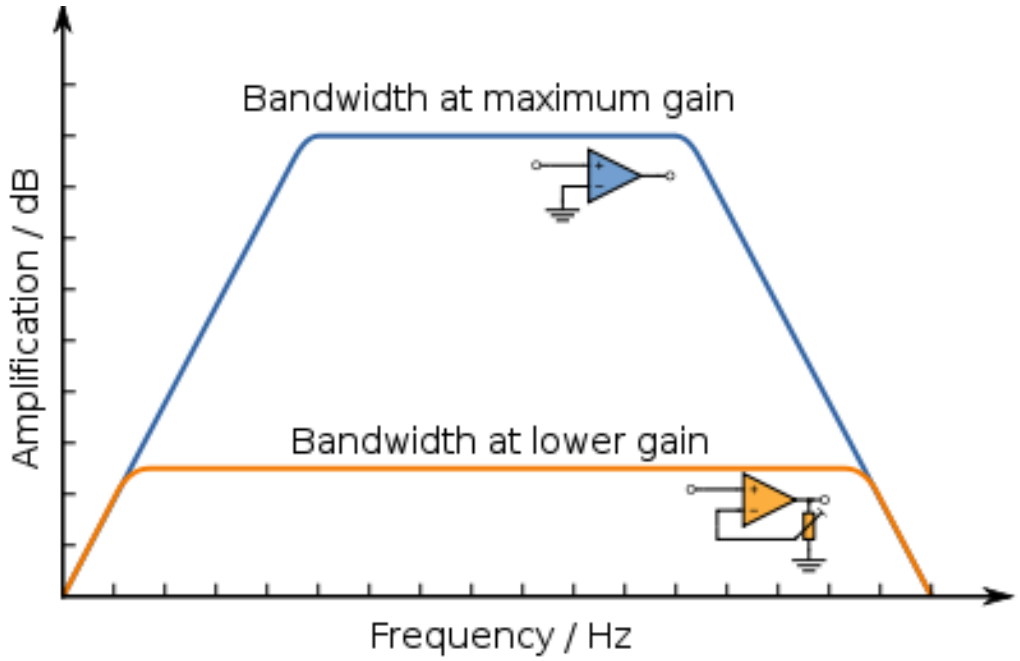

Figure 1.12. Amplifier GBW. The GBW remains constant in both high and low gain configurations, because of that, lowering the gain increases the bandwidth, which is what happens when connecting the Op Amp in some voltage feedback configuration. Adapted from *http : //en.wikipedia.org*

Input impedance

In the ideal Op amp model the input impedance is infinite, but in real Op amps is not. The input impedance is a really high finite number, and the order of magnitude of its value varies depending the application in which the amplifier is needed. Audio amplifiers, for example, usually have lower input impedances than other Op amps thanks to the low impedances found in audio applications.

In order to measure something, some part of the energy of the system under study must be taken by the sensor. If this "stolen" energy is considerable high with respect to the total energy of the measured system, the sensor acts as a load to the system, changing its configuration and characteristics. That is why a high input impedance is required to measure voltage in a circuit: to avoid loading the system

[7] Adapted from $http : //it.wikipedia.org/wiki/Prodotto_guadagno - larghezza_di_banda$

and change its configuration; in other words a high input impedance device does not allow significatively current flow into it, preserving the system energy as if no measuring were taking place.

This parameter is found in datasheets as a resistor value in parallel with a capacitive value (the input capacitance of the Op amp). For EMG measuring, devices with input impedance lower than $100M\omega$ are not recommended as input stages for EMG amplifiers [16].

Common Mode Rejection Ratio

The concept of differential and common mode signal has been introduced in Subsection 1.4.2, therefore is already clear that the common mode must be rejected as much as possible in the front-end stages of the EMG measuring system. The parameter quantifying how well a device rejects the common mode, is called the Common Mode Rejection Ratio and is given by the expression 1.9

$$CMRR = 20Log(\frac{A_d}{|A_{CM}|}) \tag{1.9}$$

The CMRR is a DC parameter defined as the ratio of the differential voltage amplification A_d and the common mode voltage amplification A_{CM}. As A_d falls with frequency, the CMRR does it too.

Bias Current

As seen before in the explanation of the input impedance, an Op Amp input impedance must be high enough to avoid loading of the source, and because its high values (easily found between 10^7 and 10^12), the Op amp ideal model assumes no current flow into the device. But the operational amplifiers need a DC operation intimately linked to the *input bias current*.

The input bias current is a current that actually flows into the amplifier to bias all its internal transistors, and it is really important to provide a DC path to this current flow. An amplifier without this path cannot work properly. Not providing a proper way to DC ground is a common error in design, three examples of it are shown in the figure 1.13.

1.4.3 Filters

A filter is a device that passes electric signals at certain frequencies or frequency ranges while preventing the passage of others. [14] These devices are used in many

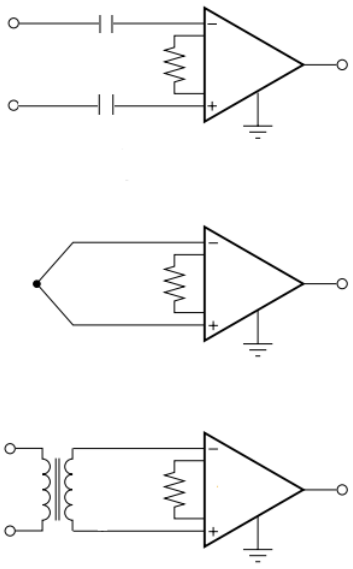

Figure 1.13. Three different configurations with no bias path are shown. The first figure shows a badly AC coupled Op amp. This arrangement can function "without" problem until the capacitor fills, then the DC path for the input bias current breaks and the Op amp does not work properly any more. The second and third image shows an example in which the loop created in the amplifier inputs does not allow a path to DC ground.

engineering fields, from telecommunication to systems power supplies, in many types, ranges and configurations. In digital data acquisition systems, *antialiasing* filters are always required to ensure optimal sampling, but are also used in other stages for conditioning signals, for example selecting the frequency band in which the useful information is.

There are many types of filters and are classified depending of the function they perform: phase shift, notch filters, low pass, high pass, band pass etc. Another classification is made depending of the type of components used in their construction: passive or active filters. Passive filters consist of resistors, capacitors and inductors and therefore are also known as RCL filters. Usually are used at frequencies in the range of Megahertz or higher. On the other hand, active filters are constructed with Operational amplifiers, resistors and capacitors, and are very common at frequencies until $1MHz$.

A quick riview behind the active low pass and high pass (band pass is just the union of one low pass and one high pass filter) will be presented below.

- **Low Pass** A low pass filter is a filter configuration which, ideally, allows frequencies under some *cutoff* frequency to propagate, while blocking the frequencies higher than it. It means that there are two zones: pass-band and

rejection band. But in practice, such filter does not exist.

A real low pass filter has three regions:

- Passband
- Transition band
- Stop band

The Figure 1.14 shows the gain of three low pass filters vs the normalized frequency[8].

Usually filters are composed of smaller filtering units of first or second *order*. The order of the filter is the number of poles (in the case of a low pass filter) of the filter equation (see the equation of a general n^{th} order filter 1.10), and is a parameter which express how fast the transition between the passband and the stopband is. High orders translate in shorter transition bands but also in more components and stages in the filter.

$$G(s) = \frac{G_0}{\prod_i (1 + \alpha_i s) \prod_j (1 + \alpha_j s + b_j s^2)} \tag{1.10}$$

Changing the parameters of the complex poles in the equation 1.10, three major types of second order filters can be obtained:

- *Butterworth* which gives a maximum passband flatness
- *Tschebyscheff* which gives a sharp transition between the passband and the stopband
- *Bessel* which gives a linear phase

Two configurations are available to choose when a second order filter must be designed: Sallen key and Multiple feedback topology. The *Sallen Key* topology is shown in the Figure 1.15.

[8]The normalized frequency is the frequency divided the filter cutoff frequency

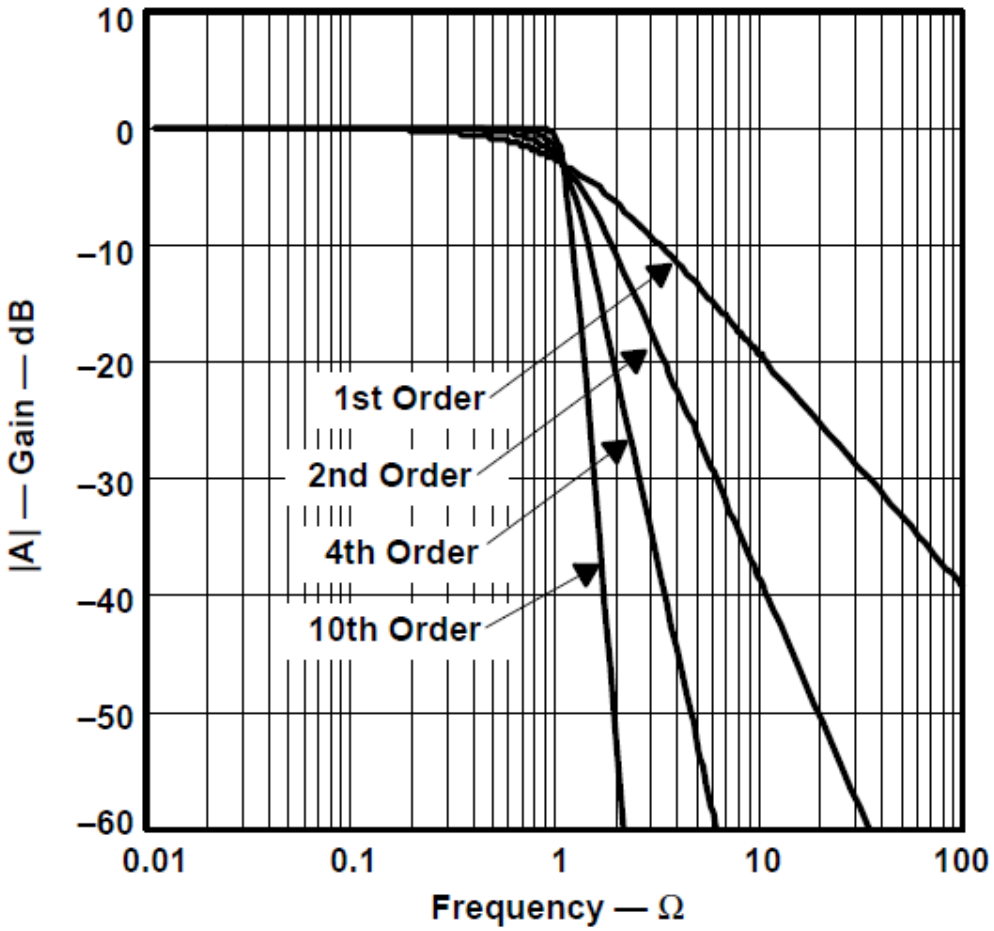

Figure 1.14. Three low pass filters of different orders. The higher the order the higher the slope of the curve and the shorter the transition band. Adapted from [14]

- **High pass filter** All the concepts of the low pass filters are applicable to the high pass filters. Its design process is really easy because is the same followed for the low pass filters, with the only additional step of interchange the components at the end: resistors per capacitors and viceversa. The Figure 1.16 illustrates the "mirroring" effect between low pass and high pass filters.

1.4.4 Analog to digital conversion

In order to transmit, process, store and display information of the world in a digital form, an analog to digital conversion must be done. Signals like temperature, velocity, force, and obviously EMG, have analog nature and need to be sampled to

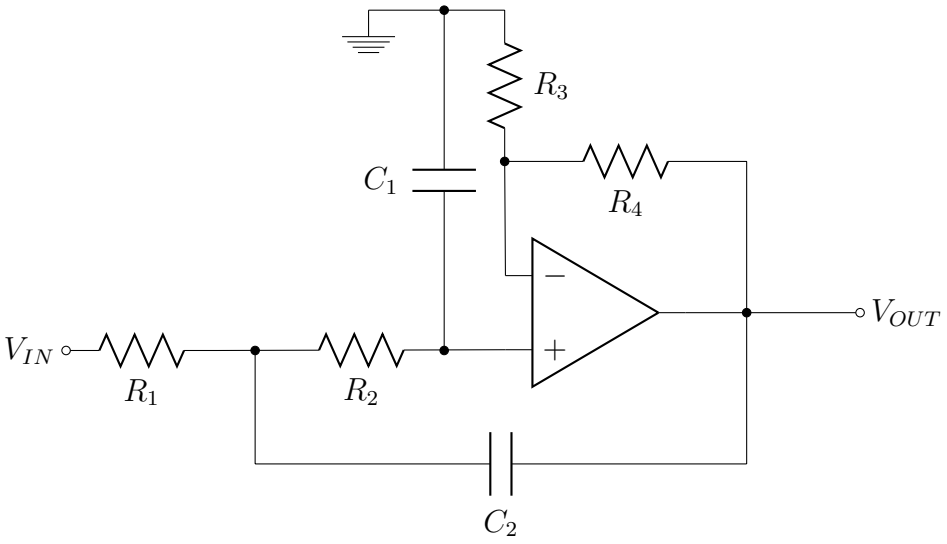

Figure 1.15. General second order low pass Sallen Key Topology. The transfer function of this configuration is: $A(s) = \frac{A_0}{1+\omega_c[C_1(R_1+R_2)s+\omega_c^2 R_1 R_2 C_1 C_2 s^2]}$ where ω_c is the desired cutoff frequency.

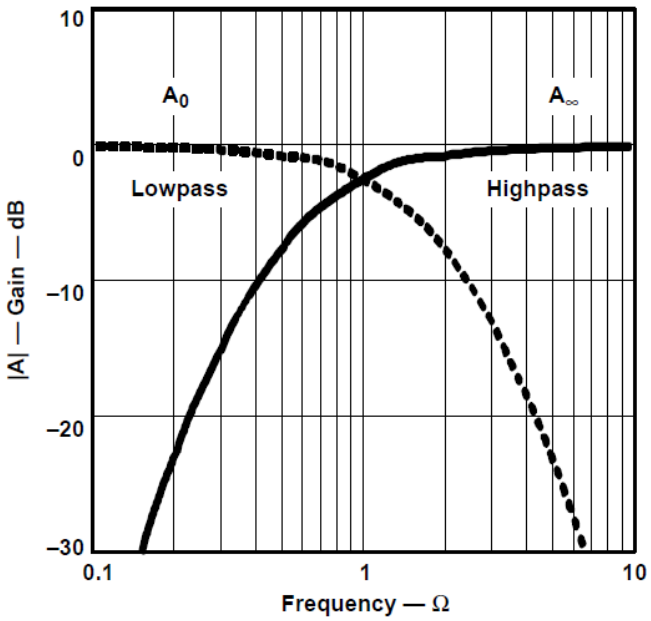

Figure 1.16. Mirror effect between low pass and high pass filters. The cutoff frequency for both is the same, if the places of capacitors and resistors in the low pass filter are interchanged. Adapted from [14]

get a discrete representation of them in computers and other digital systems. This process is carried out by a device called analog to digital converter.

There are many types of analog to digital converters, with different ways to obtain discrete equivalents of continuous signals but all of them share characteristics and limits as the following ones:

- **Sampling rate** The rate at which new single discrete values, representing the continuous signal being sampled, are created is called sampling rate or *sampling frequency*. This parameter express how many discrete values are created in a given time period by an ADC converter. Higher sampling rates means more samples per time per period, and more samples per period means major capability of capturing faster changes in given signal.

  The sampling rate has to be selected taking into account the fulfillment of the Nyquist-Shannon sampling theorem, which basically says that the sample frequency must be at least two times higher than the highest frequency sampled. If this theorem is not respected, aliasing will occur.

- **Aliasing** The aliasing effect causes that discrete form of two different continuous signals cannot be distinguished from each other. When this happens, the original signal is no longer reconstructible from its digital equivalent causing information losses and big problems in the rest of the system.

  Between two consecutive signal samples, there is an "information hole" because is impossible to know what values the analog signal takes. If the signal is slow it can be supposed that the analog values it takes between two sample times are similar to the previous and the actual sample, but if the signal is too fast compared with the sampling rate, it could take many different values between samples with the converter without noticing it. Figure 1.17 shows an aliasing example.[9]

  Aliasing must be avoided, and fortunately is simple to do it with *anti-aliasing filters*. Before the ADC conversion takes place, the signal must be passed through anti aliasing filters in order to block its high frequency components. Otherwise, they would be digitalized also, and its alias would be added as noise to the system.

- **Resolution** The resolution of an ADC converter is the number of discrete values that it can produce over the range of analog input values. ADC resolution limits the accuracy of a measurement. The higher the resolution (number of bits), the more accurate the measurement.

[9]Image adapted from *http://music.columbia.edu/cmc/musicandcomputers/chapter*2/02$_0$3.*php*

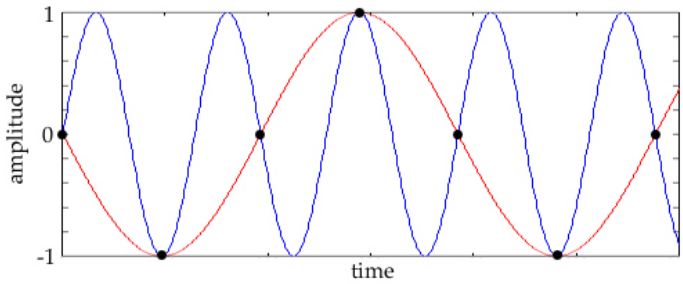

Figure 1.17. The high frequency signal (*blue*) has been undersampled. Thus is not possible to ensure if the digital representation (*black dots*) come from the high frequency signal, or from the red low frequency signal. The red signal is an *alias* of the blue signal.

An ADC converter of n bits will have 2^n different discrete levels to represent the analog signal, and because of that, for a given *dynamic range* of the input signal, more bits make higher the system accuracy. For example, a 8bit ADC converter will be able to produce 256 discrete levels, while a 12bit converter will produce 4096 levels. For an input with a dynamic range of $10V$ (from 0 to 10 volts), the 8bit ADC converter would not be capable of resolving voltage differences smaller than $39mV$ while the 12bit converter could resolve voltage differences as small as $2.4mV$.[10]

Resolution can also be defined as the minimum change in voltage input in order to make the output LSB change.

- **Simultaneous Sampling** When more than one analog channel has to be digitized at the same time, a simultaneous sampling is required. Is not as easy as it might seem because many options are commercially available.

  The two most common simultaneous sampling architectures are the *Simultaneous Sampling Architecture* and the *Simultaneous Sample and Hold (SSH)*. The simultaneous sample and hold is based in a multiplexer and only one ADC converter for all the channels. The multiplexer changes the input to the ADC converter guided by a frequency imposed by an external clock which must be selected accordingly to respect the sample and hold time of each sample. The delay time between samples can be minimized but the system limitation is given by the performance of the ADC/amplifier combination. This architecture can be used as simultaneous sampling if sample and hold circuitry is provided.

[10] http://www.ni.com/white-paper/3832/en

The SSH architecture has been popular for mid to high channel counts because of the low cost of having only one ADC unit, but in recent years with the decreasing cost of ADC converters, the Simultaneous Sampling Architecture is becoming very used.[11]

In Simultaneous Sampling Architecture one ADC converter unit per channel is provided, making a *really* simultaneous acquisition system. Normally this type of hardware costs more than the SSH, but it virtually eliminates the delay time between samples.

1.4.5 PCB Design

There is a big difference between *designing* a circuit and *constructing* a prototype of it because there are many practical considerations that need to be taken into account when passing from the paper to the copper. The PCB (*printed circuit board*) is another component of the circuit and it has to be considered for the design to be a success. The PCB must be designed such as its effect is transparent to the circuit.

Some of the aspects to take into account when designing a PCB are:

- **Materials** A table summarizing the different PCB materials is presented in 1.1

- **Number of layers** Selecting the number of layers for a design is critical. The first option is the single sided PCB, it has only one layer to place components and route and is extremely susceptible to radiated noise. Single sided PCBs are not usually recommended because of the many things that can go wrong, for example the big ground loops that are formed in absence of a common ground plane (more of the ground loops when describing the PCB construction in 4).

  The second option is the double sided pcb, which allows a second layer for tracing (although crossing traces is not recommended for analog circuitry, as it will be explained in the forthcoming paragraphs) or as a ground plane. It gives also more mechanical strength to the board.

  Multilayer boards are the best solution for a good quality PCB design for the reasons exposed in the chapter 4 of this document.

- **Tracing** How to do the PCB traces is very important for an optimal design. Length, width, angles and vias are key in reducing noise and undesired side effects as radiated noise. One of the most important nets to correctly trace is

[11] http://www.ni.com/white-paper/4105/entoc3

Grade Designation	Material
$FR-1$	Paper/phenolic
$FR2$	Paper/phenolic
$FR3$	Paper/epoxy
$FR4$	Glass cloth/epoxy
$FR5$	Glass cloth/epoxy
$G10$	Glass cloth/epoxy
$G11$	Glass cloth/epoxy

Table 1.1. Different types of PCB materials and its grade designation according to NEMA *(National Electrical Manufacturers Association)*. In typical low frequency, low temperature consumer applications $FR2$ or $FR3$ are good choices. Adapted from [14].

ground. A good grounding system is critical in the overall system performance and will be see in detail in the fourth chapter 4.

Chapter 2

EMG system: design specifications and functional blocks division

For being able to build up an EMG signal acquisition system, is not enough just to understand the physiological process whereby this type of signals are generated, nor the different techniques for their correct measurement (see Section 1.3); it is necessary to establish a performance profile which with evaluate the design's final behavior. In other words, a clear well defined objective is needed, that synthesize what is pursued with the system: type of measurement, bandwidth, maximum permitted error etc. Set up this kind of profile could be complex due to the many practical aspects that have to be taken into account during the *functional prototype* construction. Therefore, the customer requirements constitute the starting point for the development of the project, and plot the guidelines which lead the design process towards the attainment of the stated objectives.

In the case of the prototype developed for the present thesis, the customer was not very specific and required just the following:

- 16 bit output with the highest possible resolution
- At least 20 monopolar Channels
- Simultaneous sampling
- Patient Isolation

Along this chapter, the translation of the customer specifications into project restrictions will be done. The entire design will be divided into smaller and easier to define and debug blocks. Each block will be defined through an input In, an output Out and a name describing the function it does. The general structure is seen in the Figure 2.1.

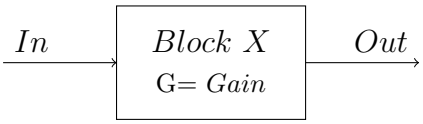

Figure 2.1. Generic functional block

It should be noted that the generality of the profile given by the customer, gave a lot of freedom in the design. The customer was interested only in the fulfillment of his specifications, and not in the typology nor the components used for that. Also a budget conditioning the system construction was not set.

2.1 System design implications

2.1.1 Signal model

The design started with the understanding of the type of signal wanted to process (sEMG[1]). Although in another chapter, the *physiological* nature of the EMG signal was explained, how it is generated and what characteristics presents (see 1.3.1), it is necessary characterize it form a *technical* point of view, for example establishing maximum amplitudes, offsets, bandwidths etc.

The input signal to the system (sEMG signal) was modelled as the combined effect of three parts: the differential EMG signal (signal of interest), the common mode interferences, and the electrodes offset (differential).

The EMG differential signal presents a maximum peak whose estimated value varies according to the author, for example: $2mV$ peak to peak [7], $5mV$ peak to peak [23], $6mV$ peak to peak [10], hence other authors characterize it as a peak of "a few mV_{RMS}" [16]. Choosing the maximum amplitude for the signal to be amplified model, is primordial to determine the system gain, which can't be so high because it would saturate the amplifiers, but neither so low because it could compromise the numerical resolution of the analog to digital conversion. Then, opting for a robust signal model, that contemplated variations above the highest maximum peak found in the literature [7], [23], [10], and that allowed a gain greater than $1000V/V$ and an output range, of the output signal compatible with the input range of the next stage; a $\pm 4mV$ maximum value for the input signal model was selected. The Figure 2.2

[1]sEMG refers specifically to the EMG signals picked up by superficial electrodes and not by other electrode types as, for example, needle ones. However the system prototype was initially conceived to work with superficial sensors and therefore sEMG and EMG terms are used indistinctly in this document to refer the electromyogram signals.

shows the time characterization of the *ideal* input sEMG signal.

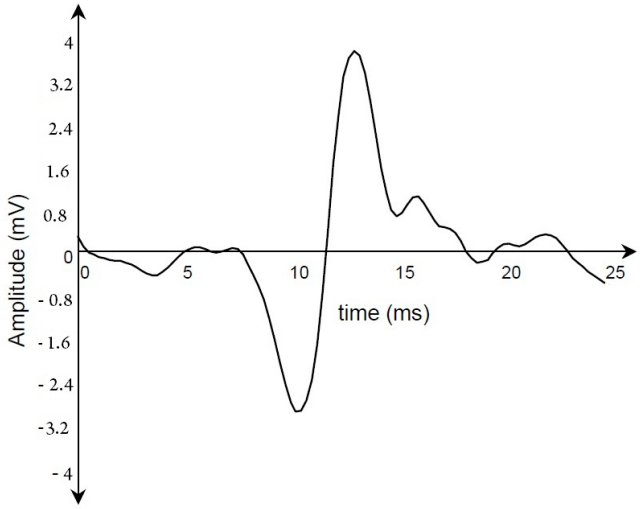

Figure 2.2. EMG *bipolar* model signal. Adapted from [7]

The same thing happened with the frequency band: each author defines it a little different from the rest(between 10 and 20Hz to between 500 and 1000Hz[7], $5Hz-2KHz$[23], $10Hz-500Hz$ [16]). But for this model parameter, the customer then fixed the upper cutoff frequency in $1KHz$, this because he wanted to see if there was some information in the range of $500Hz$ to $1Khz$, which is usually discarded by commercial EMG sensors. The frequency band was set in $10Hz-1KHz$ specting a power spectrum like the one shown in the Figure 2.3. The highlighted band is where the power line frequency is located ($50Hz$ or $60Hz$ depending on the country [2]), which is where the major common mode contribution, yields.

That is the other element present in the EMG system's raw input: the interference picked up by the human body from the power line, fluorescent lights etc. This EMI (electromagnetic interference) is coupled to the body through the skin and it is represented in the Figure 2.4. The capacitors C_2 and C_T represent the path between the body and the ac ground, C_{CB} is the capacitance coupling from the ac power supplies through the cables. C_B is the existing coupling between the ac ground and the isolated ground of the EMG system. This interference should be common to all electrodes, and if the Common Mode Rejection Ratio (CMRR) of the front-end amplifier were ideal (infinite), this common mode would be totally rejected. The problem is that the CMRR is not infinite (although it is expected to be very large) and that the common mode interference is converted to a differential mode signal,

[2] *http : //www.kropla.com/electric2.htm*

which is amplified by the system. That happens as the result of some mismatches in the signal's path impedances.

The third element present in the very input of the EMG system is a possible DC offset, "caused by factors involving skin impedance and the chemical reactions between the skin and the electrode and gel" [5]. As is reasonable to assume that every electrode-skin contact is different from the other, there will be differences in the DC offsets from an electrode pair input, creating a differential signal that would be amplified by the system. The problem is that the DC offsets signals can be greater than some hundred of millivolts ($> 300mV$, for example) [1], and therefore the differential signal could be large enough to saturate the system's amplifiers after being amplified. For further details on the electrode-skin model and the DC suppression see Section 3.

Summarizing, the signal entering the system can be splitted as shown in the Figure 2.5, from where is only interesting the signal labeled as EMG signal, the one containing the muscle electrical information.

With the system input signal model, and knowing what was the useful part of it, the design process continued taking care of implementing the actions to guarantee a clean and precise measurement of the, now fully described, EMG signal. The next step was the translation of the user specifications into design constraints.

From the requirements given by the user. The next restrictions were derived:

- **16 bit simultaneous ADC conversion**

  In order to get the analogic information relative to the EMG signal in a usable digital form, an ADC conversion had to be done. The choosing of the ADC converter depends on factors like the type of sampling and the expected resolution. The first parameter was already fixed as "simultaneous sampling" by the user. Based on the resolution of the ADC converter, two implementations were possible. The first one was with low-noise amplifiers and high gain, which allowed low resolution ADC, as long as the amplified noise did not become the dominant noise in the system. The second implementation alternative was with a lower gain but with higher resolution to allow an optimal representation of the Noise-free dynamic range.

  When a larger noise is present in the system, high resolution is worthless because many of the LSB become useless information (digitized noise); on the other hand, when low noise is present, the danger of losing many LSB representing the noise, decreases; making the high resolution implementation, a good choice for this types of cases, with such a few noise presence.

  The indications given by the user solved the dilemma: he had already asked for a 16 bit output, which is not considered high resolution, making the low noise - high gain option the most appropriate.

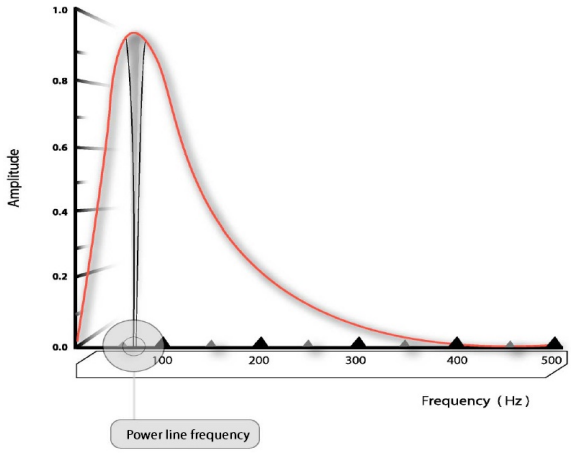

Figure 2.3. Schematic representation of a typical sEMG power spectrum. Adapted from [5]

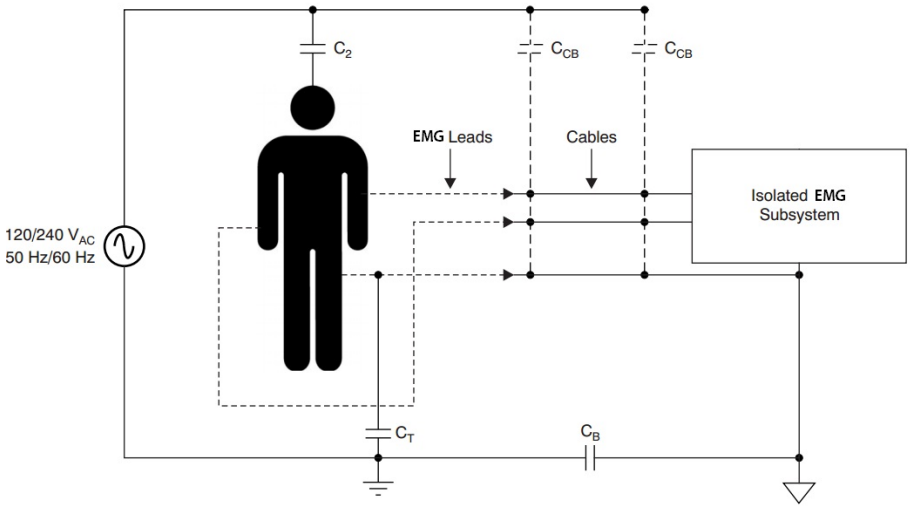

Figure 2.4. Typical EMG common mode parasitics. Adapted from [1]

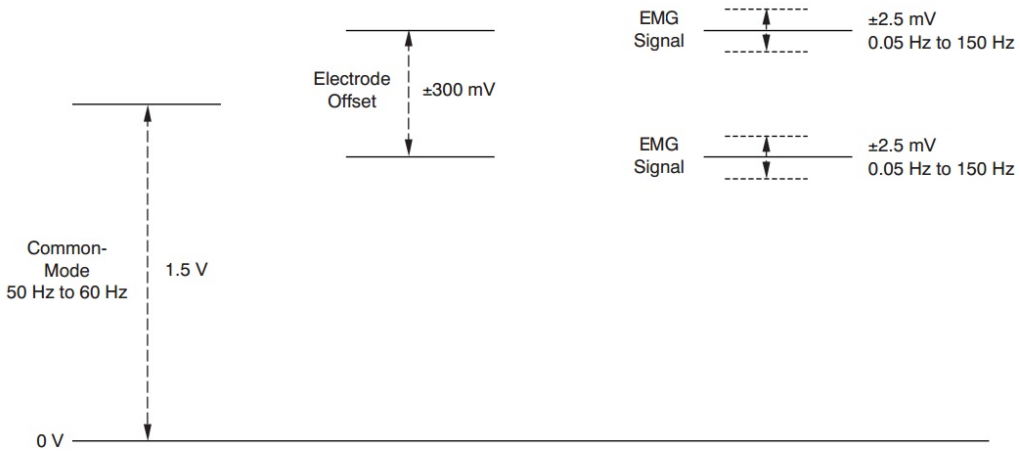

Figure 2.5. EMG system raw input signal composition. Adapted from [24]

- **Reference electrode** It's an electrode providing a point against which to measure the rest of the electrodes. Given that the measurement was wanted to be monopolar and not differential (further details in 3), the generic x electrode had to be compared to some reference. The reference could have been chosen in many ways, depending on the monopolar detection technique to implement. Was envisaged to use the *virtual reference technique*, which is a method consisting in the detection of each channel with respect to the average of all the other channels, assuming they are affected by the same interference [15]. This method is based on the fact that the line integral of the EMG potential over its entire support in the fiber direction, as well as the integral of the EMG on a surface that covers the entire spatial support of the potential generated by the active sources, is zero citereferenceE. But this approximation is only valid for an electrode array large enough to cover the entire active sources generating the signals. This condition is difficult to verify in practical EMG recordings, thereby, the application of the virtual reference technique may lead to filtering effects modifying the EMG signals shape [15].

  At the end, an additional electrode as reference was implemented an in order to avoid the circuit asking high currents to the human body through the mentioned reference electrode, a buffer was thought to be placed in between; in such a way the current was provided by the amplifier without loading the body. The buffer only makes sense because the projected system was a high channel system (32 channels), and each of those channels were going to be draining current from the body, situation that had to be avoided.

- **High CMRR** In 2.1.1 it has been showed that one of the raw EMG components is a common mode signal. This signal has to be rejected by the system,

otherwise it will saturate the front end amplifier. Ideally, the operational amplifier (OPAM) has an infinite CMRR (see Subsection 1.4.2), but in practice is, although large (usually $> 100dB$), a finite quantity. But to avoid the effects of common mode in the system is not enough to have high CMRR, because of the common mode to differential mode conversion has to be also taken into account.

This critical and almost unavoidable effect when constructing biopotentials acquisition systems, for example; is the result of mismatching impedances on the inputs of the front-end amplifier.

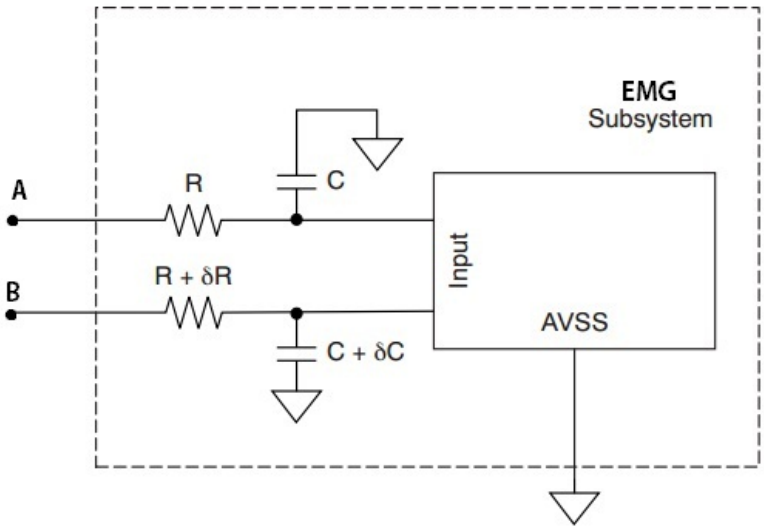

Figure 2.6. System input impedances mismatches. Adapted from [1]

When $\delta R = 0$ and $\delta C = 0$, the common mode present in A and B passes equal paths with equal impedances, making the voltage in the non inverting input just the same as the voltage in the inverting one.

In the case of mismatches (represented as δR and δC) the equation 2.1 defines the common to differential mode conversion. Z_i is the input impedance of the front-end amplifier, Z_a and Z_b are the complessive impedances in the A and B paths, respectively. V_{CM} is the common mode voltage and V_d is the resulting differential voltage. In order to apply the equation 2.1, $Z_i >> Z_a$ and $Z_i >> Z_b$ need to be assumed.

$$V_d \approx V_{CM} \frac{Z_a - Z_b}{Z_i} \tag{2.1}$$

The voltage V_d is now seen as a differential signal, and amplified by the system

differential gain. Since the common mode voltage, may be of the order of a few volts while the signal to be amplified may be up to 6 orders of magnitude smaller, the reduction of the undesired voltage V_d (generated by V_{CM}) is very important [15]. The selected strategy to minimize V_d and increment the system CMRR, will be explained in detail in the Section 3.

- **Driven shielded cables** To avoid the effect of parasitic capacitances between the system and the power line, and to reduce the general noise, the cables between the electrodes and the EMG system circuitry had to be shielded. In Section 3 the shielding will be explained in more depth.

- **Isolation and ESD protection stages** In order to protect the patient connected to the EMG system from possible high currents, the system and the power line will be galvanically isolated. There is also necessary an electrostatic discharge protection stage (ESD) to protect the system from eventual electrostatic peaks transmitted from the patient body.

With the signal model and the constraints derived from the user, there is enough information to build up the system's block diagram showing the general configuration of the prototype.

2.1.2 Blocks Diagram

To conclude this chapter the whole system blocks diagram is presented in the Figure 2.1.2 with a compact block notation. This diagram will be recalled constantly in 3, when talking about each system piece in detail. However, at this time, the overall scope of the EMG multichannel acquisition system, should be clear to the reader. The general [20] and most important things to have in mind to fully understand the specific solutions exposed in the next chapter are listed below:

- **Gain** The circuitry has to be able to amplify the low voltage input signal (see Figure 2.2) to suitable levels for recording, displaying, processing, storage etc.

- **Frequency response** The system must select the frequencies to be amplified and attenuate the non interesting ones. The band is defined by two corner frequencies, in which the signal loses $3dB$ of amplitude (see Figure 2.3).

- **Common mode rejection** The human body acts like an antenna, picking up all kinds of electromagnetic radiation present in the environment (see Figure 2.4). To avoid that, the acquisition system must reject the interference that obscures the measures.

- **Noise and drift** The designed prototype has to avoid intrinsically adding additional unwanted signals that contaminate the EMG signal under measurements.

- **Input impedance** The input impedance of the system (which depends on many factors as the amplifier choice, the electrode-skin interface impedance etc) must be sufficiently high so as not to attenuate considerably the already low voltage EMG signal.

- **Electrode polarization** The front end amplifier must be able to deal with extremely weak signals in presence of dc polarization components, like the half-cell potential, resulting of the transduction of the muscle activity into voltage signals (see Figure 2.5).

- **Patient safety and circuit protection** Connecting a patient to an electrical circuit could be dangerous and safety must be guaranteed above all. Therefore isolation must be provided.

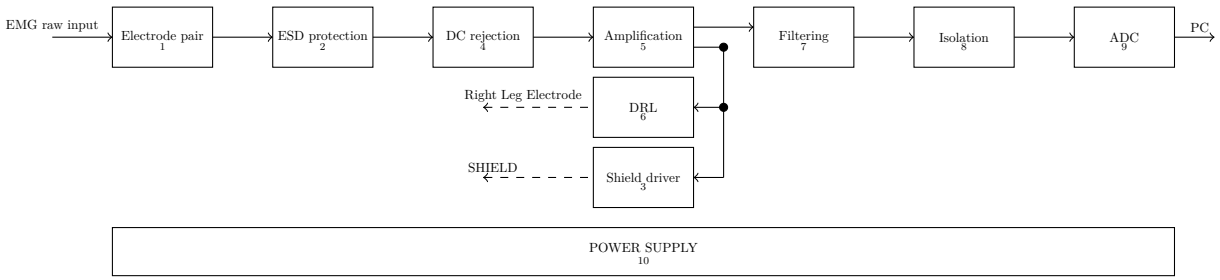

Chapter 3

Functional blocks

EMG signals measurement is the core part in many fields such as rehabilitation and sports medicine, ergonomics and kinesiology. Interfacing the muscles with the processing software is not an easy task, and although its success might depend on a variety of factors like electrode design and its optimal attachment to the patient, skin preparation, environmental noise etc, the key for good results relies in the analog circuitry in between them. This section will review some of the available technologies to amplify, filter, isolate the patient etc with the scope of proposing a suitable EMG multichannel acquisition system that satisfies the specifications seen in Chapter 2.

3.1 Electrodes

A *surface EMG* [1] electrode can be defined either as a sensor of the electrical activity of a muscle or as a transducer of the ionic current, flowing in the tissue, into the electronic current, flowing in the metal wires [16]. It is designed to obtain selectively the sEMG signal while minimizing the artifacts, DC potentials and environment noise picking. The quality of an electrode depends on its shape, size, construction material etc. but no matter the electrode type, they all share some general characteristics:

- Contact skin electrodes *always* introduce noise. Electrodes interface ionic currents, flowing through tissues and live cells, into an electronic current flow through a high conductive material, the resulting process introduces noise (see 1.4.1).

[1] There are EMG invasive electrodes known as *needle electrodes* used to record directly from the muscle fibers. Since such electrodes are very invasive, their use is limited to only highly specialized and supervised clinical or research applications, for example in needle recordings based techniques as the single−fiber EMG and macro EMG.

- To transform the ionic current into an electronic current, a chemical reaction takes place in the transducer. The transducer is composed by an electrode and an electrolyte. Current can pass from an electrolyte to a non polarized electrode oxidizing the electrode atoms. The resulting cations and electrons flow in opposite directions: the electrons go through the metal cables attached to the electrodes meanwhile the cations go to the electrolyte. In that way, a potential difference known as "half cell potential" is formed between the *negative* electrode and the *positive* electrolyte, as the Figure 3.4.2 shows. Although the DC voltages that appear in each electrode−skin contact are similar between them, they are never the same; in other words the half cell potential is a *differential* voltage that have to be handled carefully in order to avoid the amplifier saturation.

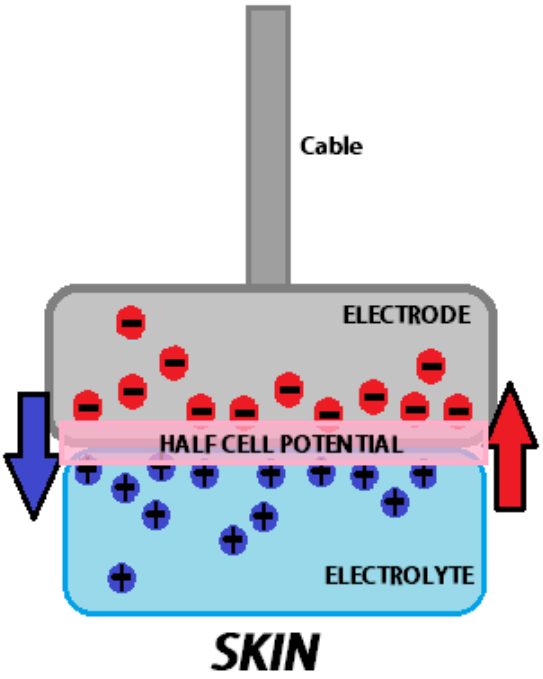

Figure 3.1. The half cell potential is the result of the chemical reactions between the electrode and the electrolyte. It is an undesirable effect when transforming ionic muscle currents into electronic currents that has to be minimized and properly treated in the following system stages.

- The electrode−skin interface is frequency and current dependent. It presents a complex impedance that can be modeled as a capacitor (C_1) in parallel with a resistor (R_1). This impedance may vary range from a few $K\Omega$ to a few $M\Omega$, depending on electrode size and skin condition, with larger electrodes

having lower impedance and noise [16]. The effect of this impedance and how it conditions the amplifier choice will be treated in Section 3.4.1.

- The electrode metal surface forces all the contact area to be at the same potential, and it modifies the potential distribution of the skin. The modification of the skin potential distribution introduced by the finite area of the electrode can be approximated if the electrode size is assumed to be small with respect to the geometrical extension of the biopotential distribution [16]. If many small electrodes are placed in some area A, the detected voltage will be the average of the individual measured potentials creating a two dimensional filtering effect.[16]. In other words, just the act of placing electrodes in contact with the skin to pickup the EMG "pure" signals introduces many undesirable effects, for example filter the signal.

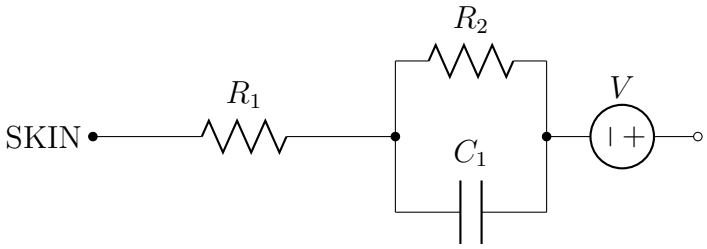

Figure 3.2. Electrode−Skin circuit model. V represents the DC voltage produced thank to the half cell potential plus the intrinsic noise.

One way to classify electrodes, is depending of the material with which are made, the size they have or even the shape. Three of the most used electrode alternatives are presented in the list below and represented in the Figure 3.3:

- **Silver−Silver Chloride Electrodes** Silver−silver chloride based electrode design is known to produce the lowest and most stable junction potentials [27] and usually an electrolytic gel is applied to the electrode to improve its conductivity and low junction potential without causing skin irritation. The Electrode−skin contact when using Ag or Ag−Cl has an impedance almost resistive, it means that compared to other metals it has a negligible capacitive component and therefore there are not important filtering effects in the EMG frequency band.

- **Gold Electrodes** Gold electrodes maintain a really low impedance (and even lower if conductive gel is applied in between them and the skin) and although are more expensive than other choices, are reusable and durable. Are often used in EEG recording.

- **Conductive Polymer Electrodes** Some polymeric materials have adhesive properties and are attached to aluminium or silver foil to make themselves conductive. Electrodes made of this materiales do not need additional adhesive or electrolytic gel, but because of their relatively high resistivity are not suitable for low noise systems construction

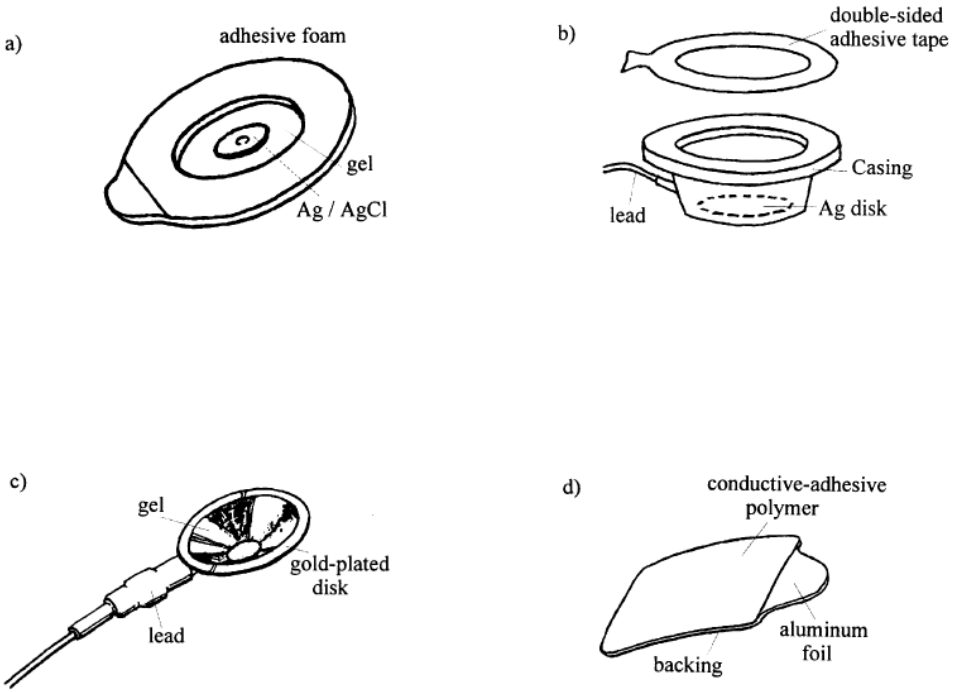

Figure 3.3. Different types of electrodes. *a*) Disposable $Ag - AgCl$ electrodes. *b*) reusable $Ag-AgCl$ disk electrodes. *c*) Gold disk electrode. *d*) disposable conductive polymer electrode. Adapted from [27]

There are two other things to define apart the electrodes type: the skin preparation and the electrode placement. In the system designed for this thesis, the electrode placement consisted in a classical monopolar distribution with n electrodes along the arm (this number could vary between 8 and 32 electrodes), a *reference* electrode away from the other n and located preferably in a "bony" part and one more electrode in the right leg to drive the common mode into the patient body. The system is designed to measure all the signals in a differential way and each time, with respect the reference electrode.

To achieve minimum electrode impedance and low DC offsets custom−made micro−needle electrodes will be used as transducers in the final EMG acquisition system. Figure 3.4 resumes the performance of the microneedle and compares it with the one of conventional Ag surface electrodes.

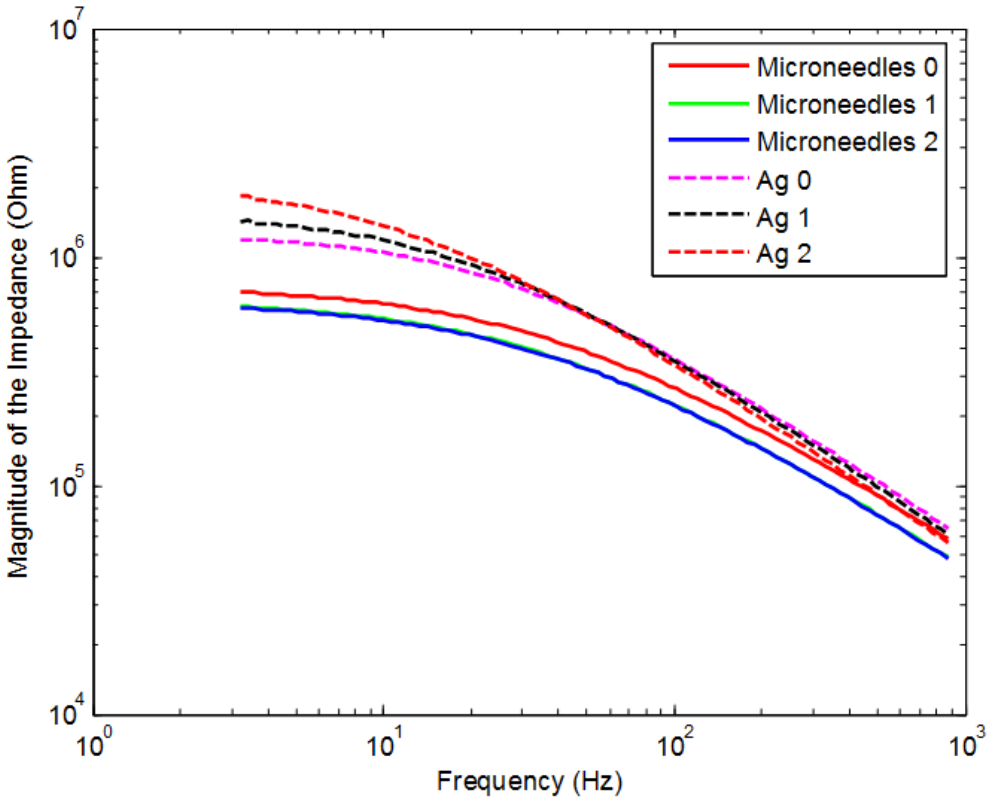

Figure 3.4. Magnitude of the electrode-skin impedance between two micro-needles[2] electrodes and between two Ag electrodes (flat surface). The two types of electrodes had the same dimensions (0.5 cm x 0.5 cm). For each electrode type, three curves are reported (Measure 0: T= 0; Measure 1: T= 10 min; Measure 2: T= 20 min). Adapted from [3]

The distance between the electrodes array is not established yet, but for future prototypes will be defined along with a skin preparation protocol. However The Surface Electromyography for Noninvasive Assessment of Muscles *SENIAM* proposed in the year 2000 a skin preparation protocol that consisted of shaving, massaging with sandpaper or abrasive paste and rinsing the skin with water to remove the abrasion flaky residuals [15].

3.2 ESD protection

An electrostatic discharge (ESD) is a high voltage transient with fast rise time and fast decay time that occurs when an electrically charged object discharges through another at lower potential. Everyday activities can electrostatically charge the

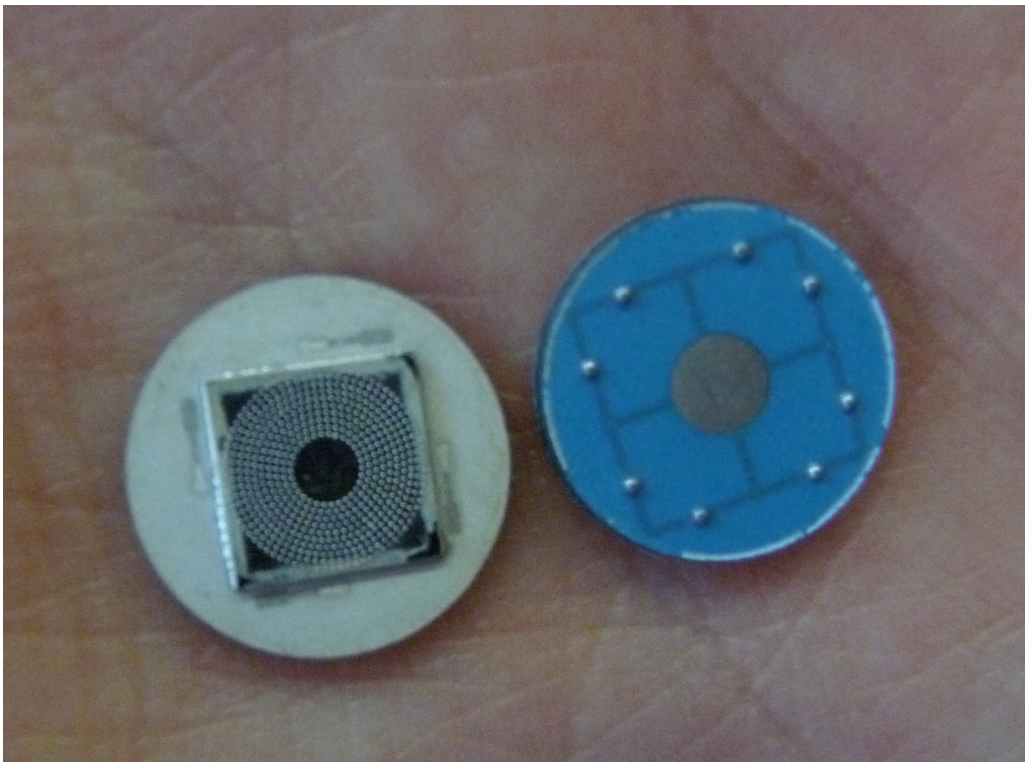

Figure 3.5. Micro−needle electrodes pair. In the backside there is some space to put the amplification stage in further prototypes.

human body in a process denominated *triboelectric charging*[3]: walking across a carpeted floor, sliding out of an office chair etc. The subsequent transfer of the acquired electrical charge to sensitive electronic devices can permanently damage them. Therefore is very important to protect sensitive devices and even more if they are in direct contact with the human body, like the electrodes of the EMG acquisition system.

Many solutions to the ESD problem are nowadays available: Metal Oxide Varistors, transient voltage suppression diodes, Zener Diodes, even regular or bipolar clamp diodes can be used to shunt the ESD energy providing protection to the ICs. These solutions are designed to handle electrostatic discharges introduced into the system without going through sensitive circuitry. A ESD protection unit should be provided for each circuit I/O port, especially if they are in direct contact with the human body (as in the electrodes case). In the Figure 3.6 a general ESD protection stage is presented.

[3]Triboelectric charging is a type of contact electrification in which two materials come into contact and then separate with some electrons exchanged by a process called adhesion

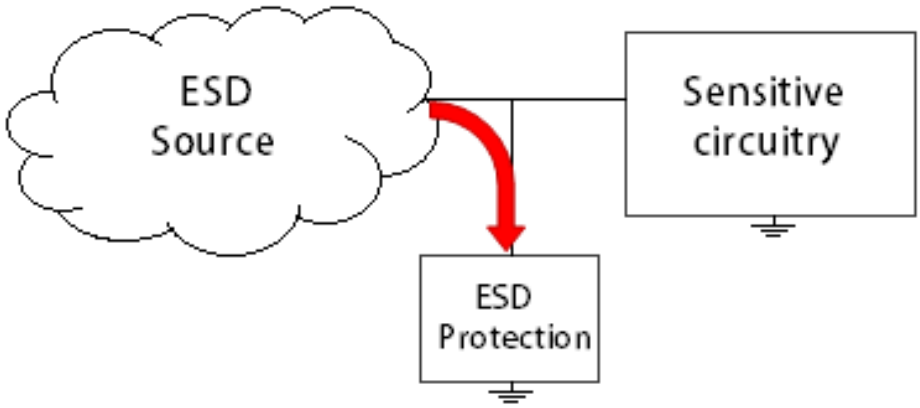

Figure 3.6. The ESD protection connects the sensitive circuitry input to ground when some voltage threshold is surpassed.

A crucial thing to take into account when choosing the better ESD protection alternative is the data rate of the sensitive signal path. If it is considerably high, the previous alternatives are not appropriate solutions due to the parasitic impedance they introduce. The first ESD protection strategy adopted for this EMG system prototype consisted in the implementation of ESD capacitors.

The charge released in the ESD event is initially stored in the human body and its quantity depends on the human body capacitance, [4] which is related to the voltage by the Equation 3.1, where Q is the charge in Coulombs, C is the capacitance in Farads and V the voltage in Volts.

$$Q = CV \tag{3.1}$$

Adding a capacitor to the input line exposed ESD, makes the protected circuit to see in its input, the voltage of the protective capacitor and not the high ESD voltage. Part of the charge then is transferred to the protective capacitor until it gets filled. An example of how to calculate the capacitance C_p for a maximum given permitted input voltage is shown in the Equation 3.2. V_{ESD} is the high ESD voltage, V_{max} is the maximum permitted voltage by the sensitive circuit and 100pF is the human body capacitance according to the HBM.

$$\mathrm{V}_1 = V_{ESD}$$

[4] According to the ANSI/ESD association Human Body Model (HBM) this capacitance is around $100pF$

$$\mathrm{V}_2 = V_{max}$$
$$\mathrm{C}_1 = 100pF$$
$$\mathrm{Q}_1 = C_1 V_1$$
$$\mathrm{Q}_2 = C_1 V_2 + C_2 V_3$$
$$\mathrm{Q}_1 = Q_2$$
$$\mathrm{V}_2 = V_3$$
$$\mathrm{C}_1 V_1 = C_1 V_2 + C_2 V_2$$
$$\mathrm{C}_1 V_1 = (C_1 + C_2) V_2 \quad 100\mathrm{pF} \times V_{ESD} = (100pF + C_p) \times V_{max}$$

$$C_p = \frac{100pF \times V_{ESD}}{V_{max}} - 100pF \tag{3.2}$$

After implementing those protective capacitors (see Chapter 5) some tests revealed that they were introducing important quantities of noise in the circuit, and another solution was designed: ESD protection using clamping diodes.

Using a circuit that clamps the maximum voltages to the maximum operating extremes (positive and negative rails) is also an alternative to prevent the voltage rising above a level that would damage the interface device. Reverse biased diodes (high−speed $1N4148$ diodes) from the input line to the voltages rails were used as ESD protection in the EMG system prototype. The Figure 3.7 shows the final implementation.

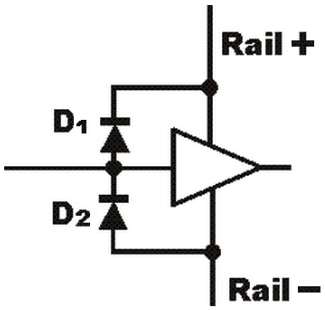

Figure 3.7. The diodes D_1 and D_2 are reverse biased under normal operating conditions. When a pulse occurs raising the input voltage above the positive rail voltage, D_1 will conduct. In the same way, if the voltage falls below the negative rail voltage, D_2 will conduct.

3.3 DC Rejection

As it has been explained in Subsection 2.1.1 the raw input to the EMG system consists of several parts, including a DC offset caused by the electrode−skin contact. This DC offset has to be treated carefully because if not, problems as saturation of the whole system could occur.

Two main strategies are commonly used to deal with DC input levels:

- **DC coupled amplifier with low gain.** This option does not filter the DC component but follows the principle of preamplification, meaning that the total circuit gain is splitted into two (or more) medium to low gain stages. In this way, the front−end amplifier has a low gain to prevent DC saturation of its operational amplifiers, then the DC is filtered among the other not relevant frequencies with a passband filter and the resulting signal is fully amplified by additional gain blocks. Another option is to block the DC component at the very output of the amplifier with an integrator in feedback configuration that cancels the mean output, leaving it, ideally, at zero.

  This approach has the advantage that no additional filtering is required, besides the passband of the general system, and that the CMRR is not decreased by additional highpass filters at the amplifier input. How the CMRR is lowered by the addition of typical filters at the amplifiers input will be reviewed in the following paragraphs.

- **AC coupled amplifier with high gain.** The second option to deal with the DC offset in the raw input EMG signal is with AC coupling. In this way, there is no need of preamplification and the entire system gain can left to one single block. Having a really high gain stage is advantageous because it drastically increases the SNR (*signal to noise ratio*) making the amplified signal more immune to interferences and noise than it would be with medium to low gain preamplifiers.

  The Figure 3.8 shows a typical high gain AC coupled amplifier.

Both options present good characteristics depending on the specific application and circuit configuration, but for the prototype developed in the present thesis, the second choice was more suitable due to the SNR increase it provides (the constructed prototype has a lot of “sensitive” traces where the signal can be easily degraded if not early SNR improvement is implemented). The problem with this alternative is that typical AC coupling is achieved by series capacitors, but in order to provide a bias path for the amplifier, grounded resistors are usually included, which degrade the common mode rejection ratio (CMRR).

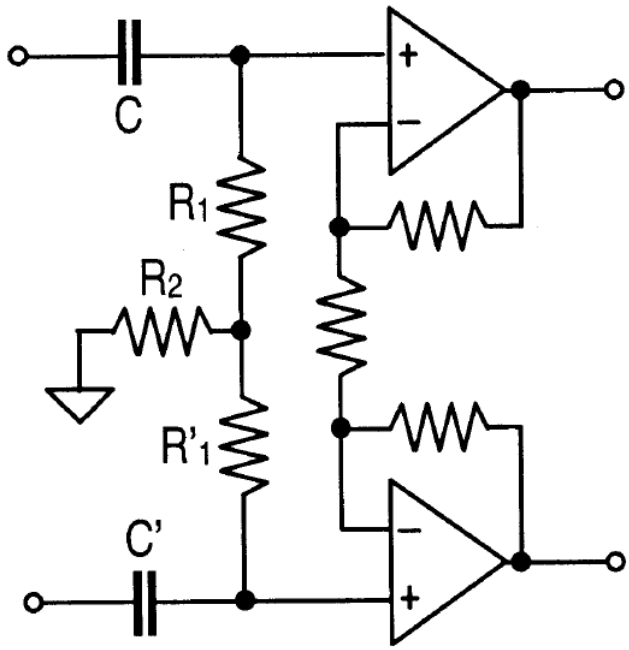

Figure 3.8. Typical circuit for balanced ac coupling. The DC rejection it provides, allows the front−end amplifier to have an advantageous high gain. Adapted from [25]

In the circuit of Figure 3.8 R_2 resistor reduces the amplifier input common mode impedance, degrading the effective CMRR by the potential divider effect (see Section 3.5). Because the CMRR of this coupling network depends on component tolerance, it is strongly worsened by any kind of mismatches in the components value, making it really difficult to construct without significant CMRR compromise involved.

Although the input impedance and the CMRR are improved with higher R_2 values, this resistor cannot go to infinite nor excessively high real values because the amplifier needs a bias path and the current noise of the system would be significatively incremented. The effective value of grounded resistors can be increased by bootstrapping, but this is also inconvenient due to the relative high offset values, that at the end also limit the maximum amplifier gain.

The solution implemented in the EMG system prototype, includes the novel, balanced ac coupling network shown in Figure 3.4.2. This circuit provides AC coupling for differential signals and at the same time, a DC path for amplifier bias currents, which drain to ground through the DRL electrode [25].

The transfer function of the filter, assuming $R_2C_2 = R_2'C_2'$ (see [25]) , is reported in the equation 3.3. The values selected for the actual implementation are $R_1 = R_2 = R = 4.99M\Omega$ and $C = 3.3\mu F$ for a cutoff frequency of ≈ 0.06Hz. The choice was made taking into account regulations as the ones presented in [2].

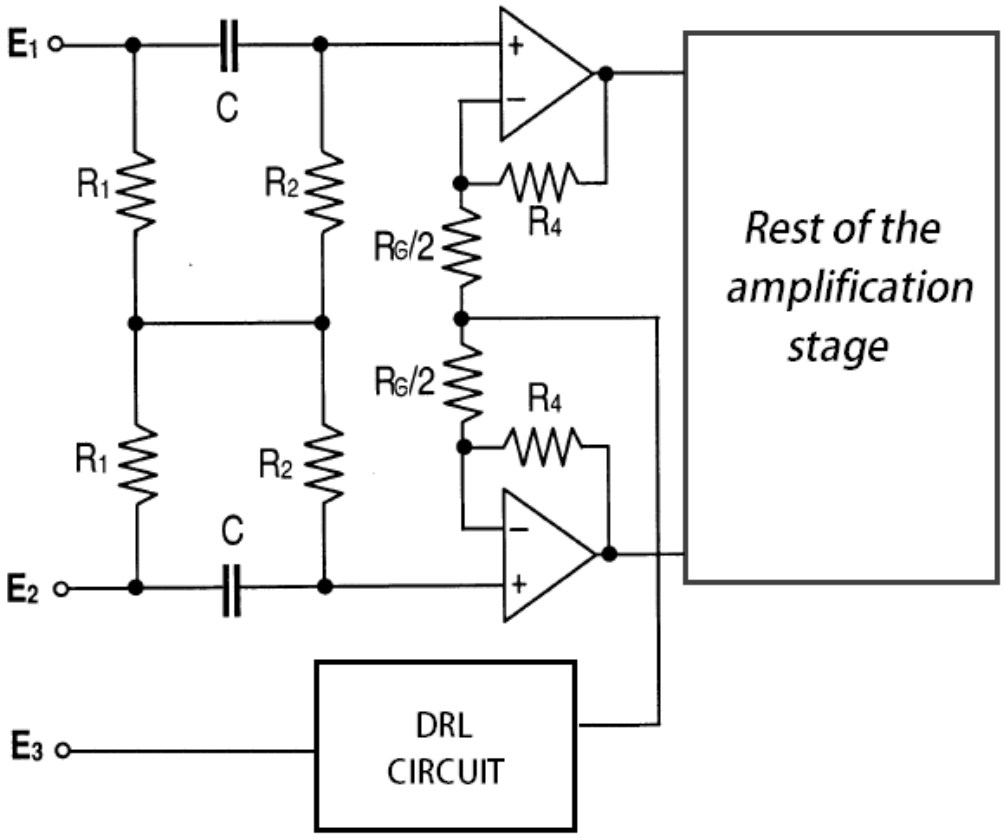

Figure 3.9. Proposed amplifier circuit, with a differential DC filter allowing CMRR and high impedance preservation while providing a DC path for the amplifier bias current. Adapted from [25]

$$G_F = \frac{sRC}{1 + sRC} \tag{3.3}$$

3.4 Amplification

An EMG acquisition system could not work properly without each one of the blocks introduced in 2.1.2 of Subsection 2.1.2, but it can be said that the core unit of the whole process is the amplifier. The amplifier is the part in charge of taking the low level EMG signals into a suitable voltage range for processing, displaying and storage, improving their SNR making them immune to coupled interference and environmental noise.

There are two basic forms of amplifying a signal (introduced in Section 1.4): single ended and differential. The construction of the EMG system prototype in

this thesis used a differential amplification because of the multiple advantages that presented over the single ended alternative, for example the high rejection to the common mode (for more details see Section 1.4). In every single channel, one of the inputs is the direct output of one electrode (after going through the ESD protection stage) and the other is the reference, which is the same for all the channels. Therefore the signal to be amplified is the *difference* between the voltage lecture of one electrode (signal A), and the reference (signal Ref). If the amplifier is close enough to the electrodes, it can be assumed that electrical interference, as the one caused by the 50Hz power line, will affect both signals A and Ref more or less in the same manner, being rejected as common mode by the amplifier. How the electrodes are physically connected to the amplifier is explained in the Chapter 4.

3.4.1 Amplifier

The selected device for EMG signals amplification was a 3-Op amp instrumentation amplifier. This type of device has many desirable characteristics in medical applications, for example its high CMRR, high input impedance, high gain, optimal bandwidth etc. (see Section 1.4). It allows to amplify the difference between two floating signals, and gives a single ended output referred to the system ground. And although the instrumentation amplifier was the selected choice, there are many types of In-amps that differ a lot from each other in several properties. The table 3.1 resumes the amplifier requirements.

Parameter	Value
Input Impedance	$> 100M\Omega$
Common Mode Rejection	$>$ 100dB
Gain	1000
Bandwidth at gain of interest	$\geq$ 1000Hz
Power Supply	$\pm$5V

Table 3.1. Requirements to choose an optimal instrumentation amplifier.

The first considered option was the very low-noise, low-distortion, instrumentation amplifier INA163 of Texas Instruments. This amplifier fulfilled all the requirements of Table 3.1 except for that of input impedance: “The input impedance for a sEMG amplifier must be at least 100 times greater than the largest expected

electrodeâskin impedance" [16]. The INA163 has input impedance of 60||2 MΩpF, which could be high enough if the output impedance of the electrode skin interface were below 500kΩ; however in the worst case, this impedance is about 1MΩ [16]. With such a high electrode-skin interface impedance, the approximate $60M\Omega$ amplifier input impedance loads the EMG signal, diminish and, possibly, distorting it.

The Figure 3.10 shows the amplifier configuration using the INA163 and Figure 3.11 shows the results of the simulation of the system using the Texas Instruments simulator TINA.

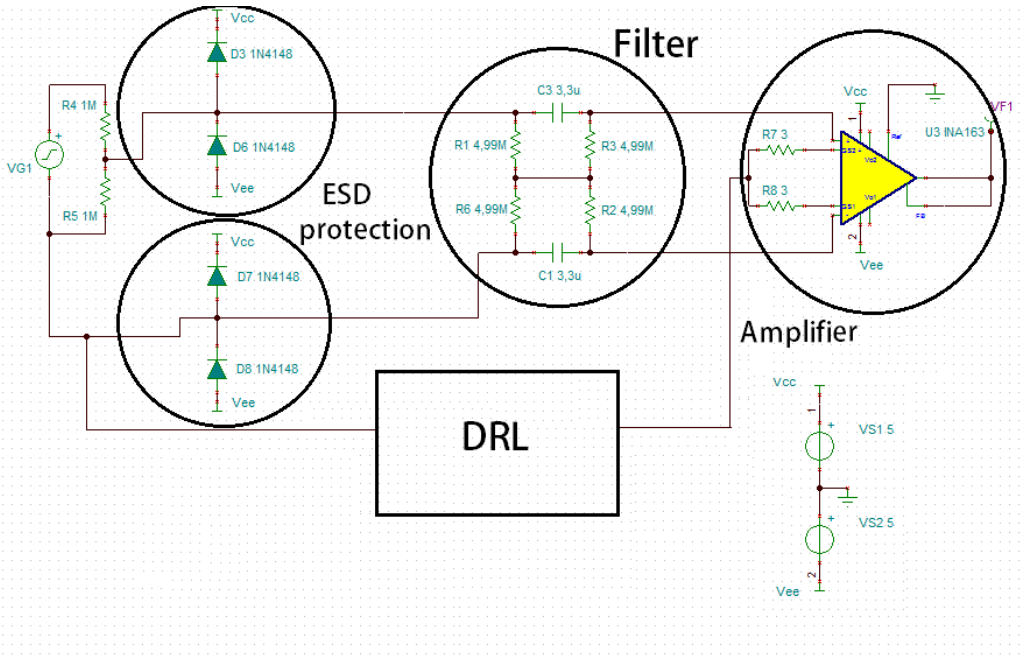

Figure 3.10. EMG acquisition system input. The ESD stage, DC rejection and the amplifier are circled and labeled.

The INA163 gain (G) is given by the expresion $G = 1 + \frac{6000}{R_G}$ where R_G is the *gain resistor*, which corresponds to 6Ω for a 1000 gain. Although the 6Ω resistor is placed as R_G in the circuit of Figure 3.10, the gain does not exceeds 50V/V. The solution to this problem was to find another device with higher input impedance to avoid loading the input signal.

The second alternative and definitive choice was the INA114 of texas instruments. This instrumentation amplifier is commonly used in biopotential amplifiers, it fulfills all the requirements listed in the Table 3.1 and exhibits a far higher input impedance than the INA163: $10^{10}\Omega||6$pF vs 60 MΩ||2pF. The INA114 was used with a 1000 gain achieved with a 50Ω gain resistor, this high gain allowed to improve the SNR of the EMG signal making it practically immune to noise and interference pickup;

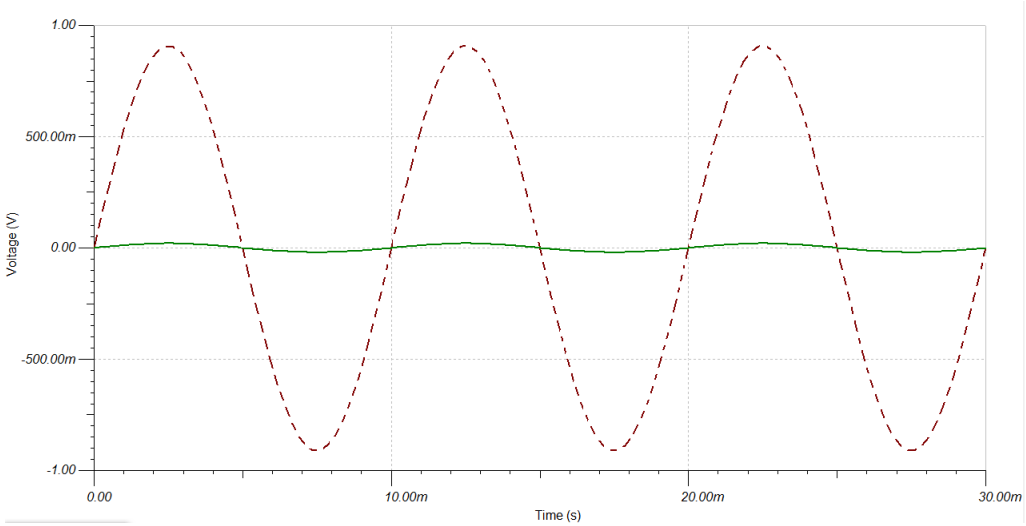

Figure 3.11. The dashed line (output) is the amplified version of the continuous line (input). The desired amplification of 1000 is not reached due to the load effect of the INA163 to the EMG signal because of its low input impedance.

however the INA114 is not a railtorail instrumentation amplifier and the high gain could easily saturate the amplification stage if large inputs enter the device. The Table 3.2 summarizes the principal characteristics of the INA114 and Figure 3.12 shows the simulation results for the same configuration of Figure 3.10, but with the INA114 instead of the INA163.

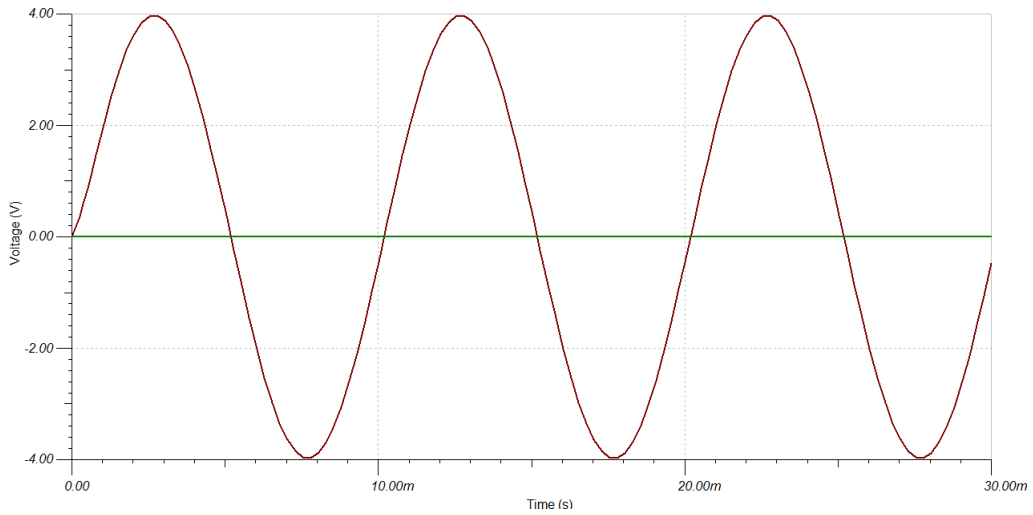

Figure 3.12. Simulation of the INA114 performance. The input is a 4mV signal and the output is a 3.97V signal.

Parameter	Value
Input Impedance	$10^10 \| \| 6\Omega$pF
Common Mode Rejection at 1000 gain	120dB
Resistance for 1000 gain	50Ω
Bandwidth at 1000 gain	1kHz
Power Supply	±15V
Voltage input noise at 1kHz bandwidth	$11\text{nV}/\sqrt{Hz}$
Current input noise at 1kHz bandwidth	$0.2\text{pA}/\sqrt{Hz}$

Table 3.2. Texas Instruments INA114 specifications.

The noise characteristic curves of the INA114 were really important during the design of the front-end amplification stage, which is practically the only noise sensitive part of the circuit. This sensitivity is given by the low voltage level of the signal that could be compared with noise amplitudes, if so, both (signal and noise) are amplified and filtered by the rest of the circuit, making really difficult to identify what part is noise and what part is not.

Applying the concepts reviewed in 1.4.1, the three main types of noise referred to the input of the amplifier were calculated as follows:

- Thermal noise produced by the equivalent filter resistor R_f of 4.99MΩ, and the electrode-skin resistance, which in the worst of the cases could be as high as 1MΩ [16]. Equation 3.4.1 shows the resulting equivalent thermal noise referred to the input E_{th} at 300K temperature with a bandwidth of 1kHz.

$$\text{E}_{th1} = \sqrt{(4 \cdot 1.38 \cdot 10^{-23} J/K \cdot 300K \cdot 4.99M\Omega \cdot 1000Hz)},$$

$$\text{E}_{th2} = \sqrt{(4 \cdot 1.38 \cdot 10^{-23} J/K \cdot 300K \cdot 1M\Omega \cdot 1000Hz)},$$

$$\text{E}_{th}^2 = (E_{th1})^2 + (E_{th2})^2,$$

$$\text{E}_{th}^2 = (9.09\mu V)^2 + (4.06\mu V)^2,$$

$E_{th} = 5.06\mu V$. (3.4)

- Equivalent amplifier voltage noise referred to the input, which according to the datasheet at 1kHz is $11nV/\sqrt{Hz}$. Equation 3.4.1 shows the resulting equivalent amplifier voltage noise referred to the input E_v.

$$E_v = 11nV/\sqrt{Hz} \cdot \sqrt{1kHz},$$

$E_v = 0.348\mu V$. (3.5)

- Equivalent amplifier current noise referred to the input, which according to the datasheet at 1kHz is $0.2pA/\sqrt{Hz}$. Equation 3.4.1 shows the resulting equivalent amplifier current noise referred to the input E_c where R_{eq} is the equivalent resistance that the current going into the amplifier encounters, in the worst case is given by the parallel between R_f and 1MΩ of the electrode-skin impedance.

$$E_c = 0.2pA/\sqrt{Hz} \cdot R_{eq} \cdot \sqrt{1kHz},$$

$$E_c = 0.2pA/\sqrt{Hz} \cdot 0.83M\Omega \cdot \sqrt{1kHz},$$

$$E_c \approx 0.2pA/\sqrt{Hz} \cdot 1M\Omega \cdot \sqrt{1kHz},$$

$E_c = 0.632\mu V$. (3.6)

The total noise referred to the input (E_{in}) is given by Equation 3.4.1. It can be noticed that the major contribution is given by the thermal noise, meaning that the performance limit is not given by the INA114.

$E_{in} = \sqrt{5.06\mu V^2 + 0.348\mu V^2 + 0.632\mu V^2}$.

$E_{in} = 5.11\mu V$. (3.7)

This result is very significative and will be relevant during the validation because it establishes that the noise is given by the discrete resistors of the pre-amplifier network and will be the limiting factor to the system performance. However, this noise will not be the major problem of the constructed prototype because its amplitude after the amplification is expected to be of 5.11mV, representing just the 0.1% of a 5V output. However, in further prototypes it should be reduced because this value limits the output accuracy to a maximmum of 10 bits.

3.4.2 Integrator

It has been already discussed the problem that the DC offset represents to the acquisition system in Subsection 3.3 when the DC rejection stage was explained. An although the major DC level contribution at the amplifier input is from the half cell potential created in the electrodes (see Figure in Section), there are other DC voltages than can cause problems, even if they have lower amplitudes, and that might not be rejected by the DC filter in Section 3.3.

The circuit in Figure in Section 3.3 is intended to filter DC input voltages, but the *DC offset voltages* of the amplifier itself, can substantially reduce the effective dynamic range of the system because they are amplified as part of the signal. This DC voltage offsets can be also produced by *offset currents* passing through large resistors, as in the case of the EMG acquisition system (the electrode skin interface impedance can until 1MΩ in the worst cases[5]).

In particular, the selected instrumentation amplifier for the prototype construction, the INA114 presents a maximum offset current of ±2nA (at 25^{o}C) with a typical increment of ±8pA per each ^{o}C of temperature increment[6]; it means that the equivalent offset voltage for a 1MΩ electrode skin impedance could be as high as 2mV at 25^{o}C, which is then amplified and seen at the output as a 2V DC offset.

To remove the offset voltage and reduce low frequency noise ($1/f$), the amplifier itself must reject low frequencies (see Section 3.3). A integrator in a feedback loop between the *reference* and *output* pins of the INA114 was implemented as the solution for the offset problem. Figure 3.13 shows the circuit configuration with the integrator in place.

Low impedance must be maintained at the INA114 *Reference* pin node to assure good common mode rejection. This is achieved by buffering with an operational amplifier. The device selected as buffer was the LF351 which is a JFET input operational amplifier with an internally compensated input offset voltage. This operational amplifier has a input impedance of about 10^{12}, ensuring no load effects at the output of the INA114. In addition to the LF351, two resistors of 1MΩ and one capacitor of 330nF were used to configure the network as is seen on Figure fig:intedc.

Combining the effect of the integrator with the previously explained DC rejection filter (see Section 3.3), results in the Equation 3.8 partial transfer function of the EMG system[7]. Where R is the resistor value and C is the capacitor value of the DC

[5]No proper skin preparation, not suitable electrodes and bad contact between the electrodes are some examples of the possible "worst cases" when measuring EMG signals.

[6]Texas Instruments INA114 datasheet: http://www.ti.com/lit/ds/symlink/ina114.pdf

[7]This transfer function does not take into account the lowpass effects that the amplifier itself produce in the circuit

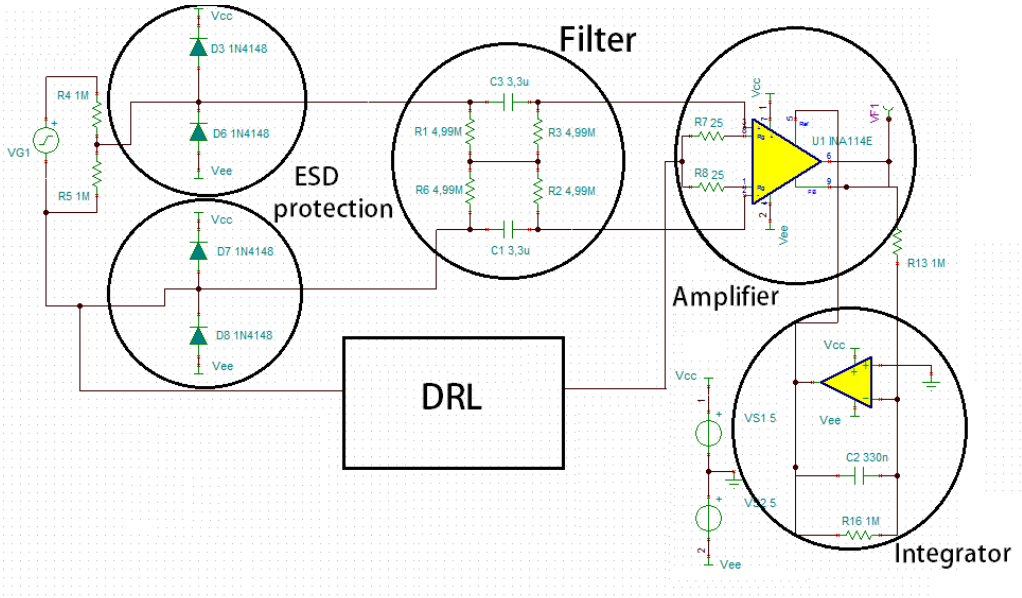

Figure 3.13. EMG acquisition system front end with integrator in feedback loop as solution for the amplifier offset voltage problem.

rejection filter, R_i and C_i are the resistor and capacitor values used in the integrator network and G is the amplifier gain.

$$T(s) = \frac{sRC}{1+sRC}\frac{sR_iC_iG}{1+sR_iC_i}. \tag{3.8}$$

3.5 Shield Driver

The most sensitive part in the EMG system design is the path between the electrodes and the amplifier because is where the EMG signal has the lowest voltage level and is most vulnerable to noise and interference pickup. The longer the signal has to travel, the most interference and noise get coupled electromagnetically. This aspect is so critical that in further prototypes and in the construction of the final EMG acquisition system at the DLR, the amplification stage will be soldered at the back of the electrodes of Figure 3.5 (see Section 3.4.2).

The interference can be coupled into the measurement system electrically, in the form of currents flowing into the wires of the circuit, or magnetically, which in theory should be easy to avoid just by reducing the area of the loop formed by the measurement cables; hence, it would not appear with the amplifier attached to the back of the electrodes. But because in this prototype design and construction, soldering the amplification stage at the electrodes was not an option, some mode of

reducing the interference coupling had to be found.

The largest and most easily encountered interference in biopotentials measuring comes from the common power line interference. This interference can be hundreds of times higher than the EMG signal to be measured and cause serious interference in two main ways: when the commonmode rejection ratio of the amplifier is limited and more important, when there are differences in electrode or input impedances which convert common mode voltage into a differential input voltage by a mechanism called "the potential divider effect" [22]. The common mode voltage transformed into differential mode can approximated as follows:

$$V_d \approx V_{CM} \frac{Z_a - Z_b}{Z_i}. \tag{3.9}$$

How this mechanism operates is explained in Section 2.

The mismatches in the paths of a pair of electrodes should not exist in theory, but often these differences are not easy to avoid in practice. Differences in input impedances are often found in multichannel measuring systems (as the EMG acquisition system of this thesis) caused, for example, by the use of shielded input cables of different length[22].

However in a carefully designed system (without the option of soldering the amplifier in the electrodes directly), the only practical solution is to reduce as much as possible the actual commonmode of the measuring. One of the most popular and effective methods to achieve such reduction is called Driven Right Leg (DRL) and will be discussed in Section 3.6. *Shielding*, the implemented technique for reducing the interference currents in the wires, will be reviewed below.

To shield a cable means to surround it with a common conductive layer. This allows that the *electromagnetic interference* (EMI) does not reach the signal in the conductors, by means of reflecting the EMI energy or conducting it to ground. There are many types of shielded cables as it can be seen in Figure 3.14, each one for specific purposes.

There are also many techniques to *drive* those shields and two of the most popular are discussed here:

- **Shields connected to the interference−type noise ground** It consists simply in connecting the cable shield to the ground of the interference source. However for the purposes of this thesis, this solution is not convenient because the main interference comes from the power line, and connecting the shield to the power line common would create *ground loops*, introducing further problems of noise and interference to the circuit. This technique is useless if the interference signal is not grounded [21] and in the EMG system prototype, the amplifier common is not the same power line common because of the isolation stage.

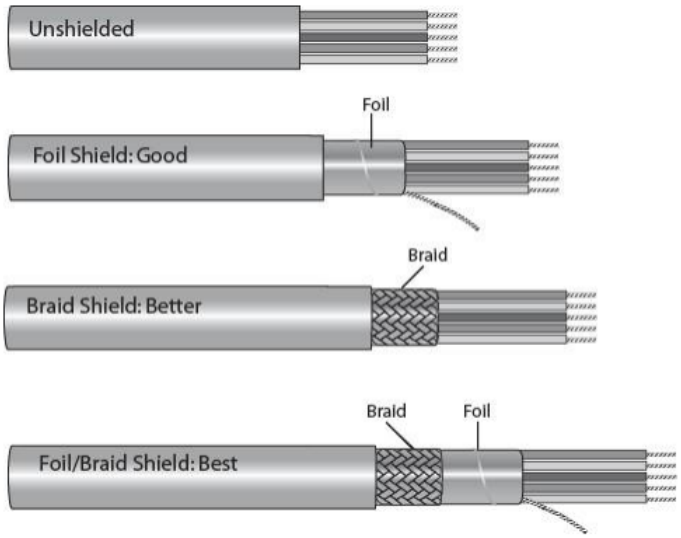

Figure 3.14. Different types of shielded cables

- **Guarding with the common mode** Guarding has many useful purposes: It reduces the common-mode capacitance, improves the CMR, and eliminates leakage currents in high impedance measurements [21]. This technique cancels the potential difference between the shield and the inner conductor, and therefore does not allow signals to flow. One shield driver is needed for each different cable and the configuration is represented in Figure 3.15. This second technique was implemented on the EMG system with the LF351 as the buffer unit, a voltage divider made by one 10kΩ and one 100Ω resistors to feedback, not the 100%, but the 99% of the common-mode and prevent possible instability.

3.6 Driven Right Leg

It has been mentioned repeatedly that one of the major problems in biopotentials measuring is the voltage divider effect, which is the transformation of common mode interference into differential signals that are amplified by the system. In fact, the CMRR is not so important if there are large mismatches between electrode-to-amplifier lines and the efforts must focus in how to reduce the common-mode itself.

There are many techniques to improve the CMR performance and to try to reduce the common-mode itself in order to avoid the voltage divider effect:

- **Shielding** It has just been explained in the previous section that shielding

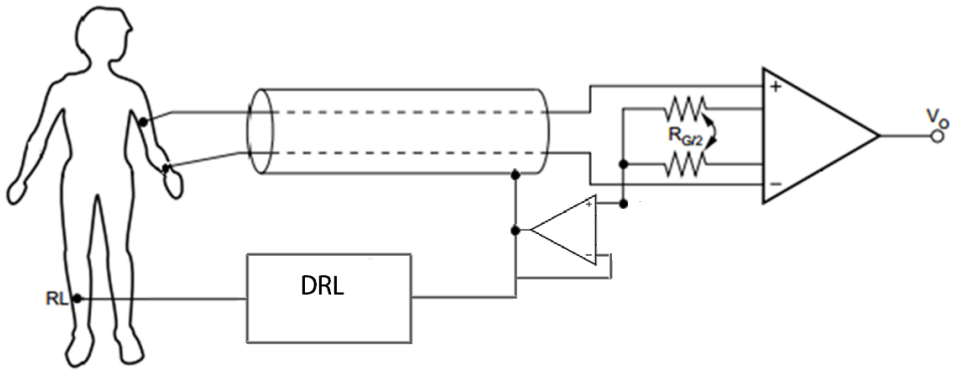

Figure 3.15. Representation of how to drive the shields in each measurement channel. Adapted from INA114 datasheet.

the circuit and the sensitive lines reduces dramatically the common-mode interference (as happened during the construction of the EMG prototype, see Section 4) and may also prevent EMI irradiation from the circuit itself.

- **Notch filter** Filter the power line interference with notch filters has been a popular practice, is based on the elimination of the 50Hz component from the measurement. Some filters are analog and come after the amplification stage, and some of them are digital, acting after the ADC conversion like the finite-impulse response (FIR) adaptive filters. However, especial attention has to be taken with such operations so that real-world signals are not compromised with this type of filtering, it has to be ensured that phase information is not skewed because of the filtering operation [1]. In fact, one of the conditions imposed at the beginning of the project was to *avoid* analog notch filters because they also eliminates the part of signal information located at 50Hz, and the final user of the system wanted the raw EMG signal for further processing.

- **Isolation Capacitance** Improving the isolation between the device ground and the patient ground helps to improve the system CMR. Given that the prototype was not intended to work with batteries, especial attention to the power supply and patient isolation had to be taken into account.

- **Driving the Common-Mode Voltage back to the body** The driven right leg (DRL) circuit has initially designed for interference reduction in ECG recordings and later applied to other biopotential recordings [16]. The system is based on a feedback circuit that drives the common mode voltage back to the patient body, amplified and phase reversed by 180^o. This feedback loop improves CMR by an amount equal to (1 + A), where A is the closed-loop gain of the feedback loop [1].

A DRL circuit was implemented in the EMG system prototype for reducing the common mode of the patient body and improve the measurement, but also to provide the third electrode whereby the bias current of the amplifier had to flow, due to the presence of the DC rejection filter (see Section 3.3). Figure 3.16 shows the front-end network configuration with the DRl circuit in place.

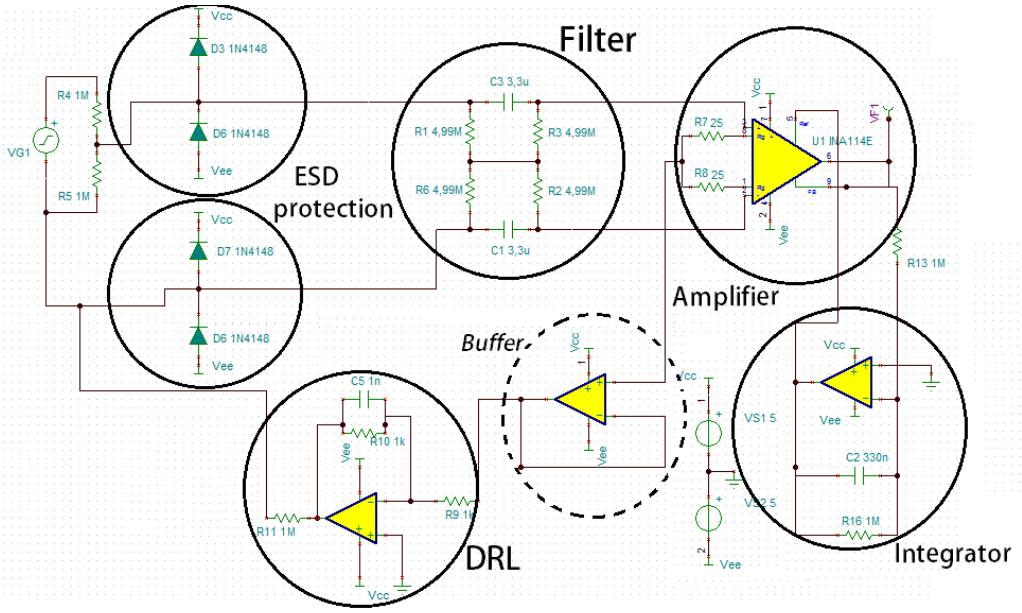

Figure 3.16. Front-end configuration with DRL circuit in place. The DRL circuit makes a feedback loop between the patient (represented by the voltage source V_{G1} and the EMG acquisition system.

The buffer is used for taking the common mode voltage without loading and compromising the gain resistance of the amplifier and its output is connected to the DRL input and to the channel shield for driving it. The DRL circuit is composed of a LF351 operational amplifier, a 1nF capacitance to reduce high frequency gain and possible instability [16] in parallel with a 1kΩ resistor, and a final resistor of 1MΩ in between the DRL circuit output and the human body. This resistor was chosen with a high value to protect the patient, (in case of a fault condition where the patient body is accidentally connected to the system ground [1]) and although the IEC standards[8] allow a lower resistor value, it was oversized for prototype construction purposes (in future prototypes and in the final version of the EMG acquisition system, this value can be lowered down until 100kΩ [1] to further improve the CMR of the entire system).

[8]Safe current limits for electromedical apparatus. ANSI/AAMI ES1-1993.

One major concern about the DRL circuit is the possible instability it can cause. In any closed loop, oscillations may appear if the the *Barkhausen stability criterion* is not satisfied, however if proper care is taken, the DRL may significantly reduce the power line interference. For further details and explanation of the instability of combined driven right leg and guarding circuits see the appendix of [22].

3.7 Filtering

The EMG signal has a specific frequency band in which the muscle activity information relies (see Subsection 2.1.1), therefore, the frequency response of the acquisition system should be tuned to *that* specific spectral content, leaving aside low frequency components that can obscure the measurements, or high frequency components that could alias in the analog to digital conversion (ADC) stage.

There are two methods of data conditioning in modern biopotential acquisition systems: software and hardware based. In the prototype constructed for this thesis no software solution was implemented because the goal of the system was to provide an EMG signal as raw as possible, with just the necessary manipulation to make it suitable for the ADC stage. Therefore a pure hardware based filter was designed and constructed to adjust the frequency band of the measured signal to the EMG signal model discussed in Subsection 2.1.1.

The filtering stage comes after the amplification (as shown in the blocks diagram 2.1.2 of Section 2), meaning that the signal is expected to be in the volts range and not at the millivolts level at that point (with a significantly higher SNR and immunity to noise and interference pick up), therefore, from the filtering stage, the circuitry could be placed far from the electrodes without signal deterioration. In further prototypes and in the final version of the EMG acquisition system, where the amplification is meant to be soldered at the back of the electrodes themselves, shielded cables could connect the mentioned *active electrodes* with the rest of the system, allowing it to be bigger and bulkier without side effects on noise and interference sensitiveness. Accordingly, no noise or interference calculations will be made from this stage on.

The filter needed for conditioning the signal is a *bandpass* filter (see 1.4.3). The highpass part to remove low frequency components due to movement artifacts, instability of the electrode skin interface [16], some common mode potentials, electrode polarization, and other interfering low frequency signals that often obscure the biopotential signal under investigation [20]. On the the other hand, the lowpass part of the filter is necessary to remove possible high frequency noise introduced by the measuring circuit and to avoid *aliasing* (see 3.10) undesired effects. However in the literature there is no consensus regarding the adequate bandwidth of sEMG (see Subsection 2.1.1 in Subsection 2.1) and each author defines it quite different

from the others. But according to the EMG signal model used for the design of this thesis acquisition system (see Subsection 2.1.1), the band pass should go from around 10Hz until around 1kHz.

A second order butterworth filter was implemented for both low and high pass filters with a Sallen Key topology (for the high pass filter, however, an additional resistor was added between the output and the inverting input of the amplifier, modifying the classical sallen key configuration) (see 1.4.3). The design process consisted in comparing the sallen key transfer function with the standard second order transfer function and adjust the values for the desired cutoff frequencies. Figure 3.17 shows the low pass configuration of a sallen key topology filter (the high pass is obtained by the mirror effect explained in 1.4.3).

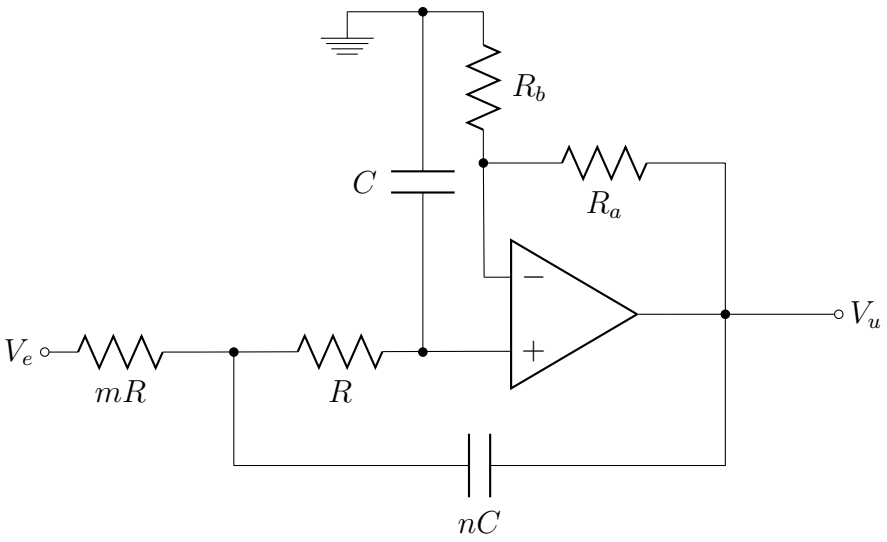

Figure 3.17. Low pass filter based on a sallen key topology.

The expresion for low pass sallen key filter[9] is reported in Equation 3.10 .

$$\frac{V_u}{V_e} = \frac{\frac{R_b+R_a}{R_b}}{s^2 mnR^2C^2 + sRC(m+1-\frac{R_a}{R_b})+1}, \tag{3.10}$$

By comparing Equation 3.10 and the later obtained high pass filter equation with the standard second order filter equations the selection for the actual values of capacitors and resistors was made. Four cells were implemented as Figure 3.18 shows, two for the low pass part and two for the high pass. The chosen operational amplifier was the low noise rail to rail OPA211 of Texas Instruments which has not

[9]http://www.science.unitn.it/ bassi/Signal/TInotes/sloa049.pdf

a very high input impedance as the LF351, but that was suitable for this stage of the circuit.

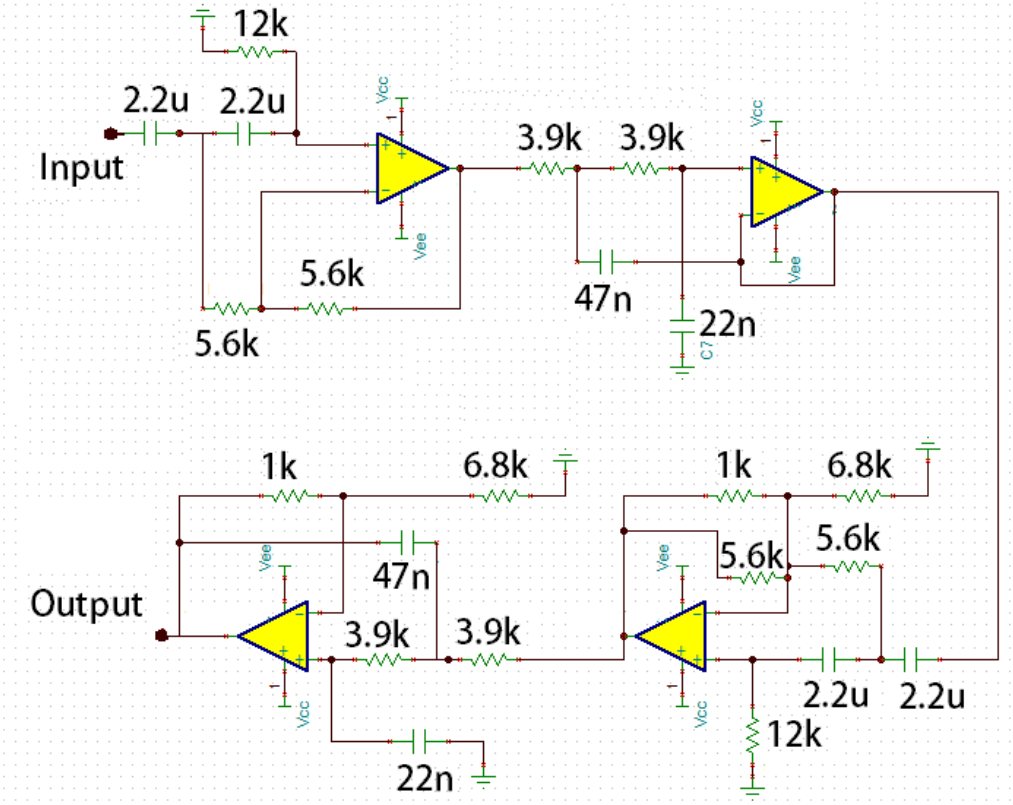

Figure 3.18. Filtering stage of the EMG acquisition system. There are four cells that allow a -40dB slope for both low and high parts of the filter. The resistors and capacitors are labeled with their respective values.

The amplitude of EMG system frequency response after applying the filter is shown in Figure 3.19 next to the system response *without* the filtering stage.

3.8 Isolation

No matter what characteristics are pursued in a medical device, safety is a primary objective. Dangers involved when the human body is connected to electrical equipment are big if proper care is not taken, for example a 60Hz current of barely 10μA flowing through the heart has the potential of causing permanent damage and even death. There are many standards for protection against electrical shock but the most significant technical standard is IEC−601, Medical Electrical Equipment, adopted by Europe as EN−60601 which has been also harmonized with UL Standard

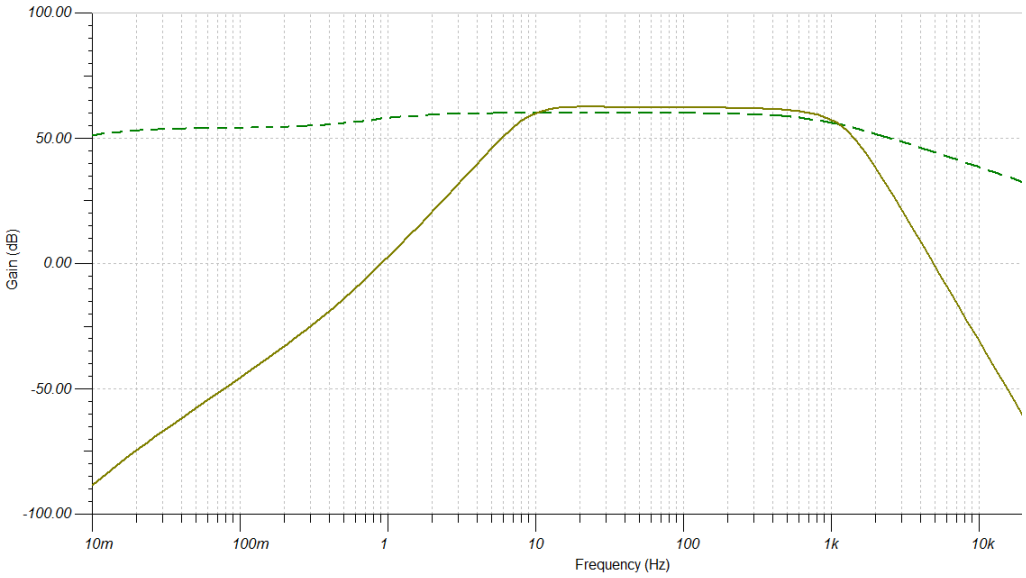

Figure 3.19. The dashed line is the EMG acquisition system output *without* any filtering, and the solid line represents the output when the filtering stage is applied. It can be seen that before the filtering, there is a low pass effect at around 1kHz given by the amplification stage limited bandwidth, and a subtle high pass effect cause by the DC rejection passive filter. Adding the effects of the filtering stage, the limited amplifier bandwidth and the DC rejection, the effective system bandwidth goes from around 3Hz until around 2kHz.

2601−1 for the United States, CAN/CSA−C22.2 601.1 for Canada, and AS3200.1 and NZS6150 for Australia and New Zealand, respectively [20]. Safety standards have classified the risks posed by various parts of medical instruments and have imposed specifications on the isolation barriers to be used between different parts. There are three main parts: the accessible part, the live part and the signal−input and signal−output parts [20], however the scope of this thesis was not to build a final medical device, but a prototype circuit. The electrical safety for the circuit consisted in the isolation of the patient and the parts of the circuit connected to the power line ground, this do not apply to devices that are powered exclusively by low voltage batteries, but because of the AC power line supply of the prototype, isolation was mandatory.

The first step taken to deal with the patient−circuit isolation was to provide a power supply for the amplifiers in contact with the patient electrically isolated from the power supply of the circuit connected to the power line. This feature will be discussed in Subsection 3.9 when the explanation of the power supply block will take place. A second isolation step had to be taken because in somehow the amplified and filtered signal had to be connected to the ADC stage to be sent to the computer.

This isolation could have been implemented in several ways:

- **Optical isolation** A basic optical isolation barrier has two basic elements: a light source and a photosensitive detector. These two elements positioned together and inserted in an electrical circuit form an optocoupler. The most important feature of an optocoupler is that there is a physically insulating gap between the light source and the detector, therefore no current passes through this gap, only light representing the data. Thus the two sides of the circuit are galvanically isolated from one another. When placed on medical devices, the optical isolating barrier counts with an isolation up to 4−6 kV, satisfying medical standards [16] and saving more space in the PCB than other options like transformer−based isolators.

- **Isolation amplifiers** Isolation amplifiers also provide electrical isolation from one part of the circuit to another. They protect from potentially high currents flowing between to different grounded systems by breaking possible *ground loops* (see Chapter 4). They can amplify at the same time they isolate signals and, depending on the device, they can also provide user−available front−end isolated power supplies like the AD215 of analog devices does.

The chosen isolation solution for the EMG acquisition system prototype was the AD215 Analog Devices isolation transformer. It provides complete galvanic isolation between the input and output of the device including the user−available front−end isolated power supplies. The AD215 has a typical nonlinearity of ±0.005% and total harmonic distortion of typically â80dB at 1kHz, allowing signal isolation without loss of signal integrity or quality[10]. Figure 3.20 shows an schematic of the measuring situation when the isolation amplifier is in place.

At the beginning the AD215 was mainly chosen for providing also the user−available front end isolated power supplies, but then in later stages of development, a power supply with a DC−DC converter of its own was thought. However, the AD215 fulfilled its role and separated the system in two parts: the patient floating part and the non−isolated part connected to the power line and to external devices like the PC. Figure 3.21 shows the AD215 configuration for unity gain.

3.9 Power Supply

When choosing a power supply, there are two main alternatives: battery power supply or some type of AC to DC power supply. The first option is the most easy

[10] AD215 datasheet. $http://www.analog.com/static/imported-files/data_sheets/AD215.pdf$

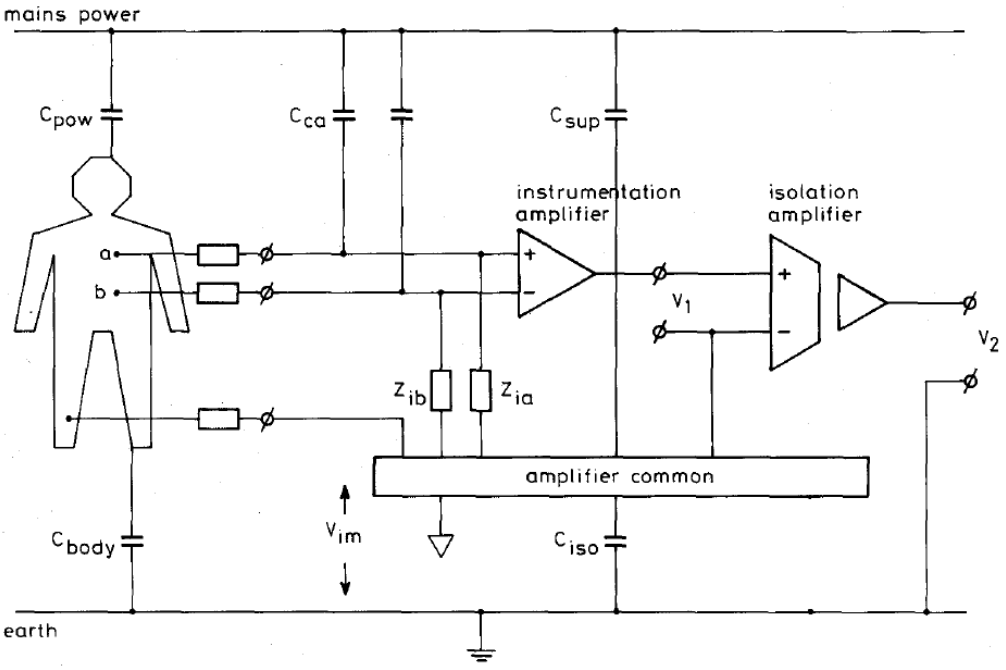

Figure 3.20. The main objective of the isolation stage is separate the two grounds of the system: the one associated to the patient and the one associated to the power line. The schematic shows how the isolation amplifier interfaces both ground systems isolating them. V_{im} is the potential difference between the isolated ground (amplifier common) and earth. Some of the parasitic capacitances coupling the patient and cables with the mains power and earth are also shown. Adapted from [22]

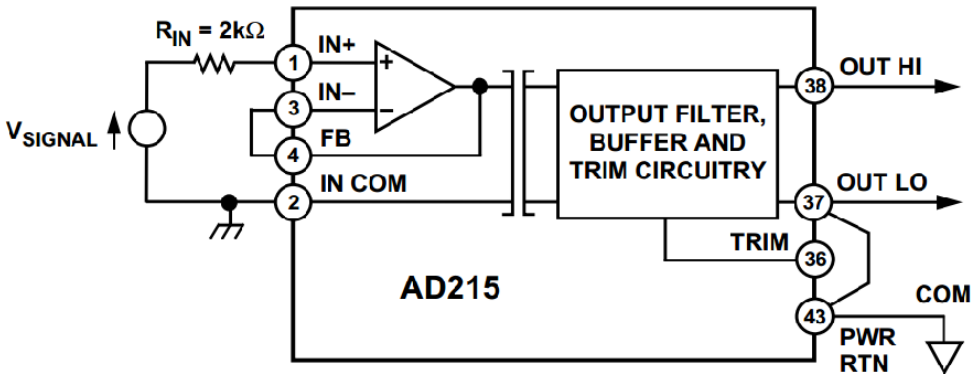

Figure 3.21. AD215 configuration for unity gain. The input V_{Signal} comes from the output of the filtering stage and is referred to the isolated ground given by the *isolated power supply*; the output OUT HI goes directly into the ADC subsystem and is referred to the non−isolated ground of the system. Taken from AD215 datasheet.

to implement because it saves efforts on isolation stages between power line mains and earth, and in rectifiers and filters to DC conditioning. It can be said also that batteries constitute a clean power supply, free of undesired frequency components remaining form the rectification and filtering of the AC power line and possible switching frequencies of DC−DC converters.

However for this prototype construction, a Switched−mode power supply was the selected choice because of the requested power of the overall multichannel circuit. Batteries would have been an easy option at the beginning, but the supervisor of the current thesis wanted to avoid constant replacement of dead batteries. So, knowing that the power line was going to supply the whole circuit, isolation and good voltage filtering were the major concerns of this block design.

The power supply block can be divided in four parts:

- Rectifying
- Filtering
- DC−DC conversion
- Filtering

The rectifier was not implemented as part of this project and a medical DC voltage source as input to the power supply system of the prototype was assumed. This voltage was thought of ±15V and its only function, besides feeding the DC−DC converter to then feed the rest of the circuit, was to supply the needed voltage to the isolation amplifier AD215. The AD215 was the only device of the EMG system that had its power input non isolated. The first filtering stage was put on the design to filter possible voltage ripple from the 15V voltage input source.

3.9.1 The DC−DC converter

A DC−DC converter is a circuit that converts a DC source from one voltage level to another.There are two main types of DC−DC converters:

- **Linear regulator** This type of converter is very inefficient for big voltages drops because it dissipates heat equal to the product of the output current and the voltage drop, therefore they are not used for conversions involving large voltage drops. The heat must be correctly irradiated away from the circuit to avoid damages, making the circuit bigger and bulkier. This devices nowadays are used as a complement in switching power supplies to reduce the output voltage ripple.

- **Switched−mode** A switched−mode regulator is a circuit that uses a power switch, an inductor, and a diode to transfer energy from input to output. The changing from one DC level to another is done by storing energy to release it at the output at a different voltage. Prior to the invention of the Vertical Metal Oxide Semiconductor (VMOS) power switch, switching supplies were generally not practical; but nowadays are the most efficient conversion method.

Given that the voltage drop in the EMG system power supply was high (from ±15V down to ±5V), linear regulation was not an option. Hence, a switch DC−DC converter had to be selected.

In order to properly select the DC−DC converter, an approximation of the maximum power consumption per channel was calculated. The first assumption to perform this calculation was that the major power consumption was from the active parts of the circuit: the instrumentation amplifier and the operational amplifiers of the filters. This was motivated by the fact that the biggest resistors were placed in the parts of the circuit in which the signals are at their lowest level; and where the signal is in the volts range, the resistors are sufficiently small, therefore the major power consumption lies in the amplifiers. Table 3.3 summarizes the power consumption of each amplifier in the worst case.

Device	Devices per channel	Power consumption
INA114	1	$10V \times 3mA$=30mW
LF351	3	$10V \times 3.4mA$=102mW
OPA211	4	$10V \times 4.5mA = 180mW$

Table 3.3. Maximum power consumption of each active device per channel. The total power consumed for one channel is approximately of 312mW

From Table 3.3 the power consumption per channel was estimated in *at least* 312mW, and for a 8 channel PCB the power consumption scales up until at least 2.5W (it has to be recalled that this power consumption is only for the active parts of the circuit because of the previously made assumption). Taking these calculations into account a 3W capable DC−DC (5V) converter was needed.

One of the DC−DC converters of the THN−15 series of TRACO POWER fulfilled the requirements providing at the same time a high 88% efficiency: The THN 15−1221 was selected.

3.9.2 Power supply filtering

The inherent switching inside the DC-to-DC converter gives rise to potential sources of noise. This noise manifests itself on the output voltage as spikes at the switching frequency [4]. For circuits that need lower noise levels than the supply is capable of, there are two techniques to apply: LC filtering or an output filter capacitor.

The classical capacitor at the output acting as a filter meets its limit because of the Effective Series Resistance (ESR) and Effective Series Inductance (ESL) parameter. Basically what happens is that the high frequency components that should be "smoothed" by the capacitor connected to ground do not, due to the equivalent circuit of the real capacitor with parasitic resistance and inductance shown in Figure 3.22.

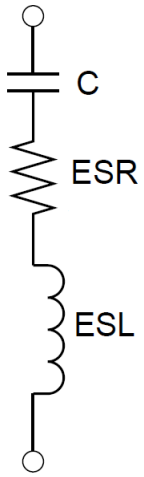

Figure 3.22. Non ideal capacitor equivalent circuit.

The impedance that the capacitor offers against signals decreases with the frequency but until certain minimum point. Thenceforth it begins to increase again thank to the ESR and ESL. Paralleling several capacitors might help to reduce the minimum impedance point but does not help to avoid the ESR and ESL parasitic effects. Figure 3.23 exemplifies the situation.

For circuits that need high accuracy and the lowest noise possible (as the EMG system), there is only one option left: LC filtering. Figure 3.24 shows an schematic version of the actual LC filter implemented during the prototype construction.

The cutoff frequency of the lowpass filter was calculated to be less than the tenth part of the switching frequency of the used DC−DC converter which, according to its datasheet, is typically 400kHz. Then, the cutoff frequency (f) was set around 30kHz and the inductance (L) fixed to 6.8μH to obtain a capacitor value of:

C= $1/(4\pi^2 f^2 L) \approx 3.3\mu F$

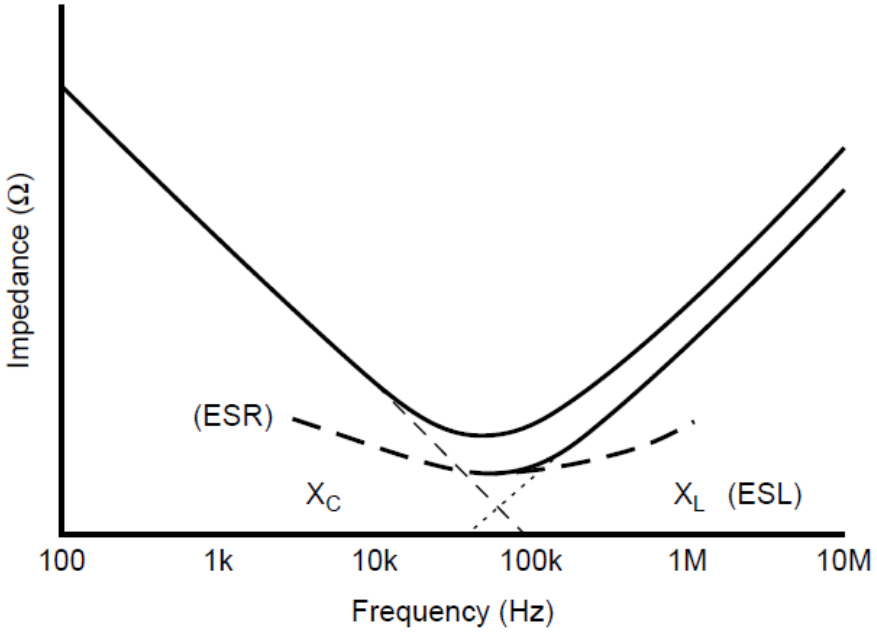

Figure 3.23. Impedance vs frequency capacitor characteristic. (1) Improvement from paralleling several capacitors with equal total capacitance. It can be seen that higher frequencies find some impedance in the capacitor and therefore pass to the output in the form of ripple or spikes.

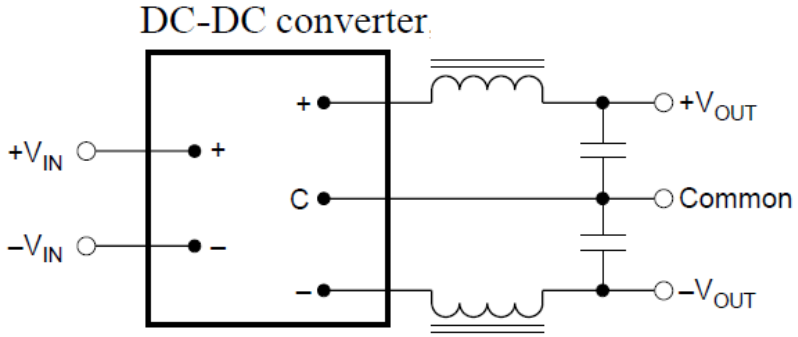

Figure 3.24. Filter circuit for DC−DC converter. Adapted from [4].

3.10 ADC

The last block in the hardware chain between the muscle and the PC is the Analog to Digital Conversion (ADC), in charge of sampling and converting an analog continuous quantity into a digital discrete time representation. As it was discussed in 3.10, there are many ways of doing this conversion, each one with its own advantages and problems.

Given that the EMG system is intended to be a multichannel system, a *simultaneous* ADC is required to avoid phase shifts between signals of different channels. There are two main alternatives to implement simultaneous sampling: *Simultaneous Sampling Architecture* and the *Simultaneous Sample and Hold (SSH)* (see Section 3.10). The first alternative was the one chosen to be part of the EMG acquisition system prototype because is the one that performs sampling in a real simultaneous way by providing each channel with its own ADC converter.

The ADC board purchased by the DLR Bionics group was the National Instruments NI PCI−6143 of the NI S series. It has dedicated ADCs per channel (real simultaneous sampling) and because of this, there is less concern with settling time and the noise and error caused by switching input channels (what happens, for example, in the case of Simultaneous Sample and Hold (SSH) that needs a multiplexer in order to use the only available ADC converter). Table 3.4 summarizes some of the NI PCI−6143 characteristics and Figure 3.25 shows its internal block diagram.

Analog features
8 differential Channels
16 bit resolution
250 kS/s/Channel sampling rate
±5 input range

Table 3.4. NI PCI−6143 main analog features.

To avoid aliasing, the Nyquist criteria must be fulfilled (see Section 3.10). In the specific case of EMG measuring, where the highest frequencies expected are between 1kHz and 2kHz (according to the model discussed in Subsection 2.1.1), the sampling frequency must be at least of 4kHz. The NI PCI−6143 has a 250 kS/s/Channel sampling rate, which largely meets the Nyquist frequency requirement.

The resolution (R) of the system can be calculated as the total input range over the total number of different values for a 16 bit representation:

R=5-(-5)$\frac{}{2^{16}}$

It means that the limit imposed to the system minimum useful value by the ADC stage is 153μV, however the thermal noise is much more limiting (see Section 3.4.1) and even more limiting are the effects produced by the potential divider effect as it was observed during the circuit tests (see Chapter 5).

Also, the value of the amplifier gain (see Section 3.4.1) was chosen taking into account that any effort to amplify the EMG signal above 5V was going to be useless

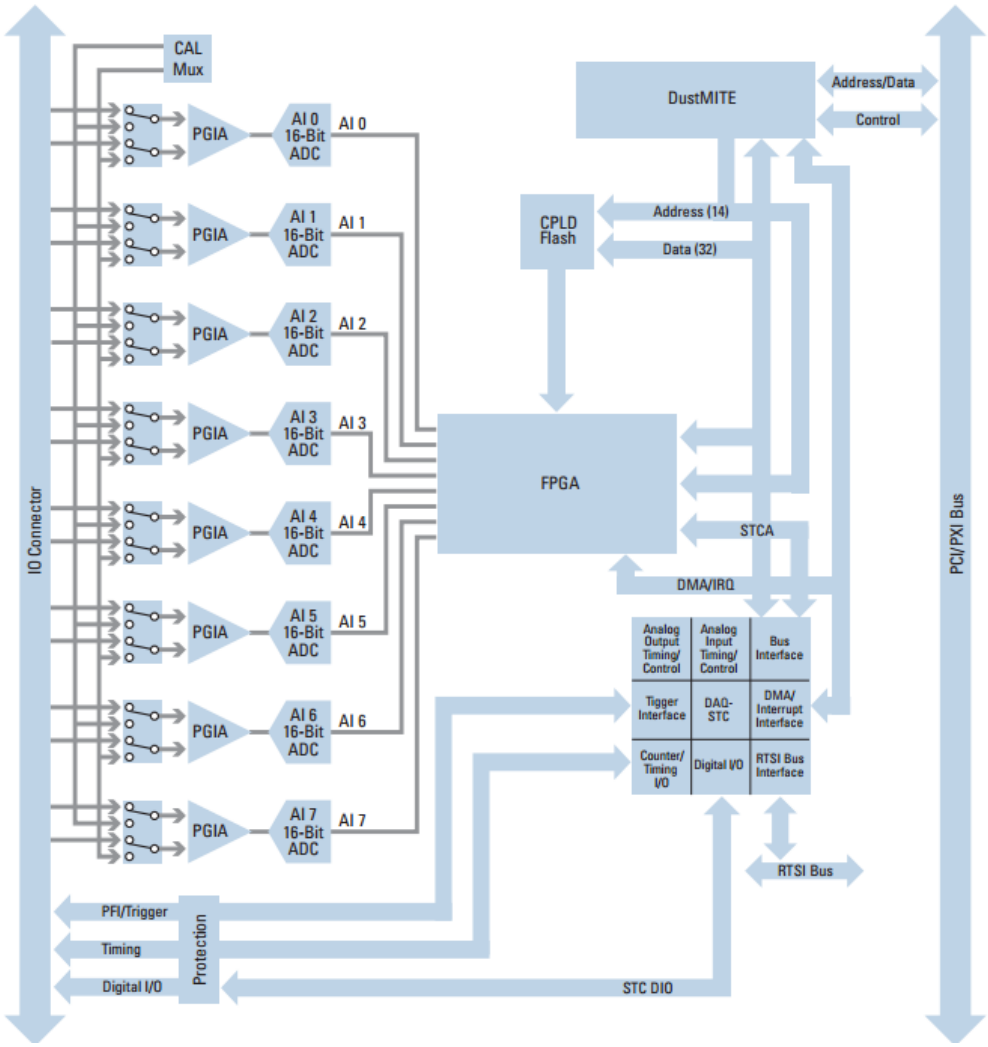

Figure 3.25. NI PCI−6143 blocks diagram. The dedicated ADC converter for each channel and the PCI/PXI Bus output can be seen. Taken from NI PCI−6143 datasheet.

because of the ADC converter input range. Therefore the gain was set in such a way to match the maximum expected EMG value (4mV) with a little less of the ADC converter input range maximum value (4.8V).

Chapter 4

Circuit construction

The last chapter covered the design process and the concepts behind each block of the EMG acquisition system. Once the design was complete and reviewed by the supervisors of this thesis at the DLR, the construction process of the prototype began. Instead of using breadboards or perfboards for a rapid circuit construction, the prototype was done directly in a custom designed PCB. The construction process started with the PCB layout design and finished with the manual soldering of each component in place for testing and validation.

The steps followed for the PCB construction [6] were:

1. Draw a complete schematic on paper.
2. Prepare a bill of materials (BOM).
3. Hold a preliminary design review.
4. Order components.
5. Create schematic symbols and layout footprints for components not found in the standard library.
6. Draw a schematic with the PCB schematic editor.
7. Draw and route a layout with the PCB layout editor.
8. Hold a final design review.
9. Generate and inspect Gerber files for your board.
10. Send your Gerber files to a manufacturer.
11. Correct any manufacturability errors and resend the Gerber files.

12. Assemble the components onto the board.
13. Test the board.
14. *Repeat the steps above to fix errors in the initial board*[1].

Two different programs of the PADS suite were used: PADS Logic©for the schematic entry of the designed circuit (step 6), and PADS Layout©which allows to draw and route the actual PCB layout (step 7).

- PADS Logic©is a schematic capture tool designed to build a simple front−end environment for PADS Layout©. This program offers instant access to every sheet in the design, as well as online parts editing, fully integrated with PADS Layout©making the transfer between schematic and layout easy and efficient. However many of the devices selected as parts of the EMG system (the INA114 and LF351 for example) were not available in the DLR PADS library and had to be created for the first time (step 5).

- PADS Layout©is the Mentor Graphics tool that supports drawing and routing of the PCB layout itself. It interfaces with PADS Logic©allowing efficient design transfer between schematic and layout and also fast identification of corresponding components, ensuring fast placement and accuracy.

4.1 PCB design considerations

The printed circuit board on which the circuit is located constitutes an additional circuit component that has to be considered carefully for good results in prototypes construction. Listed below are the practical considerations that most affected the development of the EMG prototype.

- **Tracks** The tracks between connexions should be as direct as possible without forming 90° curves or peaks, being the most continuous possible. Two main characteristics have to be set: the width and the space between tracks and other PCB elements (clearance). In this prototype, the tracks width was set in 0.3mm by default (there were areas in which thinner or wider tracks were required) and the clearance width in 0.2mm (except the clearance to board line that was set in 0.5mm). This values were selected because in this first prototype PCB area optimization was not pursued, hence there was no need of selecting really small widths as 0.2mm to fit everything in little space.

[1] *Missing step*

When drawing the tracks for the power supply, wider tracks were needed because of the higher current transport. The following indicative rule was used [26]: 0.4mm x Amper. A 0.6mm track width was used, expecting currents of 1.5A currents (see Subsection 3.9).

In general, tracks have to be as short as possible to avoid parasitic effects, noise and/or interference pick up.

- **Number of layers** The construction of the EMG prototype was made in a Multilayer PCB. Four layers were used: the top layer for components placing and routing, the second layer as a ground plane (splitted ground plane due to the presence of two independent commons), the third layer as power plane (splitted in ±5V and ±15V areas) and the fourth layer for routing if necessary. Some of the reasons for choosing a multilayer approach are listed below:

  – Better routing for power as well as ground connections.

  – Easier signal routing.

  – Distributed capacitance between the power and ground planes, reducing high frequency noise [14].

  – Better EMI/RFI rejection thank to the desirable effects of the *Image Plane Effect* equivalent image currents.(Further details in [8]).

- **Ground planes** There are two different grounds in the EMG system: one isolated from the power line earth in contact with the patient and other non−isolated connected to the isolation amplifier and ADC stage in contact with equipment directly connected to the power line, like the PC for example. One layer was used to locate those two grounds allowing direct ground connection everywhere in the board and reducing the effects of *ground loops*[2]. Figure 4.1 shows the ground plane division in the layout design.

- **Power distribution** Power planes are also highly recommended because they deliver power at any point of the circuit, avoiding the use of large tracks carrying and distributing the power. In the EMG prototype there are four power nodes: 5V, −5V, 15V, −15V; all of them were placed in the same layer as Figure 4.2 shows.

[2] *Ground loop* A ground loop is created when an undesired current flows between two points that should be at the same potential, but which are not for some reason, causing noise and interference in the system. In the next chapter, a problem involving a ground loop in the validation setup will be discussed.

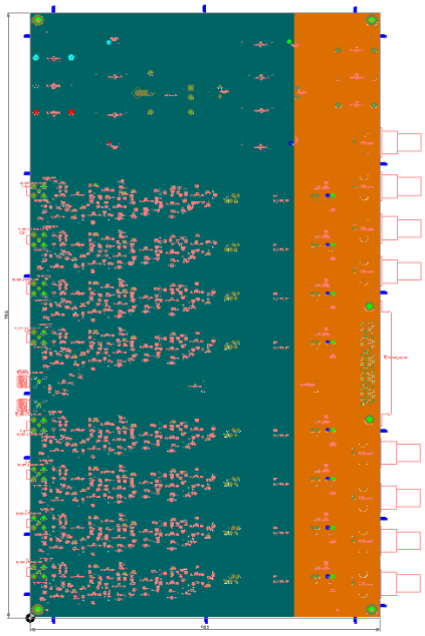

Figure 4.1. Ground plane of the EMG prototype circuit. The left part is the isolated ground and the right part the non−isolated one. In between them, below the position of the isolation transformers, there is a gap of 0.5mm.

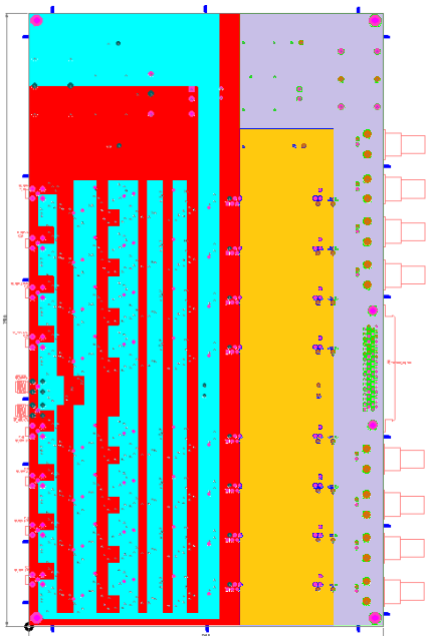

Figure 4.2. Splitted power plane. The two right areas correspond to the ±15V and the left interlacing areas to the ±5V.

The method most often used to *decouple* the high−frequency noise is to include a capacitor connected from the Integrated Circuits (ICs) power pins to the ground pins. It is important to keep the traces on this decoupling capacitor short. If not, the traces on the PCB will have significant self−inductance, defeating the purpose of the capacitor [14]. Large bulky capacitors, electrolytic for example, are recommended to be placed in parallel with one smaller high frequency ceramic capacitor as close as possible to the IC to decouple power and ground. Figure 4.3 exemplifies how a coupling capacitance for an IC should be placed.

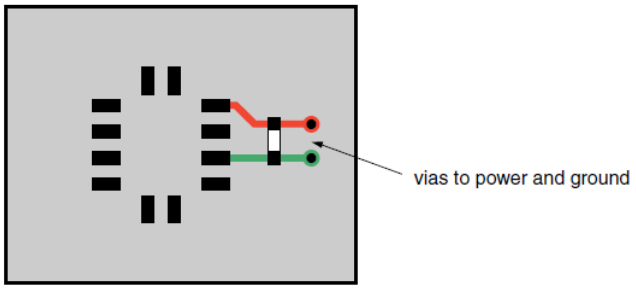

Figure 4.3. The capacitance should be as close as possible to the IC and the vias to the ground and power planes should also be very close to avoid long loops.

- **Board structure** Some structure has to be followed in order to place the components in the PCB, and the most convenient is by *functional groups*, in other words, all the components used for some specific purpose should be place together and not far away from each other. The blocks diagram presented in Subsection 2.1.2 served as a guide to the components placement, in that way there was not unnecessary crossing between signals or back turns in the signal flow, helping to minimize tracks length and therefore, noise and interference pick−up.

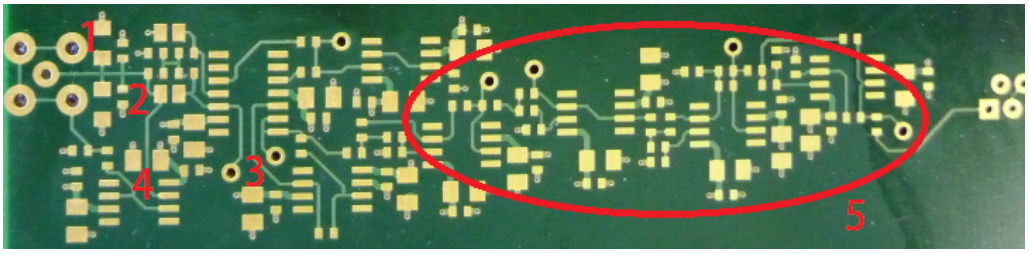

Figure 4.4. Detail of a single channel layout. It can be seen how the signal flow determined the component placement: (1) ESD protection. (2) DC rejection. (3) Amplifier. (4) Shield Driver. (5) Filtering stage.

4.2 Prototype structure

As it has been already mentioned, the EMG system is intended to be a multichannel acquisition system, meaning that the whole block diagram discussed since Subsection 2.1.2 has to be repeated for each channel (all the channels must be treated and constructed identical to avoid any external difference between the measured EMG signals).

The final version of the EMG acquisition system is expected to have more than 20 monopolar channels[3], but given that the National Instruments ADC cards can handle only 8 channels at the same time, a modular approach in which boards of 8 channels are interconnected to support 16, 24 and 32 channels, was developed. However, all the channels are compared to the same reference electrode and only one DRL electrode is placed in the human body, therefore a common subsystem in charge of those two aspects and able to manage any of the four configurations (8, 16, 24 or 32 channels) had to be developed. The solution was achieved with the construction of two different PCBs: one where the reference electrode is buffered to be then connected to n number of channels and where the DRL is implemented; and another PCB where the amplification, filtering etc. of 8 channels are implemented. Figure 4.5 shows the situation.

For the first prototype (the one constructed for this thesis) just one PCB1 and one PCB2 were made. And although many revisions were conducted before their manufacturing, some footprint and tracks errors had to be corrected with soldering and wiring after the PCB production. PCB2 is not power independent, in other words it needs to be connected to one PCB1 to get the power from. It was implemented like this because in any case, a PCB2 is never going to be used alone without at least one PCB1, therefore there was no need of powering it independently.

The DRL circuit placed on the PCB2, and explained in 3.6, has a modification that allows it to select a different feedback resistor depending on the number of PCBs1 (which translates in the number of used channels) connected to it. If only 8 channels are used for a certain measurement, the common mode of each channel has a weight of 1/8 of the common mode value fed back to the human body. If 16 channels are used, the weight then is 1/16 and so on. The resistor selection is made manually with a jumper. Figure 4.6 shows the PCB1 and Figure 4.7 shows the PCB2.

The splitting into two boards solution explained above is just *temporary* and for *rapid prototyping* purposes, in a final EMG acquisition system is not an option because it is a really bulky and impractical setup, and the many cables between

[3] A monopolar measure is made between one electrode and one reference point where no muscular activity is assumed.

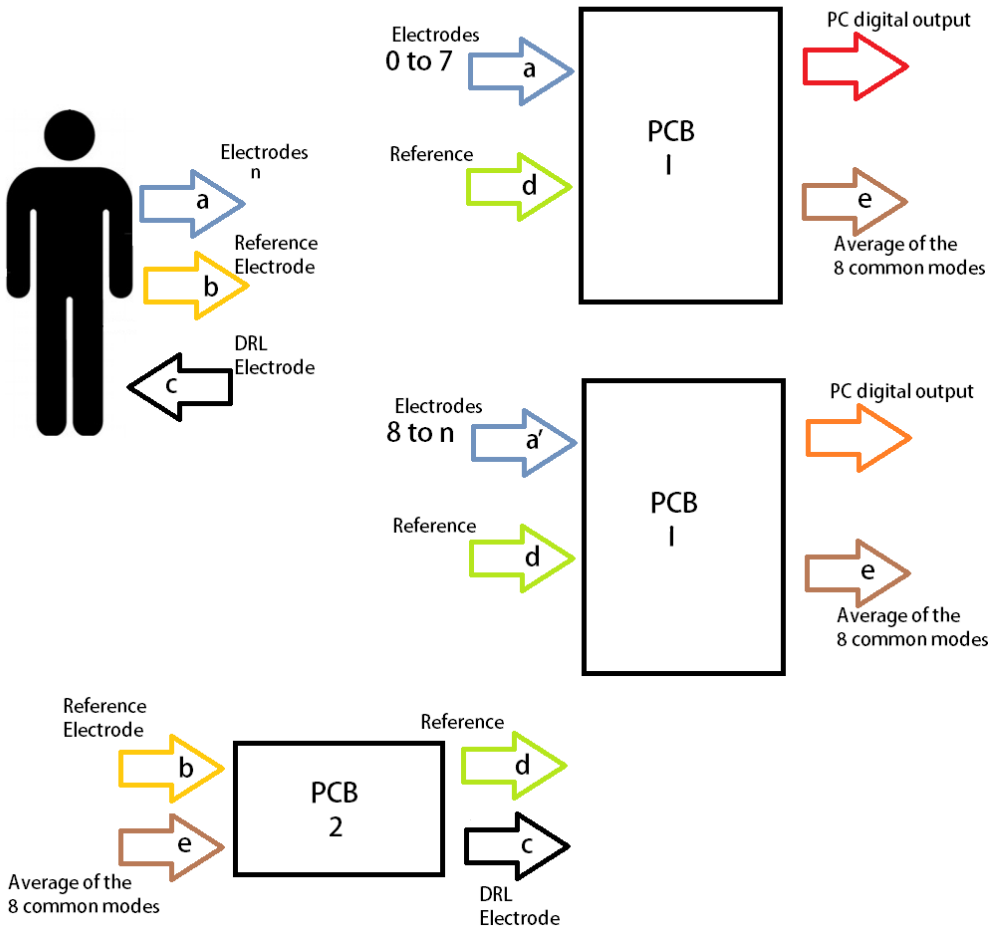

Figure 4.5. The arrows with the same letter are connected to each other and represent the different inputs and outputs of the different PCBs of the system. The PCB 1 represents one of the four possible boards where the blocks between the electrodes and the ADC stage, for 8 different channels, are placed. The PCB2 is the auxiliary board that buffers the output of the reference electrode before connect it to all the used channels, and also performs the average of the PCB1 averages for the DRL stage.

boards flying around, pick up a lot of noise and interference, making even more difficult the EMG signals measuring. Figure 4.8 shows the prototype set up with PCB1 and PCB2 connected to each other.

Another important aspect in the PCB construction is the type of cables used to connect the electrodes to the main board and to interconnect the signals (excepting power and ground) between PCB1 and PCB2: Samtec RG 178 cables as shown in Figure 4.9 were used. And although these cables were shielded as explained in Section 3.5, interference problems arose (see Chapter 5) because of their length and the loops that the cables themselves formed.

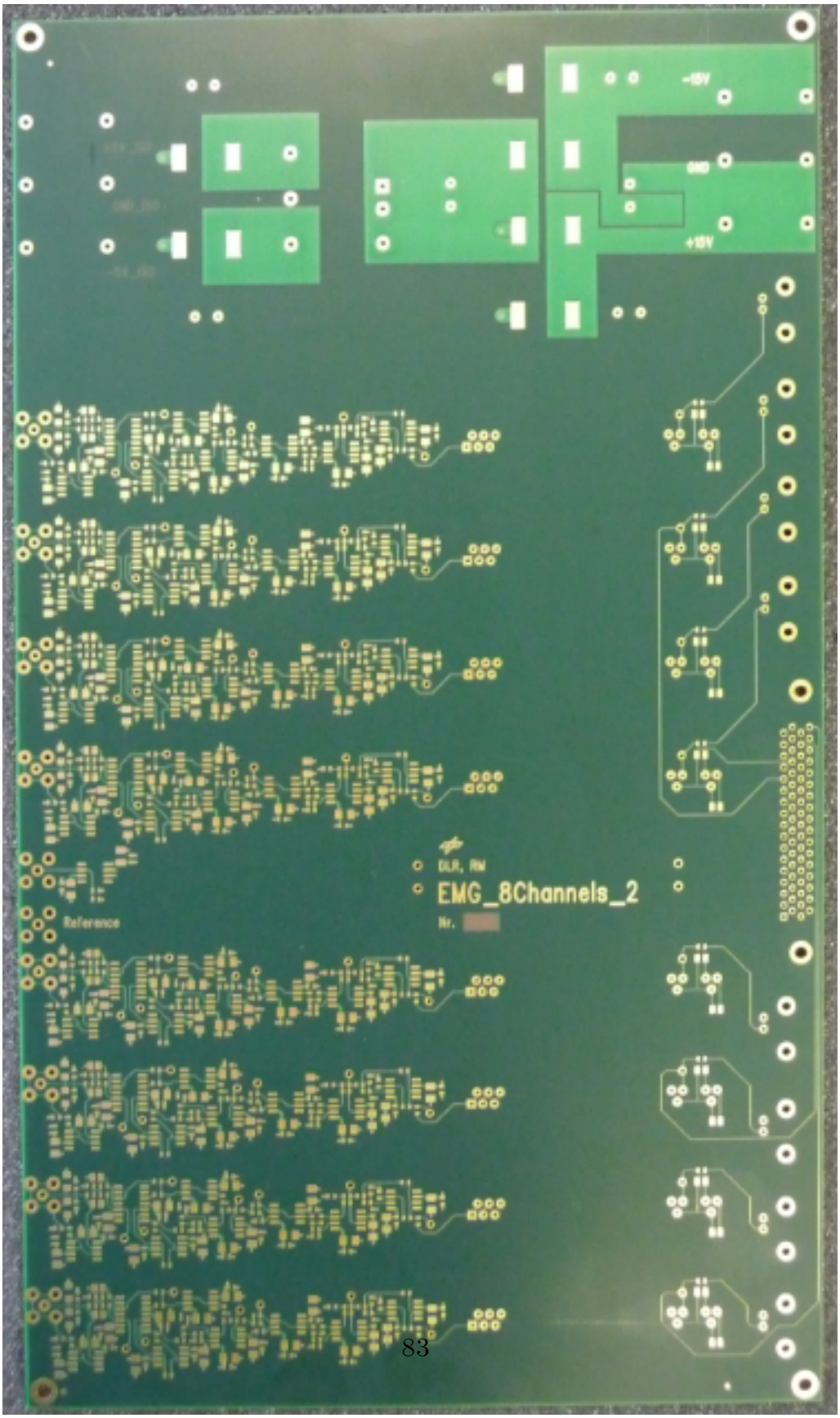

Figure 4.6. Unsoldered PCB1. This PCB supports eight channels when connected to PCB2. In the upper part lies the power supply which powers also the PCB2, then there are 8 identical amplification and filtering circuits (one for each channel) and around the PCB center, the connection for the reference (input) and the average of the common mode of all the channels (output) is placed.

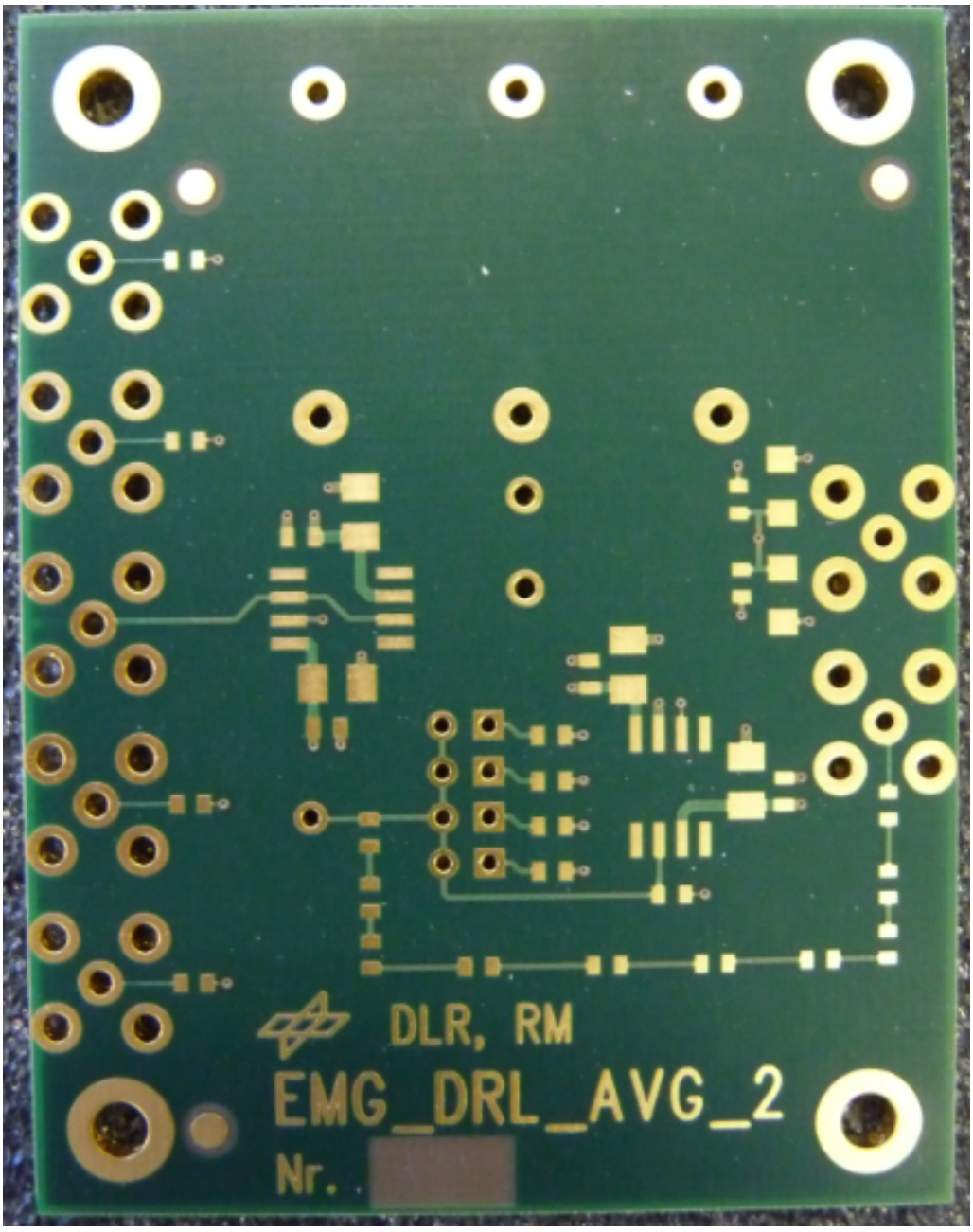

Figure 4.7. Unsoldered PCB2. This PCB is in charge of buffering the reference signal (coming from the reference electrode) to then connect it to the used channels in up until four different PCB1. It is also in charge of producing the DRL signal by averaging the common modes of all the channels involved in the measuring.

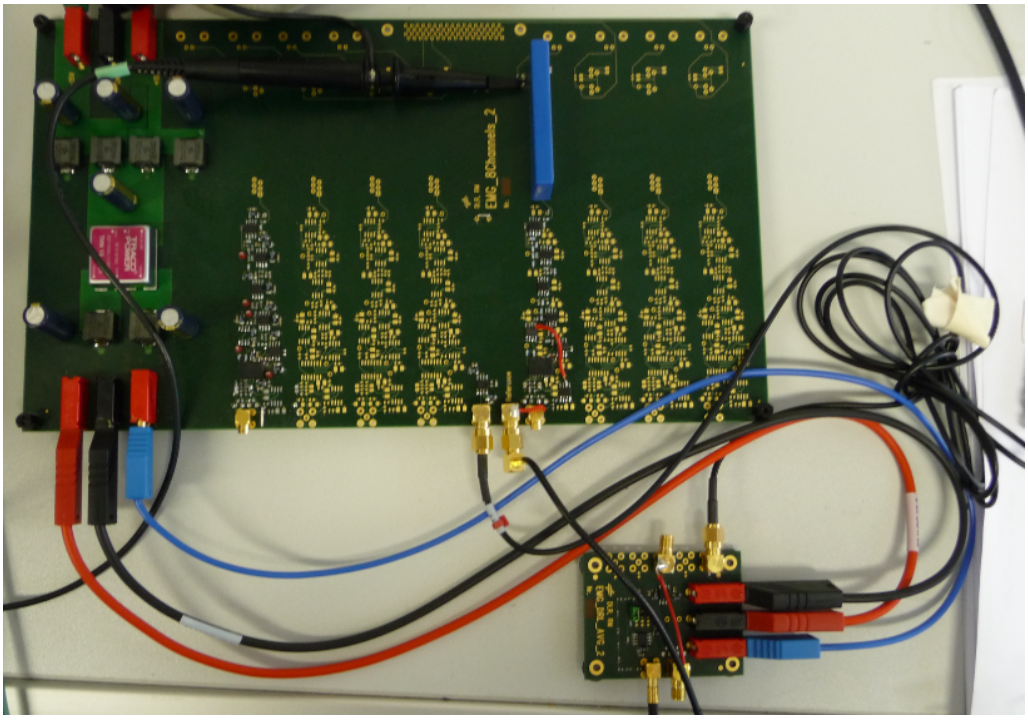

Figure 4.8. PCB1 and PCB2 connected for EMG measuring. It can be seen that the large number of *long* cables flying around are not a practical solution, even when only 8 channels are connected.

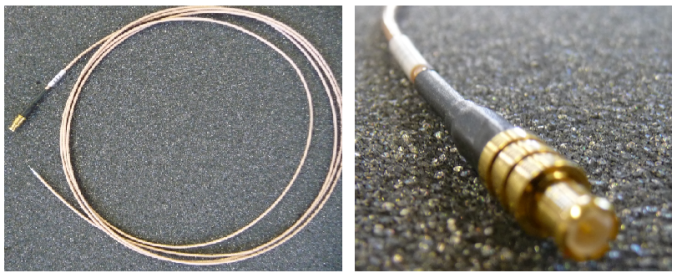

Figure 4.9. Samtec RG 178 cables used in the electrodes−main and PCB1−PCB2 connections.

Chapter 5

Circuit validation

Before connecting the circuit to the human body, each block was tested separately and the complete EMG system was characterized using a function generator and a resistive network to emulate the electrode−skin impedance. The actual gain, frequency response, common mode rejection and general aspects of the prototype are presented in this chapter with the used validation setups. The chapter ends with some notes and tips for future prototypes construction.

The equipment used to conduct the tests on the circuit consisted in a KROHN Hite frequency generator, a Tektronix TDS 2014 oscilloscope (although the images presented in this chapter were taken with a LeCroy WaveRunner Oscilloscope) and a linear isolated Power source.

A problem arose when the isolation stage was connected because a ground loop was formed. The function generator that emulated the muscle EMG signal generation was isolated (through an isolation transformer) to simulate the floating human body, but when the output of the circuit was measured with the oscilloscope, the only lecture was the 50Hz common mode. Breaking the ground loop by removing the isolation transformer solve the problem. Figure 5.1 explains the situation.

- **Frequency response** The first test was done to determine the circuit frequency response. In order to do that, a 4mV (8mVpp) sinusoidal wave at different frequencies was given (directly form the function generator) as input to the EMG prototype. Table 5.1 presents the output amplitude for some frequencies (without the filtering stage nor the DC rejection connected) while Figure 5.2 plots gain vs frequency.

  The second frequency characterization was done after connecting the band pass filter and DC rejection to the amplifier. Table 5.2 and Figure 5.3 resume the results of the total EMG system frequency characterization.

  Figure 5.3 shows a series of blue dots which represent the data collected, and some red lines that trace the asyptotic Bode plot. Three different slopes can

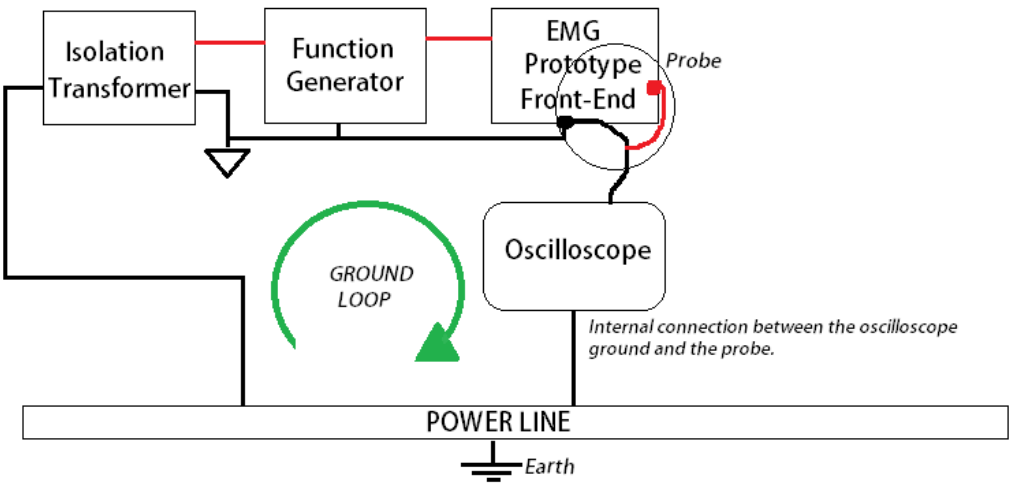

Figure 5.1. The problem was that the oscilloscope internally connects the probe negative with its own ground, therefore it was internally connecting the isolated ground of the EMG circuit with the main power earth through the probe, closing a ground loop. In this way the measuring was being done against the common mode of the power line and not against the isolated common.

Frequency (Hz)	Output value (V)	Gain
0.103	7.82	977.5
1.03	7.81	976.25
4.99	7.8	975
10.25	7.796	974.5
50.25	7.79	973.75
100	7.79	973.75
200	7.75	968.75
500	7.38	922.5
1000	6.35	793.75
1500	5.35	668.75
2000	4.5	562.5
5000	2.05	256.25
10000	1	125

Table 5.1. Amplifier output for a 8mVpp sinusoidal input.

be seen. The first slope ($+40dB/dec$) corresponds to the high pass part of the system band pass filter, the effects of the DC rejection filter are not seen because its cutoff frequency is ≈0.6Hz; this makes that the $+20dB/dec$, coming from the DC rejection filter, vanishes before that the bandpass filter affects

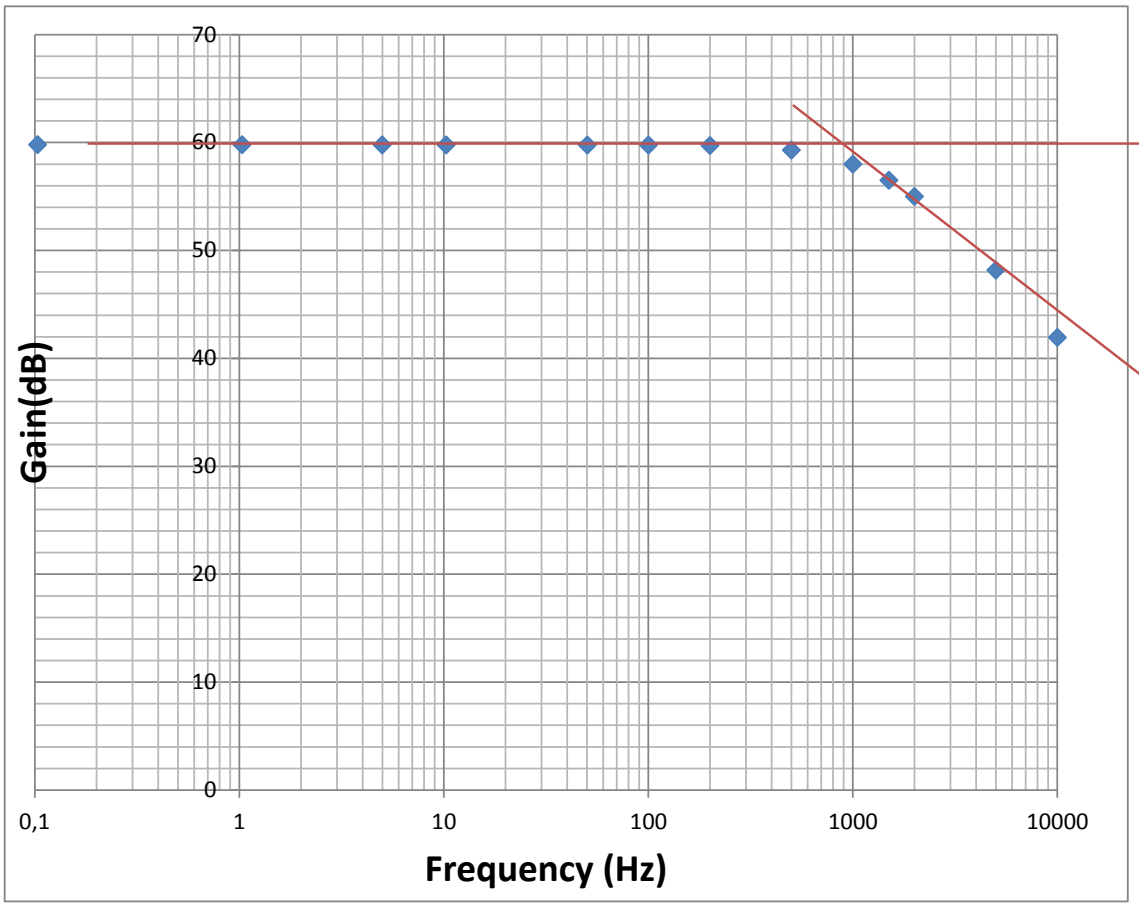

Figure 5.2. The blue dots represent the collected data and the red lines trace the asymptotic Bode plot. It can be seen that even with 1% tolerance resistors, the desired gain of 1000 (60dB) was never reached, the maximum gain was 977.5 (≈59.8dB).

the system. The second line in the asymptotic Bode is the flat pass band, with an approximate gain of 60 to 61dB (translated into 1000 to 1200 times magnitude). If these numbers are comapred with the ones in shown in 5.2, the reason of designing a *non unity* gain filter, is understood: if the gain is left *only* to the amplification stage, tolerance in components prevents reaching the desired minimum 1000 gain, however if some additional gain is left for the filtering stage, the amplification requirements are met. The last part of the filter corresponds to $-60dB/dec$ line, product of the combined effects of the lowpass part in the filtering stage among with the INA114 intrinsic low pass filter. This sharp slope ensures virtual absence of harmonics that could be aliased by the ADC stage.

Frequency (Hz)	Output value (V)	Gain
0.1	5m	0,625
1	45m	5.6
14	8.8	1100
50	9.36	1170
100	9.57	1196,25
500	8.93	1116,25
700	7.74	967,5
1000	4.85	606,25
1200	3.2	400
1500	1.6	200
2000	580m	72,5
5000	5m	0,625
10000	3m	0,375

Table 5.2. Amplifier output for a 8mVpp sinusoidal input.

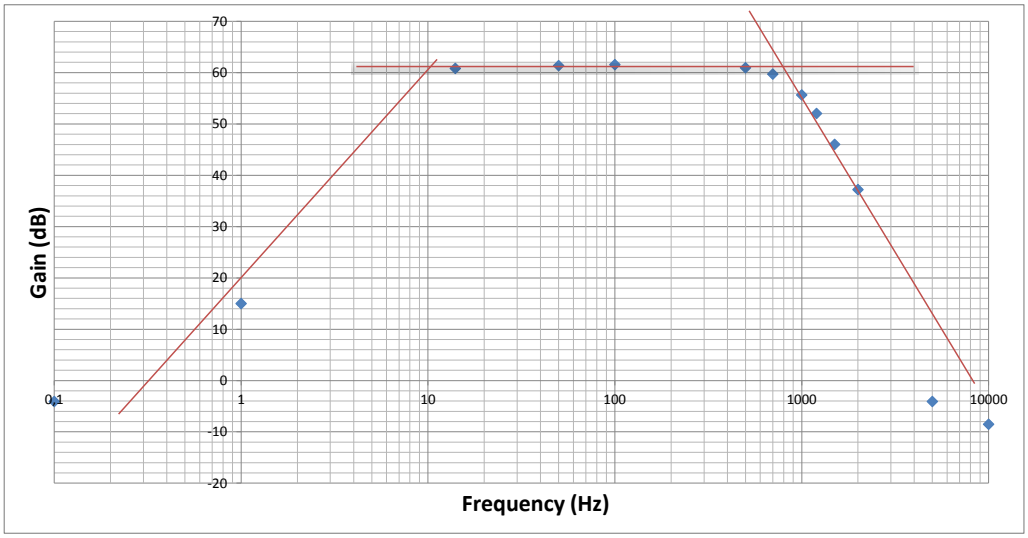

Figure 5.3. The blue dots represent the collected data and the red lines trace the asymptotic Bode plot. The band pass goes from around 10Hz until 1kHz.

Summarizing, the effective system bandwidth goes from around 8Hz until to 1kHz, satisfying the frequency specifications imposed by the model in Section 2.1.

- **Amplification** The frequency response of the circuit was determined by connecting directly the function generator to the amplifier input at the desired

amplitude (8mVpp) and measuring the output for different frequencies. However, in real applications, the circuit will not be connected to a 50Ω source, but to the human body. This means that the expected output impedance can be as high as 1M, and this changes everything and a new validation setup had to be implemented in order to simulate the human skin−electrode interface impedance.

This new setup consisted in a voltage divider with an equivalent output impedance of 100kΩ, even that the worst case happens when the impedance is 1MΩ, because this only takes place when no skin prepartion at all is done, and when bad construction electrodes are used, which is not the case of the future EMG system working conditions. Instead, 100kΩ is a high value that can be encountered even with the best measuring conditions. Figure 5.4 shows how the test signal was produced:

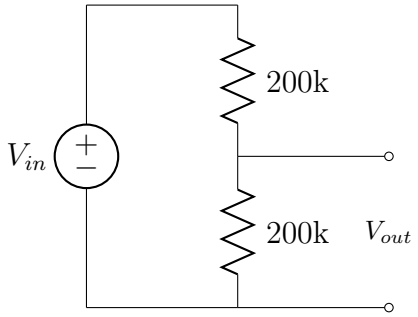

Figure 5.4. Test signal generation

The function generator voltage (V_{in}) is set at 16mVpp in order to get 8mVpp at V_{out}, the equivalent output resistor is equal to 100kΩ (parallel of the two 200kΩ) and from there the EMG system is connected. However the construction of this simple voltage divider interfacing the function generator with the EMG acquisition system was really problematic because of the interference it helped to picked up. Figure 5.5 shows this little adaptation.

The first test was performed without the shields connected and taking the signal from the adaptation output of Figure 5.5. Figure 5.6 shows the resulting amplified signal coupled with the 50Hz common mode.

It can be seen from the amplitude changes that the 50Hz signal interferes with the higher frequency sinusoidal signal (the one that represents the EMG signal) limiting the effective gain and changing the shape of the output. The same measurement is repeated connecting the shields, but this time, the result signal has minimum interference. See Figure 5.7. The remaining noise is caused by

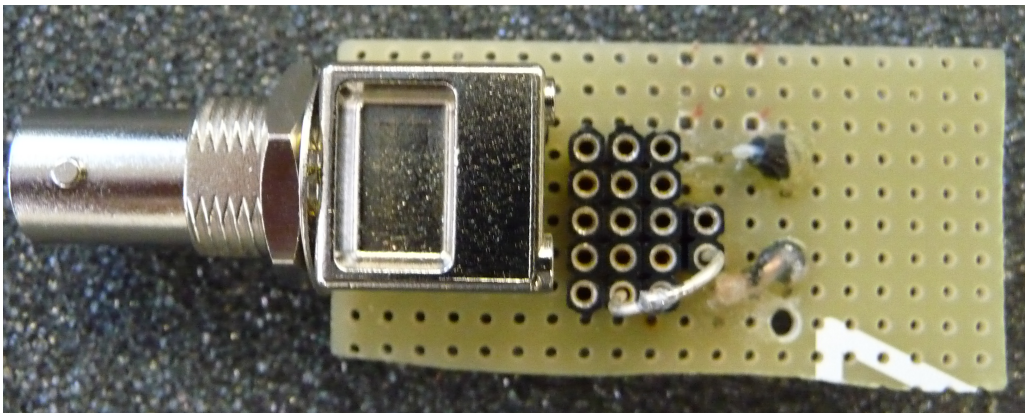

Figure 5.5. The function generator output was plugged to the BNC connector and then the resistive arrange was made by connecting different resistor values in the protoboard−like holes arrengement. The output was finally fed into the circuit through Samtec RG 178 shielded cables.

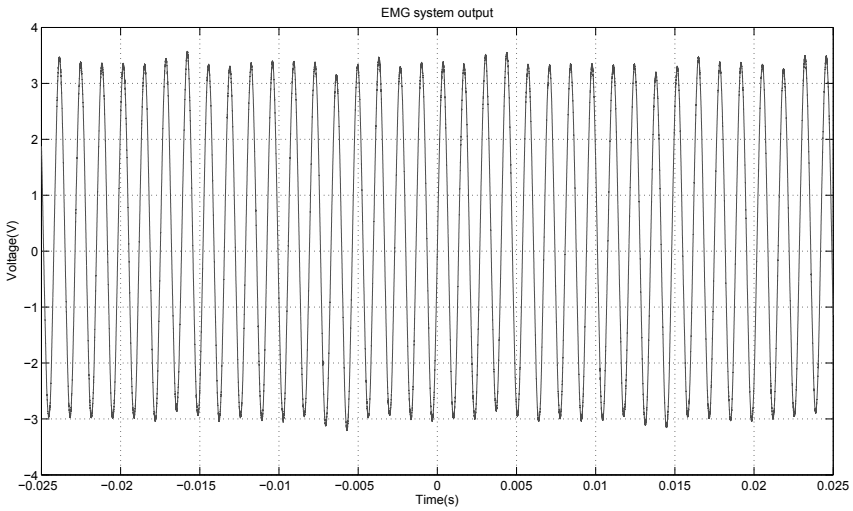

Figure 5.6. The 50Hz common mode signal interferes with the sinusoidal signal that represents the EMG, changing the effective gain and form of the amplified output.

the factors explained in previous chapters, and the remaining interference is due to the still unshielded parts, like the voltage divider of Figure 5.5.

The next test conducted had not the voltage divider connected so far away from the amplifier input, but it was soldered at the very input pins and the shielded signal arrived directly there. The result of this test reduced even more the already low interference, but did not eliminate it completely. The problem

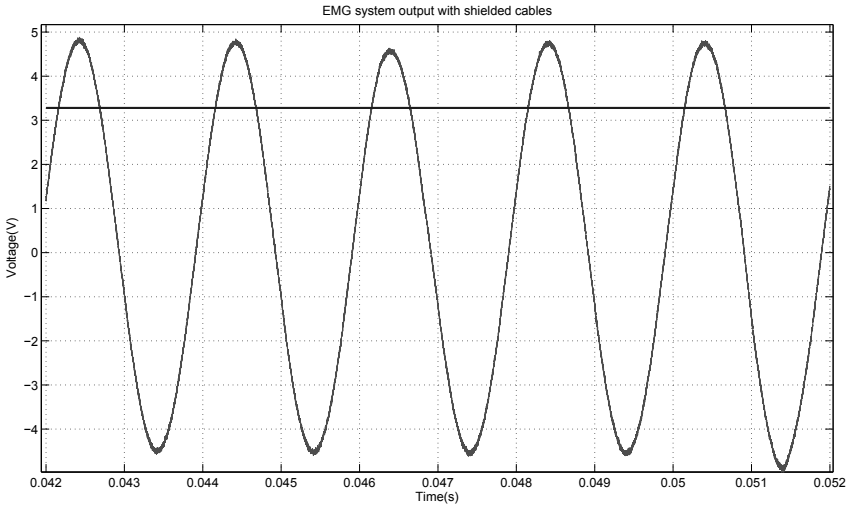

Figure 5.7. The sinusoidal signal is exposed to the same interference sources than before, but the presence of the shields reduce dramatically their impact. The horizontal line marks the RMS value.

was in one of the PCB tracks.

The prototype circuit was designed for a multi−channel system, where each electrode is connected to a different channel but always referred to a common *reference* electrode. It has been shown that this reference electrode is buffered in an auxiliar smaller PCB and then connected to all the channels. This connection can be resumed as follows: from the buffer, through a shielded cable, the signal is connected to the PCB where the measurement channels are placed and then is distributed along a big track on the back side of the PCB. See Figure 5.8.

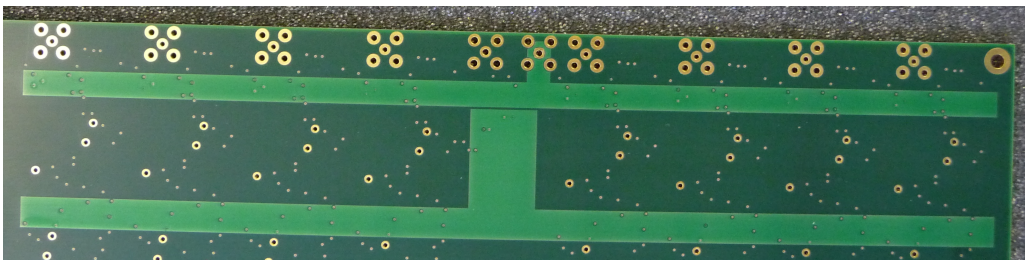

Figure 5.8. The upper track corresponds to the reference node and the lower track is the average of the common modes of all the channels in the PCB.

The problem is that the reference and average tracks, act like “antennas” and pick up interference from the surroundings, and because of their not negligible

length and impedance, they also add noise to measurement. Both interference and noise produce undesirable *currents* that affect the system especially when large resistors are connected (that is why the recordings get worse when higher impedances are connected to the input).

The solution to this problem was to decrease the length of the reference track, and put as close as possible all the channel inputs to their signal sources; in other words this a problem will be solved in further prototypes, when the amplification stage is soldered at the very back of the electrodes.

For this prototype, the effective amplification value was calculated as the circuit gain when it is connected to a 8mVpp (maximum EMG amplitude expected) 500Hz (middle frequency of the system band pass) signal coming from the voltage divider of figure 5.4. The gain of the prototype under those conditions is 1100 ($\approx 60.83dB$).

- **Common Mode Rejection.** The last validation test was supposed to measure the rejection that circuit offered against common mode. However the results of this test do not reflect the real behaviour of the circuit in presence of common mode interferences, as it was said before, the problem of the common mode is not how large the CMRR is (almost every modern instrumentation amplifier has a CMRR≥80dB), but how much of this common mode is transformed into differential mode. Time constraints did not allow to conduct this test. Only a classical CMRR test was done following the steps listed below:

  1. Short the differential inputs and connect them to a 10mV signal VCM (maximum EMG amplitude expected) at 50Hz (power line interference frequency) coming out of the voltage divider shown in Figure 5.5.

  1. Measure the output voltage V_o.

  1. Calculate the common mode gain as $G_{CM} = V_o/VCM$.

  1. Using the measured gain of the amplifier ($G_{dif} = 1100$) calculate the Common Mode Rejection as $CMRR = 20log(G_{dif}/G_{CM})$

  Figure 5.10 shows the system output when the input is the signal VCM shown in Figure 5.9. After the calculations, the CMRR turns to be:

  $G_{CM} = \frac{0.5 \cdot 10^{-3}}{7 \cdot 10^{-3}} = 0.071$

  CMRR=$20\log(1100/0.071) \approx 193dB$

  That result is not valid as a CMRR indicator because the mistmaches in the differential input paths make that part of the common mode signal enters the

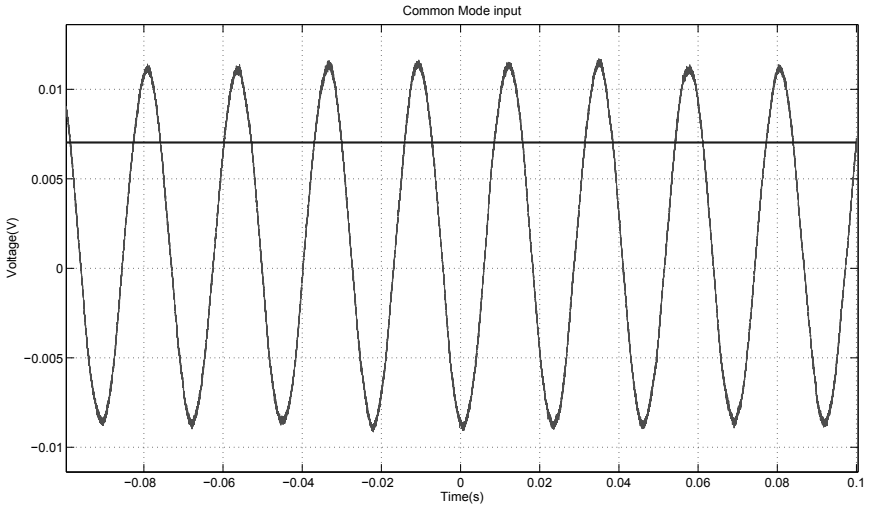

Figure 5.9. V_{CM} is a 10mV amplitude sinusoidal signal with 1mV offset at 50Hz.

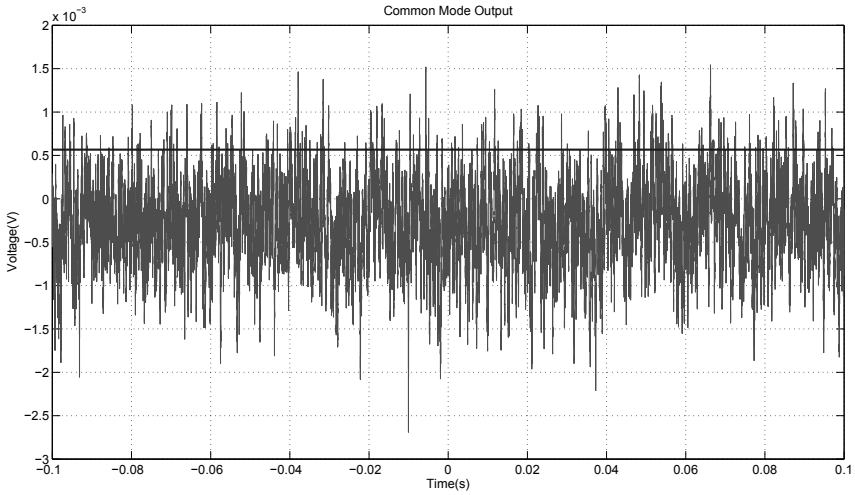

Figure 5.10. The output signal V_o is not longer linked to the input V_{CM} by a common mode gain factor, because part of the input enters the system as a differential signal.

system as a differential signal, reducing the effective common mode input, and therefore the common mode output is not longer related to the input by a gain factor G_{CM}. So it is not right to say that the system presents 194dB CMRR because it is not taking into account the common mode that enters the system trasformed into differential mode.

Another classical test in biopotential amplifiers with DRL circuits is to determine how the DRL improves the circuit performance. However in this prototype such test has not sense because the circuit does not work at all without the DRL circuit, because is through it that the amplifier is biased.

After the preliminary tests to this first EMG acquisition system prototype, the table 5.3 summarizes the results.

EMG Acqusition System Features	
Gain	1100
Bandwidth	8Hz-10kHz
Amplifier input impedance	$\geq 10^{10}\Omega$
CMRR	$\geq$80dB
AC coupled	Yes
Limit input values	$\pm$4mV
Simultaneous sampling	Yes
Driven Right Leg Ciurcuit	Yes
Driven Shield Cables	Yes
Patient−Circuit Isolation	Yes

Table 5.3. Features of the first EMG acquisition system.

Future works

The first EMG acquisition system prototype was developed, designed, constructed and validated in six months at the DLR bionics group in Munich, Germany. It sets the basis for the manufacture of an EMG high−density system at the DLR, but before arriving to a final version some aspects have to be reviewed and corrected. The list below enumerates those aspects:

- The PCB layout has to be updated because some components footprints changed and some signal connections also: the INA114 footprint has to be placed instead of the INA163, the shields of the reference and average signal have to be connected to the correct driver signal (common mode of the channel and not ground as they are connected now) and the buffer feeding the shields of each channel must be routed to the node between the gain resistors of the amplifier (to the channel common mode signal).

- The cables must be shorted because right now they are the part that is introducing most of the interference to the system. In the final version the amplifier should be soldered as close as possible to the electrodes backside.

- Currently, the reference signal is buffered and then given as one of the inputs to all the channels, however the path it crosses between the buffer output and the amplifier input is long enough to create *current* noise and to pick up interference that deteriorate the measurement. The reference signal should be buffered for each channel, but given that this solution requires more space, power consumption and it also costs more; the reference signal should be soldered in such a way that the space between the electrodes and the amplifier is minimal, and that the impedance of this trace matches the other amplifier input impedance. If the impedance of both amplifier inputs do not match, the driver potential effect will significantly degrade the measurement.

- The ADC block has to be connected and tested with the rest of the system.

- This prototype is designed to work with signals of maximum 4mV amplitude according to the discussion in Chapter 2, therefore if larger signals enter the system, the circuit will saturate. This can be prevented by rising the resistor gain value shown in Section 3.4.1.

- Only one test connecting the system to the human body was done, so further tests with real EMG signals have to be conducted.

Chapter 6

Conclusion

After spending just six months at the DLR Bionics group, the first circuit prototype for high−density EMG recording was constructed. The principles of EMG recording are in themselves, nothing new, but some unique solutions to fulfill specific requirements were found. For example: shielding the cables with their own common mode interference and filtering the DC offsets without any grounded resistor.

The first step in the design process was to research, understand and compare different EMG recording methods from classical and novelty literature, to then evaluate the most adequate solutions for the specific EMG measuirng problem imposed by the DLR Bionics group. Once the design and calculations were done, simulations were conducted to validate the circuits before their construction. Then the practical implementation took place, and after several weeks of routing, selecting componenets and manufacturing, the prototype was finished. And despite the lack of time, validation tests were done in order to evaluate performance and set basis for further development.

Although biopotentials measurement is not an easy task, because of the high interferences and noise that obscure the low voltage signal of interest, there are methods that help to improve recordings, for instance, high amplification gain (above 1000 in this prototype), adequate bandwidth selection (8Hz to 1kHz, specifically), reduction of sensitiveness to interferences and noise etc. Classical methods for reducing the human body common mode, as DRL circuits, can be used in novelty solutions for unrelated problems like electrodes half potential DC offset. In this thesis was implemented a DC rejection filter without any grounded resistor, preventing degradation of the front−end amplifier CMR properties by offering a bias path through the DRL electrode. However the relative high resistor values (5MΩ) used in its implementation, increased the noise referred to the input until 5.11μV which limited the output accuracy to maximum 10 bits.

The major problems arose due to the power line interference, making clear that proper driven shields *must* be implemented for a final useful system solution. The

best results were achieved when the common mode signal itself was used to drive the shields as it can be seen in Chapter 5, however keep connections as short as possible is essential to optimal performance. Additionally, in future versions of the EMG system, a battery power supply could be implemented to compare it with the power supply constructed in this prototype. It could not only save space but it would eliminate the need of an isolation stage.

This thesis demonstrated that it is possible to the DLR Bionics group to construct their own EMG acquisition system with their particular requirements, it set the basis for further development and spotted key issues for designing and constructing future prototypes. It also achieved the implementation of a circuit that can be used in later experiments at the Deutschen Zentrums fÃ¼r Luft und Raumfahrt (DLR) Bionics group.

Bibliography

[1] Acharya, Venkatesh: *Improving Common-Mode Rejection Using the Right-LegDrive Amplifier.* , Texas Instruments, 2011.

[2] Association for the Advancement of Medical Instrumentation 1999: *American National Standard ANSI/AAMI EC38:1998, Ambulatory Electrocardiographs. Arlington, VA: Association for the Advancement of Medical Instrumentation*, 1999.

[3] Botter, Alberto: *Short report on micro-needle electrodes.* April 11, 2011 at DLR, Munich-Germany.

[4] BULLETIN, APPLICATION: *DC-to-DC converter noise reduction.* , BURR-BROWN.

[5] Day, Dr. Scott: *Important Factors in Surface EMG Measurement.* , Bortec Biomedical, 2002.

[6] Ettinger, Sam: *PCB Design With PADS.* HMC 2012.

[7] G., De Luca: *Fundamental Concepts in EMG Signal Acquisition.* , DelSys Inc., 2001.

[8] German, Robert F., Henry W. Ott Clayton R. Paul: *Effect of an Image Plane on Printed Circuit Bord Radiation.* IEEE International Symposium on Electromagnetic Compability, 1990.

[9] Johnson., J. B.: *Thermal Agitation of Electricity in Conductors.* Physical Review, 32, 1928.

[10] JV, Basmajian De Luca CJ: *Muscles Alive. Their Function Revealed by Electromyography.* Williams & Wilkens, 1985.

[11] Kamen, Gary David A. Gabriel: *Essentials of electromyography.* Human Kinetics, 2010.

[12] Kitchin, Charles Lew Counts: *A Designer's guide to instrumentation amplifiers.* , Analog Devices Inc., 2006.

[13] Konrad, Peter: *The ABC of EMG: A Practical Introduction to Kinesiological Electromyography.* , Noraxon Inc. USA., 2005.

[14] Mancini, Ron: *OP Amps For Everyone.* , Texas Instruments, 2002.

[15] Merletti, Roberto, Matteo Aventaggiato, Alberto Botter, Ales Holobar, Hamid Marateb Taian M.M. Vieira: *Advances in Surface*

EMG: Recent Progress in Detection and Processing Techniques. Critical Reviews in Biomedical Engineering, 38, 2010.

[16] Merletti, Roberto, Alberto Botter, Amedeo Troiano, Enrico Merlo Marco Alessandro Minetto: *Technology and instrumentation for detection and conditioning of the surface electromyographic signal: State of the art.* ELSEVIER, 2008.

[17] Merletti, Roberto Philip A. Parker: *ELECTROMYOGRAPHY Physiology, Engineering, and Noninvasive Applications.* Wiley-Interscience, 2004.

[18] Motchenbacher, C.D. F.C. Fitchen: *Low-Noise Electronic Design.* Wiley-Interscience, 1973.

[19] Niel-Asher, Simeon: *El libro conciso de los puntos gatillo.* Paidotribo, 2008.

[20] Prutchi, David Michael Norris: *Design and Development of Medical Electronic Instrumentation.* Wiley-Interscience, 2005.

[21] Rich, Alan: *Shielding and Guarding.* , Analog Devices.

[22] Rijn, A.C. Metting van, A. Peper C.A. Grimbergen: *High-quality recording of bioelectric events.* Med. & Biol. Eng. & Comput. University of Amsterdam, 1990.

[23] Ruiz, A. F., F. J. Brunetti, E. Rocon, A. Forner-Cordero J. L. Pons: *Adquisición y procesado de información EMG en el modelado de sistemas biológicos.* Grupo de Bioingeniería aI instituto de Automática Industrial - CSIC.

[24] Soundarapandian, Karthik Mark Berarducci: *Analog Front-End Design for ECG Systems Using Delta-Sigma ADCs.* , Texas Instruments, 2009.

[25] Spinelli, Enrique Mario, Ramon Pallàs-Areny Miguel Angel Mayosky: *AC-Coupled Front-End for Biopotential Measurements.* IEEE TRANSACTIONS ON BIOMEDICAL ENGINEERING, 50, 2003.

[26] S.R.L, Eycom: *RECOMENDACIONES de DISEÑO para Circuitos Impresos.* .

[27] Thakor., Nitish V.: *Bipotentials and Electrophysiology Measurement.* Johns Hopkins School of Medicine.